Characterization of Follicular Lymphoma Lacking the Hallmark Translocation t(14;18)

Dissertation zur Erlangung des

naturwissenschaftlichen Doktorgrades

der Julius-Maximilians-Universität Würzburg

vorgelegt von

Ellen Leich

aus Ludwigshafen am Rhein

Würzburg 2009

Eingereicht am: 02.06.2009

Mitglieder der Promotionskommission:

Vorsitzender: Prof. Dr. Martin J. Müller

Gutachter : PD Dr. Andreas Rosenwald

Gutachter: PD Dr. Robert Hock

Tag des Promotionskolloquiums: 23.09.2009

Doktorurkunde ausgehändigt am:

Contents

1 Zusammenfassung

Neoplasien des hämatopoetischen und lymphoiden Systems können in Hodkin Lymphome (HL) und in Non-Hodgkin Lymphome (NHL) unterteilt werden. Etwa 80% der NHL sind B-Zell Lymphome (B-NHL), während etwa 20% T-Zell und NK-Zell Lymphome (T-NHL) umfassen. Genetische Alterationen, insbesondere Translokationen, welche die Immunglobulin (*Ig*) Rezeptor Gene betreffen, sind für die Klassifikation von B-NHL von großem Nutzen und sind auch in der Pathogenese dieser Neoplasien von erheblicher Bedeutung. Ein Beispiel hierfür ist die Translokation t(14;18)(q32.33;q21.3) in follikulären Lymphomen (FL).

Analog zu den *Ig* Rezeptor Genen in B-NHL, sind die T-Zell Rezeptor (*TCR*) Gene von etwa 30% der Vorläufer T-Zell Neoplasien von einer Translokation oder Inversion betroffen, die in der Regel mit der Überexpression eines Onkogens einhergehen. Die Pathogenese von reifen (peripheren) T-NHL, sowie deren zugrunde liegenden molekularen Mechanismen sind jedoch weitestgehend unbekannt. Um das Vorkommen und die Häufigkeit von chromosomalen Bruchpunkten im Bereich der *TCR* Gene in reifen T-NHL detailliert zu charakterisieren, wurden 227 Fälle im Tissue Microarray (TMA)-Format mit spezifischen Fluoreszenz in situ Hybridisierungs (FISH)-Assays analysiert. Translokationen oder Inversionen konnten in lediglich zwei der untersuchten Fälle nachgewiesen werden, was darauf hindeutet, dass reife T-NHL nur selten (<1%) von Bruchpunkten in ihren *TCR* Loci betroffen sind.

FL sind die zweithäufigste B-Zell Neoplasie, die durch ein vorwiegend follikuläres, follikulär und diffuses, oder durch ein vorwiegend diffuses Wachstum geprägt sein kann. Die Translokation t(14;18)(q32.33;q21.3), die in etwa 90% der Fälle auftritt, ist mit einer deregulierten Expression des BCL2 Proto-Onkogens assoziiert. Während bereits eine Vielzahl von Studien die morphologischen, klinischen und molekularen Aspekte dieser Entität definieren konnte, fehlt eine detaillierte Charakterisierung t(14;18)-negativer FL bislang vollständig. In der vorliegenden Arbeit wurden mittels Polymerase Kettenreaktion (PCR) und FISH Analyse 184 FL in t(14;18)-positive und t(14;18)-negative Fälle unterteilt, und die Genexpressionsprofile sowie die nummerischen chromosomalen Aberationen dieser Subgruppen untersucht. Die einzige genetische Alteration, die sich im Vergleich von t(14;18)-negativen und t(14;18)-positiven FL als signifikant erwies, waren Zugewinne und Amplifikationen in 18q11-q21, die in 32% der t(14;18)-positiven und in 0% der t(14;18)-negativen FL auftraten. Mit Hilfe von Genexpressionsanalysen und einer Gene Set Enrichment-Analyse (GSEA) konnte eine signifikante Assoziation von Keimzentrums B-Zell (GCB) Signaturen mit t(14;18)-positiven FL nachgewiesen werden, während in den t(14;18)-negativen FL eine signifikante Anreicherung von aktivierten B-Zell (ABC)-, NFkB-, Proliferations-, Zell Zyklus-, Interferon- und „Bystander" Zell Signaturen beobachtet wurde. In einem immunhistochemischen Validierungsansatz mit einer unabhängigen FL Studiengruppe (n=84) konnte gezeigt werden, dass der Keimzentrums Marker CD10/MME in t(14;18)-positiven FL häufiger exprimiert wird als in t(14;18)-negativen FL, während häufig eine erhöhte Expression des Post-Keimzentrums Markers IRF4/MUM1, des Proliferations Markers Ki67 und des zytotoxischen T-Zell Markers GZMB in t(14;18)-negativen FL nachweisbar war. Diese Ergebnisse weisen auf einen Post-Keimzentrums Phänotyp in t(14;18)-negativen FL hin. Das Vorkommen von „ongoing" somatischen Hypermutationen (SHM) in den schweren Ketten der *Ig* Gene dieser Fälle spricht jedoch gegen diese Hypothese und deutet darauf hin, dass der Phänotyp der t(14;18)-negativen FL eher dem einer B-Zelle im späten Keimzentrumsstadium entspricht.

In einer unabhängigen Studie mit 35 vorwiegend diffus wachsenden FL konnte mittels immunhistochemischer Färbungen, klassischer Chromosomenbänderung, FISH und Genexpressionsanalysen eine Untergruppe von t(14;18)-negativen FL definiert werden, die sich durch eine chromosomale Deletion in 1p36 ((del)1p36) und durch spezifische morphologische und klinische Eigenschaften auszeichnete. Das Genexpressionsprofil der diffusen FL fügte sich in das Spektrum der klassischen FL ein. Mittels GSEA konnte jedoch eine signifikante Anreicherung von T-Zell-, NK-Zell- und zwei dendritischen Zell (DC) Signaturen in diesen Fällen beobachtet werden, während die Kontrollgruppe mit klassischen FL signifikant mit GCB-, Proliferations-, Zell Zyklus- und B-Zell Signaturen assoziiert war. Die diffusen FL zeichneten sich häufig durch ein frühes klinisches Stadium, sowie durch große lokale inguinale Tumoren aus.

Zusammenfassend deuten die vorliegenden Ergebnisse darauf hin, dass t(14;18)-negative FL dem Spektrum „klassischer" FL angehören, aber dennoch spezifische molekulare und klinische Eigenschaften aufweisen. Insbesondere scheinen t(14;18)-negative diffuse FL, die durch eine Deletion in 1p36, ein frühes klinisches Stadium und große in der Leiste lokalisierte Tumoren charakterisiert sind, eine eigene FL Subgruppe zu repräsentieren.

2 Abstract

Tumors of the hematopoietic and lymphoid system are classified into Hodgkin lymphoma (HL) and non-Hodgkin lymphoma (NHL). Approximately 80% of non-Hodgkin lymphomas (NHL) are B-cell lymphomas (B-NHL) and the remainder include T-cell and NK-cell lymphomas as well as immunodeficiency-associated lymphoproliferative disorders. The presence of genetic alterations such as translocations involving the immunoglobulin (*Ig*) receptor loci in B-NHL, e.g. the translocation t(14;18)(q32.33;q21.3) in follicular lymphoma (FL), are of great value for the classification and of importance in the pathogenesis of these neoplasms.

In analogy to the *Ig* receptor genes in B-NHL, the T-cell receptor (*TCR*) gene loci are targeted by chromosomal breaks in approximately 30% of precursor T-cell lymphoblastic leukemias/lymphomas involving various translocation or inversion partners. Most of these events result in the overexpression of an oncogene by juxtaposing it to the regulatory sequences of the *TCR* genes. However, the pathogenesis of peripheral (mature) T-cell NHL (T-NHL) and the underlying molecular mechanisms are only poorly understood so far. To determine the exact frequency of breakpoints occurring in the *TCR* loci of 227 mature T-NHL cases, we designed fluorescence in situ hybridization (FISH) assays for the *TCR* loci that are applicable for large scale analysis of formalin fixed and paraffin embedded (FFPE) lymphoma specimens in a tissue microarray (TMA) format.[1] This approach revealed only two mature T-NHL cases with a chromosomal breakpoint in one of the *TCR* loci making the rearrangement of *TCR* loci a very rare event in these neoplasms that occurs in less than 1% of cases.

FL is the second most frequent type of B-NHL that can show predominantly follicular, combined follicular and diffuse, or predominantly diffuse growth patterns. The

characteristic genetic hallmark of FL is the translocation t(14;18)(q32.33;q21.3) that occurs in approximately 90% of cases and leads to a deregulated expression of the anti-apoptotic BCL2 proto-oncogene. FL has yet been a subject of many studies deciphering morphological, clinical and molecular features of this entity. However, only little information exists about cases lacking this translocation. In this thesis we divided 184 FL cases by polymerase chain reaction (PCR) and by FISH assays into FL cases with and without t(14;18) and investigated their respective gene expression profiles and copy number alterations. For FISH analysis we followed the refined conditions established for the T-NHL study.

The only genetic alterations that differed significantly by comparative genomic hybridization (CGH) analysis between FL cases with and without t(14;18) were frequent gains or amplifications in 18q11-q21 in 32% of t(14;18)-positive and 0% of t(14;18)-negative cases. Gene expression profiling and geneset enrichment analysis (GSEA) revealed an enrichment of germinal center B-cell (GCB) signatures in t(14;18)-positive cases whereas an enrichment of activated B-cell (ABC) like, NFKB-, proliferation-, cell cycle-, interferon and bystander cell signatures were observed in t(14;18)-negative cases. A validation approach by immunohistochemistry (IHC) on an independent test set of FL cases (n=84) revealed a more frequent expression of the germinal center (GC) marker CD10/MME in cases with t(14;18) and a higher expression of the post GC marker IRF4/MUM1, the proliferation marker Ki67 and the cytotoxic T-cell marker GZMB in cases without t(14;18). Although these results may suggest a post-GCB phenotype for translocation t(14;18)-negative cases, ongoing somatic hypermutations (SHM) of the immunoglobulin heavy chain genes in these cases rather point to a late GC stage of B-cell differentiation in FL without t(14;18). In an independent study with 35 predominantly diffuse FL cases, it was furthermore possible to define another subset of t(14;18)-negative FL characterized by a chromosomal deletion (del) in 1p36 and distinct morphological and clinical features by IHC, classical chromosome banding, FISH and gene expression profiling. The gene expression profiles of predominantly diffuse FL cases fell into the spectrum of FL. However, by GSEA they showed a significant enrichment of T-cell, NK-cell- and two dendritic-cell (DC) subset signatures, whereas a significant enrichment of GCB cell-, proliferation-, cell cycle- and B-cell signatures was observed in a control group of “classic” FL cases.

Remarkably, patients with diffuse FL frequently presented with low clinical stage and large, but localized inguinal tumors.

In conclusion, our results suggest that t(14;18)-negative FL are part of the spectrum of FL in general, but nevertheless show distinct molecular and clinical features. In particular, predominantly diffuse FL with (del)1p36, low clinical stage and large but localized inguinal tumors may represent a distinct t(14;18)-negative FL subtype.

3 Introduction

3.1 *Non Hodgkin Lymphoma (NHL)*

Non Hodgkin lymphoma is a diverse group of hematologic cancers that is derived from lymphocytes and can involve lymph nodes, spleen, and other organs of the immune system. Approximately 66,120 men and women (35,450 men and 30,670 women) are diagnosed with and 19,160 men and women die of NHL in the USA each year (http://www.cancer.gov/cancertopics/types/non-hodgkin).

Many subtypes of NHL have been described that can be grouped into low grade (indolent), intermediate grade or high grade (aggressive) according to their clinical behaviour, the morphology and proliferation rate of the tumor cells and to the growth pattern of the tumor. Moreover, the immunophenotype and genetic features, such as the presence of genetic alterations involving the immunoglobulin (*Ig*) receptor gene locus in B-NHL are of great value in the classification of these tumors.[2] Most NHLs are B-cell lymphomas (~90%) and the other types are T-cell and NK-cell lymphomas as well as immunodeficiency-associated lymphoproliferative disorders.[2] According to the WHO classification there are about 30 different types of B-NHL including diffuse large B-cell lymphoma (DLBCL), a fast-growing lymphoma, and FL, a slow-growing lymphoma, which are the two most common B-cell lymphomas.[2] The most common clinical sign of NHL is one or more enlarged lymph nodes in the neck, armpit or groin. NHL can be divided into stages I-IV, dependent on the number and localization of affected sites (stage I: one lymph node affected on one side of the diaphragm, stage II: two or more lymph nodes affected on one side of the diaphragm, stage III: lymph nodes at both sides of the diaphragm affected, stage IV: lymphoma has spread to one or more organs such as bone marrow, skin or liver). The information on the stage may provide prognostic information and thereby may guide the choice of treatment; however, the pathological classification is generally much more important. Approximately 50% of patients with aggressive NHL can be cured, whereas indolent forms are not currently curable but nevertheless patients with an indolent lymphoma may live up to 20 years or more. For treatment, patients may receive anthracycline based chemotherapy (CHOP), radiation therapy, biologic therapy (e.g. the monoclonal antibody Rituxan (Rituximab) that selectively targets CD20 positive B-cells), or a combination of these. However, not all patients respond to these treatments or may suffer from severe side effects. Therefore, more specialized treatment regimens that allow the specific targeting of tumor cells are needed. Bone marrow or stem cell transplantation may occasionally be used and surgery may be primarily used to obtain a biopsy for diagnostic purposes.

*3.2 **Molecular Background of B-Cell and T-Cell Derived Malignancies***

B-cell neoplasms represent clonal proliferations of B-cells and appear to mimic stages of normal B-cell development ranging from precursor B-cells to mature plasma B-cells (**Fig.1**). The process of normal B-lymphocyte differentiation is full of events which threaten the genomic integrity of a cell and then in turn may lead to neoplastic transformation. The first event which should be mentioned in this context is the process of VDJ-recombination of the immunoglobulin genes in the bone marrow that involves recombination signal sequences (RSS) guided double strand breaks initiated by recombination activating genes (*RAG1* and *RAG2)* and resolved by the non-homologous end-joining repair apparatus (**Fig.1**).[3] Sometimes these breaks are resolved aberrantly and result in translocations such as the translocations t(14;18) and t(11;14) which are hallmarks of FL and mantle cell lymphoma (MCL), respectively.[4] Furthermore, somatic hympermutation (SHM) that occurs in the GC during the process of antigen selection/affinity maturation may also lead to translocations as it is believed to be the case for the translocation t(8;14) in Burkitt lymphoma (BL) or to aberrant SHM of non *Ig* loci as it is known for the *BCL6* gene in DLBCL.[4-6] Finally, DNA breaks also occur during the process of class switch recombination and may also cause translocations as it is supposed to be the case for multiple myeloma (MM) (**Fig.1**).[4] Many of these oncogenic events result in the disruption of pathways involved in apoptosis, cell cycle and proliferation due to a deregulated expression of oncogenes such as *BCL2*, *CCND1*, *MYC* and *BCL6*.

Just like the *Ig* receptor loci (**Fig.2A**) that are frequently affected by translocations in B-cell lymphomas (e.g. t(14;18) in FL, t(11;14) in MCL and t(8;14) in BL), the *TCR* gene loci (**Fig.2B**, **Fig.5**) are targeted by chromosomal breaks in approximately 30% of precursor T-cell lymphoblastic leukemias/lymphomas.[7] According to B-cell lymphomas most of these translocations result in the transcriptional deregulation of an oncogene by juxtaposing it to regulatory sequences of the *TCR* genes thus playing an important role in the pathogenesis of these disorders. Whereas chromosomal translocations involving the *TCR*α/δ, *TCR*β and *TCR*γ loci were initially thought to be absent in mature T-cell lymphoma other than T-PLL (T-cell prolymphocytic leukemia) that carries the inv(14)(q11;q32) in 80% of cases,[2] recent data suggest that few cases of peripheral T-cell lymphoma (PTCL) do have breakpoints in one of the *TCR* loci.[8-10] In particular, the translocation t(14;19)(q11;q13) involving the TCRα/δ and *BCL3* loci, was demonstrated in two PTCL, not otherwise specified (NOS) and in one angioimmunoblastic T-cell lymphoma (AITL) recently.[10]

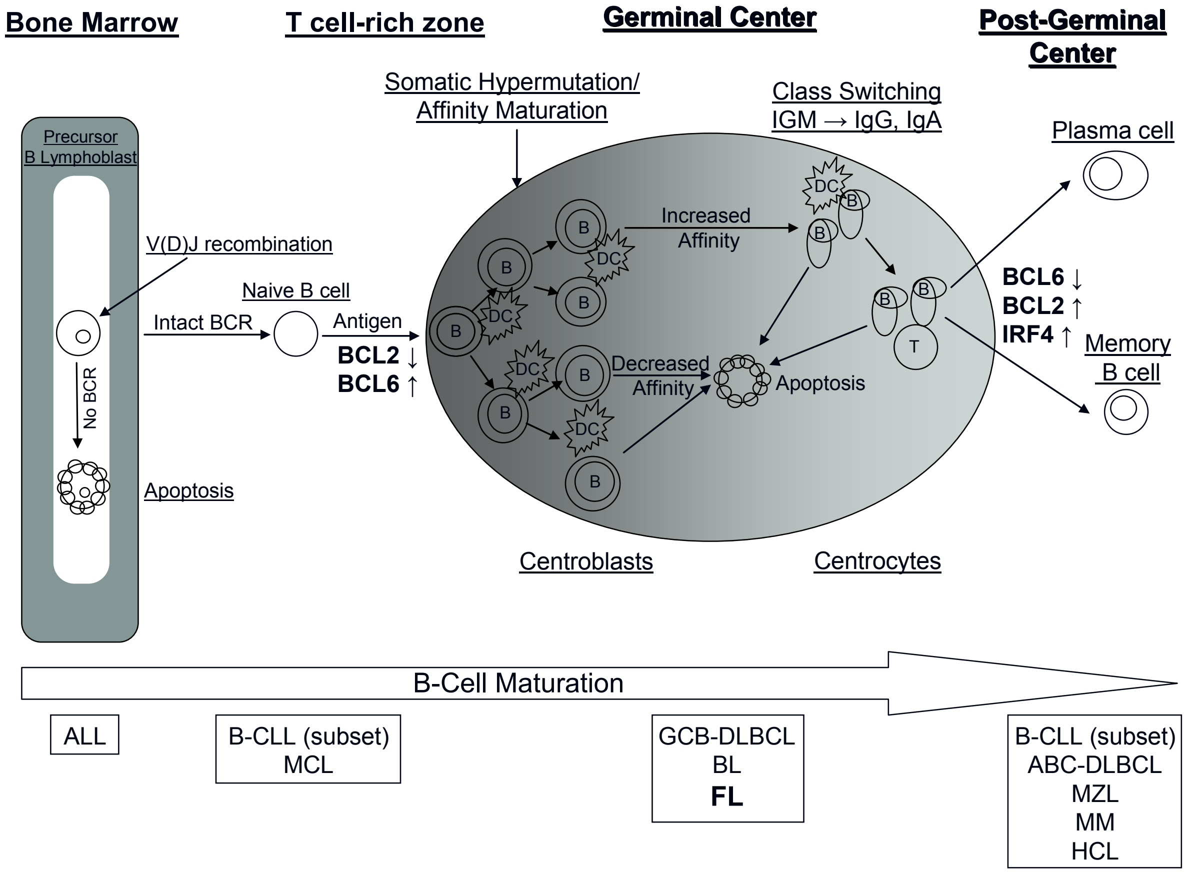

Figure 1: B-cell maturation from a precursor B lymphoblast in the bone marrow to a mature plasma B-cell or memory B-cell. Corresponding lymphoma subtypes are listed below the arrow. BCR=B-cell receptor, B=B-cell, T=T-cell, DC=dendritic cell, ALL=acute lymphoblastic leukemia, B-CLL=B-cell chronic lymphocytic leukemia, MCL=mantle cell lymphoma, GCB-DLBCL=germinal center like diffuse large B-cell lymphoma, BL=Burkitt lymphoma, FL=follicular lymphoma, ABC-DLBCL=activated B-cell like diffuse large B-cell lymphoma, MZL=marginal zone B-cell lymphoma, MM=multiple myeloma, HCL=hairy cell leukemia.

A

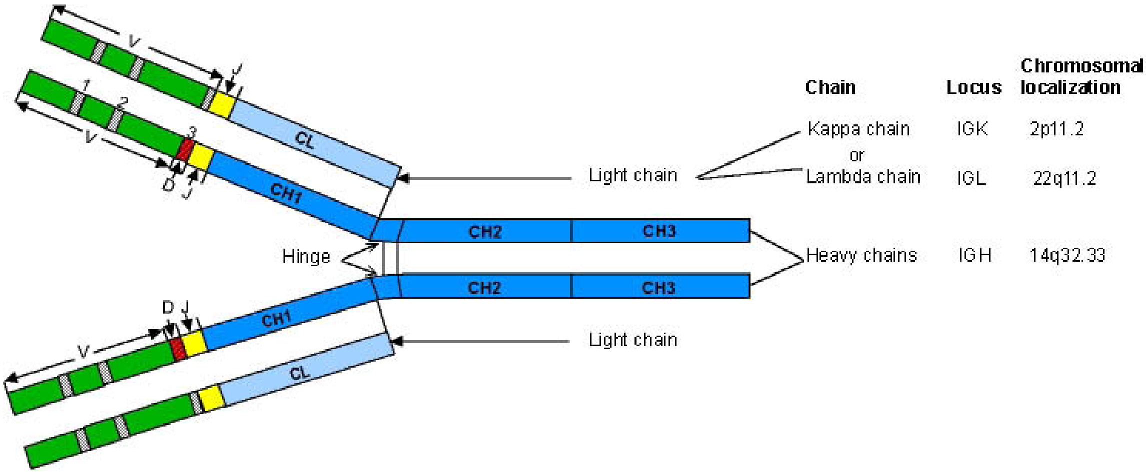

B

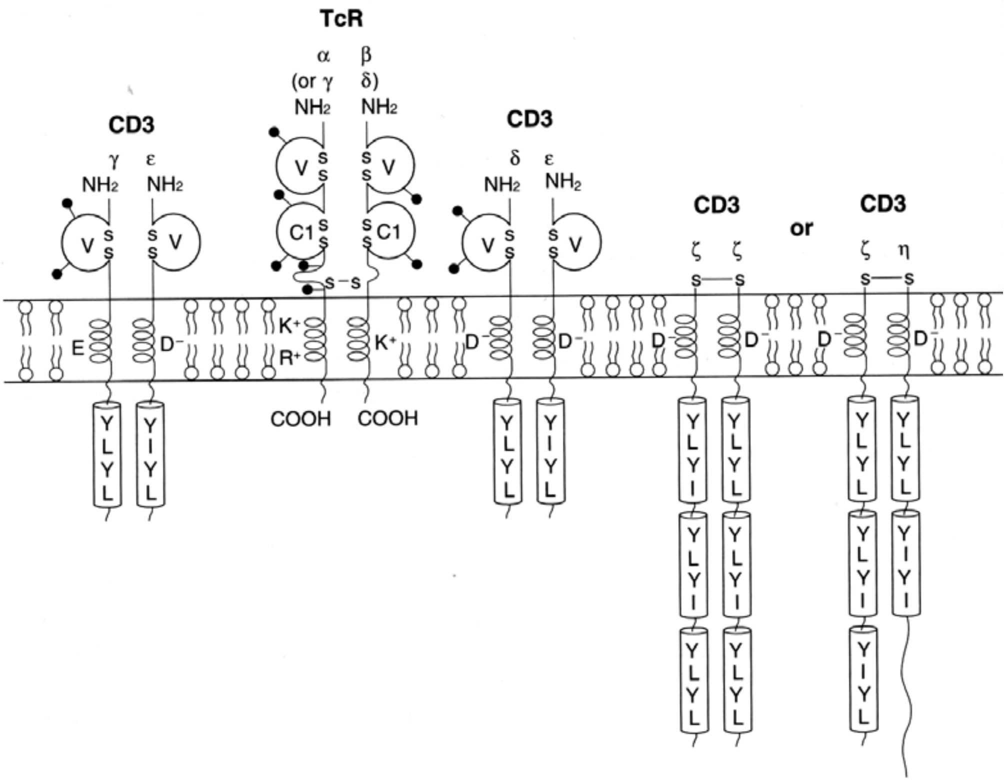

Figure 2: Structural representation of an (A) immunoglobulin (Ig) and a (B) T-cell receptor (TCR)-CD3 complex. Illustrations were derived from the T-cell receptor facts book by Marie-Paule Lefranc and Gerard Lefranc.[11,12] V=variable, D=diversity, J=joining, CL=constant light chain, CH=constant heavy chain.

3.3 *Apoptosis and Its Deregulation in Cancer*

Apoptosis is needed for tissue homeostasis, development and immune response as well as for cell death upon DNA damage, cell damage or viral infection. Disruption or deregulation of apoptotic pathways may thus lead to neoplastic transformation of normal cells into tumor cells. Apoptosis is mainly regulated by two caspase-dependent pathways which is the death receptor-induced- and the stress-mediated pathway (**Fig.3**).[13] While caspase activation in the former pathway is mediated by the Death Receptor Induced Complex (DISC), activation of these proteins in the latter pathway is dependent on the apoptosome which forms upon cytochrome C release from the mitochondria mediated by members of the BCL2 family. Proteins of this family govern the permeabilization of the outer mitochondrial membrane, can be either pro-apoptotic (BAX, BAK, Diva, BCLXs, BIK, BIM, BAD, BID, EGL1) or anti-apoptotic (BCL2, BCL_{XL}, MCL1, CED-9, BCL2A1/Bfl1) and share one or more *BCL2*-homology (BH) domains.[14]

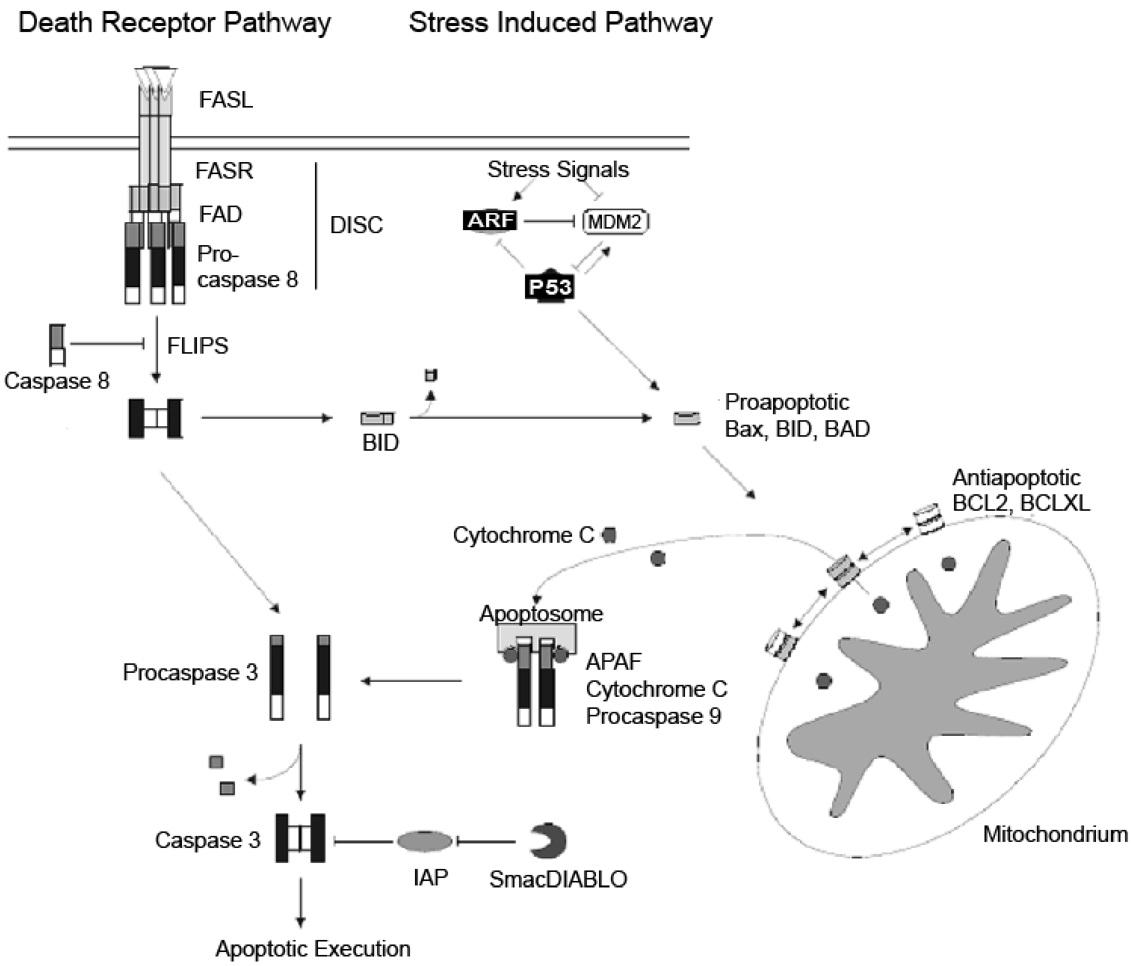

Figure 3: Caspase dependent apoptotic pathways. According to Ehlert et al., 2001.[13] Apoptosis is mainly regulated by two caspase-dependend pathways which is the death receptor-induced- and the stress-mediated pathway. While caspase activation in the former pathway is mediated by the Death Receptor Induced Complex (DISC), activation of caspases in the stress induced pathway is dependent on the apoptosome which forms upon cytochrome C release from the mitochondria mediated by members of the BCL2 family.

3.4 *Morphology and Immunophenotype of Follicular Lymphoma*

FL is a mature B-cell neoplasm composed of centrocytes and centroblasts, representing approximately 30% of NHL. Most 'classic' FL cases show a follicular growth pattern. However, FL may also present with combined follicular and diffuse, or predominantly diffuse growth patterns.[2] The growth pattern is either defined as follicular (>75%), follicular and diffuse (25-75% follicular) or minimally follicular (<25% follicular).[2] Compared to reactive lymph nodes, the follicles of FL are not clearly defined, lacking the mantle zone and the typical starry sky pattern of the GC and they proliferate less as indicated by a reduced Ki67 immunostaining (**Fig.4**).[2] Dependent on the number of blasts FL can be divided into grade 1, grade 2 and grade 3 (3A/3B).[2] The tumor cells either express IgM, IgD, IgG or rarely IgA, the B-cell associated antigens CD19, CD20, CD22 and CD79a and they are usually positive for BCL6, CD10 and BCL2.[2] Furthermore, the follicular areas are characterized by a tight meshwork of follicular dendritic cells (FDC) expressing CD21 and CD23. Since normal B-cells of the GC are BCL2 negative (**Fig.1**) this protein is useful to distinguish neoplastic from reactive follicles. However, approximately 10% of cases, in particular those with grade 3B lack BCL2 expression.[2] Notably, low grade FL cases (FL grade 1-3A) without BCL2 expression may be misclassified as reactive follicular hyperplasia.[2]

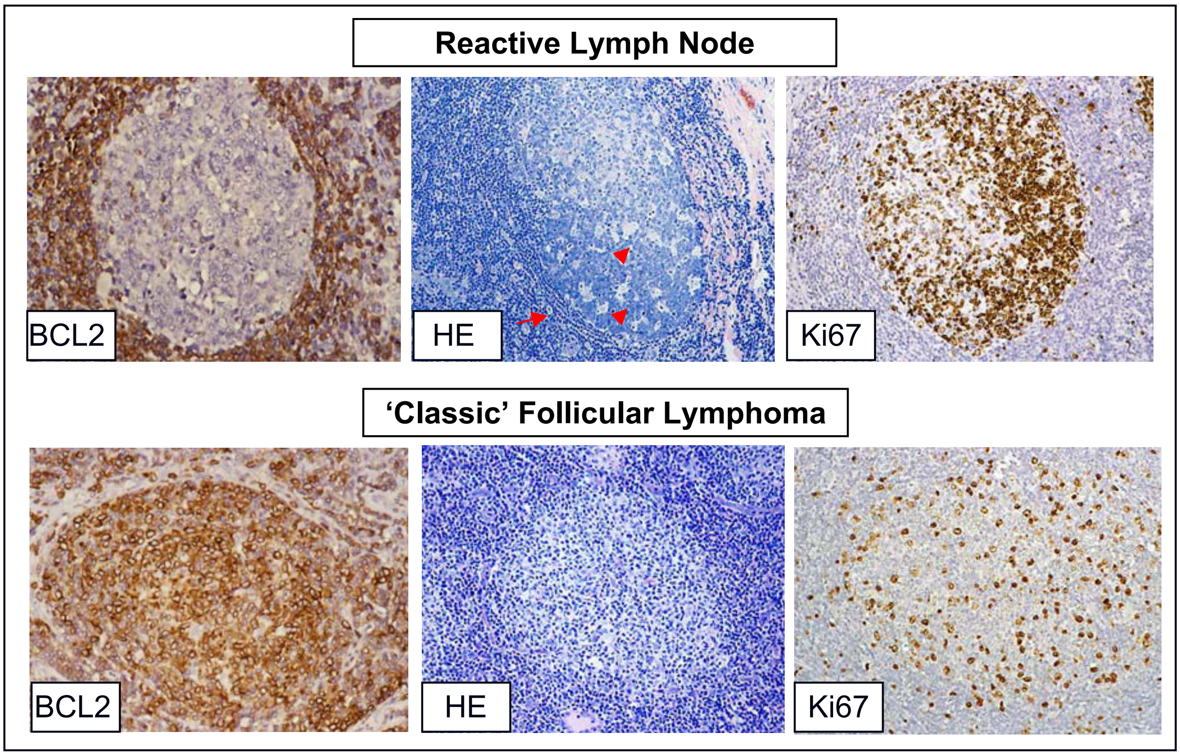

Figure 4: FL is a mature B-cell tumor composed of centrocytes and centroblasts mostly presenting with a follicular growth pattern. Compared to reactive lymph nodes, the tumor follicles are not clearly defined, lacking the mantle zone (red arrow) and the typical starry sky pattern (red arrow heads) of the GC (**middle**) and proliferate less as indicated by a reduced Ki67 immunostaining (**right**). Due to the translocation t(14;18) 90% of FL cases stain positive for BCL2 (**left**).

3.5 ***Clinical Background of Follicular Lymphoma***

FL mainly involves the lymph nodes but also spleen, bone marrow, peripheral blood and Waldeyer's ring. Generally, it is characterized by an indolent clinical behaviour with an overall median survival of eight to ten years.[2] However, the clinical course of patients can be highly variable with some patients dying within one year and others living up to 20 years.

Therefore, therapeutic approaches in FL comprise a wide spectrum which ranges from radiation over chemotherapy (CHOP or CHOP-like), immunotherapy

(Rituxan/Rituximab, Bexxar, Zevalin) and stem cell transplantation to watch and wait strategies. Most of the patients present with stage III and IV at the time of diagnosis.[2] However, not all patients respond to the current treatment regimens or may suffer from severe side effects making more specialized treatment regimens necessary. A possible strategy in BCL2 expressing NHL is to modulate the activity of members of the BCL2 family as shown for the antisense construct G3139 (oblimersen), which has meanwhile entered clinical phase III for several types of cancer.[13,15] This drug is an 18-mer oligonucleotide that binds to the first six codons of the *BCL2* gene thus inhibiting BCL2 expression. Interestingly, a synergy between oblimersen and Rituximab treatment was described for FL patients and, furthermore, oblimersen was described to overcome mechanisms of Rituximab resistance in this lymphoma entity.[15]

Clinically, the Follicular Lymphoma International Prognostic Index (FLIPI) is widely used to predict the clinical behaviour of FL at the time of diagnosis. This index includes information on age, Ann Arbor stage, haemoglobin level, number of extranodal sites affected and serum lactate dehydrogenase (LDH) level.[16] Transformation to a more aggressive lymphoma, usually DLBCL, occurs in 30-60% of cases and often goes along with additional genetic alterations such as inactivation of *TP53* and *CDKN2A* and activation of MYC.[17-19]

3.6 ***Molecular Background of Follicular Lymphoma***

Because FL are characterized by ongoing somatic hypermutation (ongoing SHM) and typically show a GC like morphology together with the expression of markers consistent with those of GC B-cells, it has been assumed that FL tumors arise from normal GC B-cells upon transformation in close association with T-helper (Th) cells and FDCs (**Fig.1**).[20] However, bystander cells such as T-cells, macrophages and DCs are not only thought to have an influence on FL pathogenesis but were also described to have an impact on patients' outcome.[21-24] In particular, a correlation approach between gene expression data and survival data identified two gene expression signatures (sets of coordinately expressed genes that can reflect the cell of origin of the cancer, the nature of the nonmalignant cells in the biopsy specimen, and the oncogenic mechanisms responsible for the cancer), namely immune response 1 (IR1) and immune response 2 (IR2) that are derived from cells of the microenvironment of the tumor. Both are highly predictive of survival, especially when using a multivariate mathematic model. Interestingly, an enrichment of the IR1 signature that is composed of genes encoding T-cell markers (*CD7, CD8B1, ITK, LEF1*) and those that are highly expressed by macrophages (*TNSF13B* and *ACTN1*) was found to be associated with a good prognosis. By contrast, an enrichment of the IR2 signature including genes preferentially expressed in macrophages (*FCGR1A, TLR5, C3AR*) and/or DCs (*SEPT10, LGMN*) were found to be associated with a poor prognosis.[25] Furthermore, the appearance of B-cell receptor (BCR) autoreactivity, ongoing SHM and the generation of carbohydrate-linking motifs, caused by SHM, in FL suggest that antigen activation might also play an important role in the pathogenesis of this entity.[26]

The genetic hallmark of FL is the translocation t(14;18)(q32.33;q21.3). The translocation t(14;18) is present in up to 90% of FL cases and probably occurs during V(D)J recombination in the bone marrow which is mediated by RAG nucleases (see also page 5, Molecular Background of B-Cell and T-Cell Derived

Malignancies). This translocation results in the deregulated expression of the anti-apoptotic *BCL2* proto-oncogene both by the *Ig* enhancers and the *BCL2*-regulatory region. Very few cases are affected by the alternative translocations t(2;18) or t(18;22) juxtaposing *BCL2* to the loci of the *Ig* light chains kappa (κ) and lambda (λ) likewise resulting in a deregulated expression of BCL2 in GC B-cells.[27] BCL2 expression in the germinal center leads to inappropriately long-lived GC B-cells which are steadily exposed to the hypermutation machinery (**Fig.1**).[28,29]

This may promote the accumulation of secondary chromosomal alterations such as gains in 1q, 2p, 7, 12q and 18q and X as well as losses in 1p, 6q, 10q, 13q and 17p which were observed in almost all FL cases with t(14;18).[30,31] Whereas deletions in 6q and gains in 1q were identified as negative prognostic markers, gains of chromosomes 7, 8 or 18 were found to be associated with a good prognosis.[32,33] Secondary alterations might be necessary to produce a fully malignant phenotype, since on the one hand t(14;18) was also detectable in peripheral blood cells of healthy individuals and on the other hand only few *BCL2/Ig* transgenic mice developed frank lymphoma but rather showed a non-clonal B-cell lymphoproliferation.[34,35]

The breakpoints at the immunoglobulin heavy chain (Ig_H) locus (14q32.33) are predominantly found within the joining elements of the heavy chain (J_H) and the breakpoints at the *BCL2* locus (18q21.3) are located within the major breakpoint region (Mbr), the minor cluster region (mcr) or dispersed in the intermediate cluster region (icr)[36].

3.7 ***Translocation t(14;18)-Negative FL***

In contrast to the detailed information regarding gene expression and genetic alterations that is available for the cases with t(14;18),[26,37] almost no information exists about the process of neoplastic transformation and pathogenesis in FL cases lacking the t(14;18) and thus also lacking BCL2 expression in the majority of cases. In particular, no reliable diagnostic marker and potential therapeutic target so far exists in this FL susbset. A subset of t(14;18)-negative FL appears to harbor genetic rearrangements of 3q27/*BCL6*, while others show BCL2 expression on the immunohistochemical level despite the lack of the t(14;18).[38-40] Furthermore, an increase in BCL_{XL} expression was observed in FL cases lacking both the t(14;18) and BCL2 expression, possibly indicating an optional pathway for tumor development.[41] Moreover, a frequent occurrence of trisomy 3 was detected using array CGH in a series of FL grades 1-3B of which the majority showed an CD10-negative and IRF4/MUM1-positive immunophenotype.[42]

The present study focused on the molecular characterization of t(14;18)-negative FL grades 1-3A since FL grade 3B cases are thought to be biologically distinct from nodal FL grades 1-3A.[43,44]

4 Aims of the Thesis

1.

Translocations involving the *Ig* gene locus in B-cell lymphomas such as the translocations t(14;18) in FL, t(11;14) in MCL and t(8;14) in BL are genetic hallmarks of these neoplasms. In analogy to the situation in B-cell lymphomas, translocations of the *TCR* loci were observed in approximately 30% of precursor T-cell lymphoblastic leukemias/lymphomas.[7] However, the occurrence of breakpoints in the *TCR* of mature T-cell lymphoma was described to be a rare event.[8-10]

Therefore, one aim of this study was to assess the accurate frequency of breakpoints affecting the *TCR* loci in a large number of mature T-NHL and to determine possible translocation partners.

2.

FL, a frequent B-NHL, are characterized by the translocation t(14;18) that leads to an overexpression of the proto-oncogene BCL2 that serves as a reliable diagnostic marker and a promising target for therapeutic approaches in FL. However, 10-15% of FL cases lack the translocation t(14;18) and the majority of these cases also lack BCL2 expression. This raises the question whether FL cases lacking the t(14;18) belong to the spectrum of “classic” FL and if this FL subset is characterized by specific clinical or molecular features. Therefore, the focus of this study was to determine the frequency of FL cases without *BCL2* rearrangement in a representative series of 184 FL cases grades 1-3A[25] and to study the differences of clinical features, gene expression, genetic alterations and the composition of the microenvironment between those cases and their t(14;18)-positive counterparts.

3.

Follicular lymphoma is a well characterized B-cell NHL that can show predominantly follicular, combined follicular and diffuse, or predominantly diffuse growth patterns.[2] Approximately 85% of FL harbor the translocation t(14;18) and consistently display a follicular growth pattern. Predominantly diffuse FL, however, are less well characterized on the phenotypical, molecular and clinical level.[2]
Therefore, a third aim of this study was to better define this FL subtype genetically and clinically.

5 Material and Methods

5.1 *Chemicals and Reagents*

Agarose	AppliChem, Darmstadt, Gemany
Anti-RbIgG (H+L) (gt) Fluorescein	Axxora, Lörrach, Germany
Anti-streptavidin-Biotin	Axxora, Lörrach, Germany
Anti-streptavidin antibody (goat), biotinylated	Axxora, Lörrach, Germany
BAC/YAC Clones	Deutsches Resourcenzentrum für Genomforschung, RZPD, Berlin/ imaGenes, Berlin, Germany
BioNick™ Labeling System (#18247015)	Invitrogen, Karlsruhe, Germany
Biotin-16-dUTP	Roche, Mannheim, Germany
Blocking Reagent	Roche, Mannheim, Germany
β-Mercaptoethanol	AppliChem, Darmstadt, Gemany
BSA	Invitrogen, Karlsruhe, Germany (for Genexpression analyis) New England Biolab, Frankfurt, Germany (for SNP analysis)
Chloramphenicol	Sigma-Aldrich, Taufkirchen, Germany
Citric acid	Merck, Darmstadt, Germany
Colcemid	Invitrogen, Karlsruhe, Germany
Cot Human DNA	Roche, Mannheim, Germany (for probe labeling) Invitrogen, Karlsruhe, Germany (for SNP analyis)
DAPI	Roche, Mannheim, Germany
Denhardt’s Solution (50x)	Sigma-Aldrich, Taufkirchen, Germany
Dextransulfate	Sigma-Aldrich, Taufkirchen, Germany

Digoxigenin-11-dUTP	Roche, Mannheim, Germany
DNA sizemarker 100 bp	MBI-Fermentas, St. Leon-Roth, Germany
DNA sizemarker 1 kb	MBI-Fermentas, St. Leon-Roth, Germany
DNA Low Mass Ladder	Invitrogen, Karlsruhe, Germany
DNA Polymerase-Buffer (10x)	Promega, Mannheim, Germany
DNA Suspension Buffer	TEKnova, York, United Kingdom
dNTP-Mix	MBI-Fermentas, St. Leon-Roth, Germany
dNTP (2.5M each)	Takara, Saint-Germain-en-Laye, France
DMSO	Sigma-Aldrich, Taufkirchen, Germany
EcoR1	MBI-Fermentas, St. Leon-Roth, Germany
EcoR1-Buffer	MBI-Fermentas, St. Leon-Roth, Germany
EDTA Disodium Salt (0.5M)	Sigma-Aldrich, Taufkirchen, Germany Ambion/AppliedBiosystems, Darmstadt, Germany (for SNP analysis)
Ethanol (pure)	AppliChem, Darmstadt, Gemany
Fetal Calf Serum	Sigma-Aldrich, Taufkirchen, Germany
Formamide	AppliChem, Darmstadt, Gemany
Fragmentation Reagent (DNaseI)	Affymetrix, Santa Clara, California; USA
Fragmentation Buffer (10x)	Affymetrix, Santa Clara, California, USA
Gentamycine	Sigma-Aldrich, Taufkirchen
Giemsa	Merck, Darmstadt

Glacial acetic acid	Merck, Darmstadt
Goat IgG	Sigma-Aldrich, Taufkirchen, Gemany
Hering Sperm DNA	Promega, Mannheim, Gemany (for chip analysis) Eppendorf, Gemany (for probe labeling)
HotStarTaq DNA Polymerase (#203203)	Qiagen, Hilden, Gemany
Igepal CA-630 (NP-40)	Sigma-Aldrich, Taufkirchen, Gemany
Ion exchanger	Merck, Darmstadt, Gemany
Isopropanol	AppliChem, Darmstadt, Gemany
Canamycine	Sigma-Aldrich, Taufkirchen, Gemany
LB Medium	Roth, Karlsruhe, Gemany
LB Agar	Roth, Karlsruhe, Gemany
Lipopolysaccharid (LPS)	Sigma-Aldrich, Taufkirchen, Gemany
Loading Dye Solution (6x)	MBI-Fermentas, St. Leon-Roth, Gemany
Magnesiumchloride 25 mM	MBI-Fermentas, St. Leon-Roth, Gemany
Magnesiumsulfate	Merck, Darmstadt, Gemany
MES hydrate	Sigma-Aldrich, Taufkirchen, Gemany
MES Sodium Salt	Sigma-Aldrich, Taufkirchen, Gemany
Metaphase CGH Target Slides (#30-806010)	Abbot Molecular, Wiesbaden, Germany
Methanol	Merck, Darmstadt, Germany
MOPS	Roth, Karlsruhe, Germany
Mouse Monoclonal Anti-Digoxigenin Clone DI-2	Sigma-Aldrich, Taufkirchen, Germany

NE-Buffer 3	New England Biolab, Frankfurt, Germany
N, N-Dimethylformamid	AppliChem, Darmstadt, Gemany
NSP1 (10.000 U/ml)	New England Biolab, Frankfurt, Germany
NucleoBond PC20 (#740571.100)	Machery-Nagel, Düren, Germany
Paraffin	Peel-A-Way Micro-Cut Parrafin, Gold Standard Series Polysciences, Inc, Warrington, PA, USA
PCR-Buffer 10x	MBI-Fermentas, St. Leon-Roth, Germany
Penicillin-Streptomycin Solution	Sigma-Aldrich, Taufkirchen, Germany
Pepsin	Sigma-Aldrich, Taufkirchen, Germany
Pertex	medite GmbH, Burgdorf, Germany
Phorbol-12,13-Dibutyrat (P)	Sigma-Aldrich, Taufkirchen, Germany
Phorbol-12-Myristat-13-Acetat (TPA)	Sigma-Aldrich, Taufkirchen, Germany
Phytohemagglutinine (PHA)	Invitrogen, Karlsruhe, Germany
Potassiumhydrogenphosphate	Merck, Darmstadt, Germany
Primer	MWG, Ebersberg, Germany
Proteinase K	Roche, Mannheim, Germany
RNAse (500µg/ml)	Roche, Mannheim, Germany
RNAse free water	LONZA, AccuGene, Belgium
RNA sizemarker	Ambion, Cambrigdeshire, UK
RPMI-1640 (with L-Glutamine / HEPES)	PAA, Cölbe, Germany
SAPE	Invitrogen, Karlsruhe, Germany
Sephadex G50	Amersham Biosciences, Freiburg, Germany

Sheared Salmon sperm DNA	Roche, Mannheim, Germany
Sodium Chloride (5M)	LONZA, AccuGene, Belgium
SSPE (20x)	LONZA, AccuGene, Belgium
STY1	New England Biolab, Frankfurt, Germany
Sodium Hypochlorite (12%)	Roth, Karlsruhe, Germany
Sodiumhydrogenphosphate	Merck, Darmstadt, Germany
Sodiumchloride	Roth, Karlsruhe, Germany
Sodium hydroxide-Pellets	AppliChem, Darmstadt, Gemany
Sodiumacetate	Merck, Darmstadt, Germany
T4 DNA Ligase	New England Biolab, Frankfurt, Germany
T4 DNA Ligase Buffer	New England Biolab, Frankfurt, Germany
TaqPolymerase	MBI-Fermentas, St. Leon-Roth, Germany
TITANUM^{TM} Taq DNA Polymerase (50x)	Clontech, Saint-Germain-en-Laye France
TITANUM^{TM} Taq PCR Buffer (10x)	Clontech, Saint-Germain-en-Laye France
Texas Red Streptavidin	Axxora, Lörrach, Germany
TMACL	Sigma-Aldrich, Taufkirchen, Germany
Tris ultrapure	AppliChem, Darmstadt, Gemany
Tri-sodium citrate	Merck, Darmstadt, Germany
Trypsin	Serva GmbH, Heidelberg, Germany
Tween-20	Thermo Scientific, Rockford, USA
Vectashield Mounting Medium	Axxora, Lörrach, Germany
X-Gal	Roth, Karlsruhe, Germany
Xylol	AppliChem, Darmstadt, Gemany

5.2 *Kits*

ALLPrep DNA/RNA Mini Extraction Kit (Qiagen, Hilden, Germany)

BigDye Terminator Cycle Sequencing Kits

(Applied Biosystems, Darmstadt, Gemany)

BioNick labeling System (Invitrogen, Karlsruhe, Germany)

CGH Nick Translation Kit (Abbot Molecular, Wiesbaden, Germany)

DNA Amplification Clean-Up Kit (Clontech, Saint-Germain-en-Laye, France)

Eukaryotic Poly-A RNA Control Kit (Affymetrix, Santa Clara, California, USA)

GeneChip IVT Labeling Kit (Affymetrix, Santa Clara, California, USA)

GeneChip Sample Cleanup Module (Affymetrix, Santa Clara, California, USA)

GeneChip Mapping 250K, NSP Assay Kit

(Affymetrix, Santa Clara, California, USA)

GeneChip Mapping 250K, STY Assay Kit

(Affymetrix, Santa Clara, California, USA)

JETprep-Kit (Genomed, Löhne, Germany)

NucleoBond Kit (Machery-Nagel, Düren, Germany)

One-cycle cDNA Synthesis Kit (Affymetrix, Santa Clara, California, USA)

Rapid Gel Extraction System (#11456-027, Marligen, Ijamsville, USA)

RNeasy Mini Kit (Qiagen, Hilden, Germany)

5.3 ***Buffers/Solutions***

Stock-Solutions

12xMES	
(Gene expression analysis)	64.61g MES Hydrate
	193.3g MES Sodium Salt
	800ml H_2O
	pH 6.5-6.7, filter through a 0.2µm filter
	store in the dark at 4°C
12xMES	
(SNP analysis)	70.4g MES Hydrate
	193.3g MES Sodium Salt
	800ml H_2O (Lonza)
	pH 6.5-6.7, filter through a 0.2µm filter
	store in the dark at 4°C
Chloramphenicol-Solution	34mg Chloramphenicol
	1ml pure EtOH
	store at -20°C
Deionized Formamide:	3l Formamide
	300g Ion Exchanger
	stirr for 30’
	filter two times through filter paper
	aliquot in 50ml Falcons
	store at -20°C

Dig 11-dUTP Mix:	17µl 1mM Dig 11-dUTP 33µl 1mM dTTP 0.5µl 100mM dATP 0.5µl 100mM dCTP 0.5µl 100mM dGTP 48.5µl ddH2O store at -20°C
10x FA Gel Buffer	200 mM MOPS 50 mM Natriumacetat 10 mM EDTA adjust to pH 7.0 with 1M NaOH store at -20°C
10xPBS	80g NaCl 2g KCl 14.4g $Na_2HPO_4xH_2O$ 2g KH_2PO_4 ad 1l ddH_2O, pH 7.3 store at RT
20xSSC	175.3g NaCl 88.2g NaAcetate ad 1l ddH2O store at RT
10% Paraformaldehyd (PFA):	900ml 1xPBS (60°C) 100g Paraformaldehyde add solid NaOH (until solution becomes clear) ad 1l PBS, pH 7.0 freeze 10ml stocks at -20°C

RNA Sample Buffer	10 ml Formamide 3,5 ml 37% Formaldehyde 1 ml 10x FA Gel Buffer 1 ml RNase free H_2O store at -20°C
Stain Buffer (2x)	41.7ml 12x MES 92.5ml 5M NaCl 2.5ml 10% Tween-20 113.3ml H_2O (Lonza) store in the dark at 4°C
TAE-Buffer (50x)	242 g Tris in 500 ml H_2O 100 ml 0,5 M Na_2EDTA pH 8,0 57,1 ml Glacial Acetic Acid ad 1l ddH_2O store at RT
10 x TN Buffer:	1 M Tris-HCl (pH 7,5) 1,5 M NaCl ad 1l ddH_2O store at RT

<u>Working-Solutions</u>

Array Holding Buffer (1x) (SNP analysis)	8.3ml 12xMES 18.5ml 5M NaCl 0.1ml 10% Tween-20 73.1ml H_2O (Lonza) store in the dark at 4°C

Anti-Streptavidin Antibody (Gene expression analysis)	dissolve 0.5mg in 1ml of H_2O
Citrate-Buffer (pH 6.0):	42g Citric Acid 20.8g NaOH-Pellets ad 10l ddH_2O pH 6.0 store at RT (boil before usage)
Citrate-Buffer (pH 7.0):	42g Citric Acid 20.8g NaOH-Pellets ad 10l ddH_2O adjust to pH 7.0 with 1N NaOH store at RT
DAPI-Mounting Medium:	1ml Vectashield 0.5µl DAPI store in the dark at 4°C
Digestion-Buffer:	3.4mM Tri-Sodium Citrate 0.1% NP-40 0.5mM Tris ad 8ml ddH_2O pH 7.6

Digestion-Buffer + Trypsin:	3.4mM Tri-Sodium Citrate 0.1% NP-40 0.5mM Tris 0.5% Trypsin ad 8ml ddH_2O pH 7.6
Digoxigenin Labeling Mix:	15-20µl DNA (~1µg) 5µl β-Mercaptoethanol 5µl DNA-Polymerase 10x Buffer 5µl Dig-Mix (see Buffers/Solutions) 5µl Enzyme-Mix (BioNick labeling System, Invitrogen) ad 50µl ddH_2O
Giemsa-Buffer:	5ml Giemsa Solution (filtered) 95ml Sörensen Buffer (see below)
Hybridization-Mix:	50% Formamide 10% Dextransulfate 2 x SSC store at -20°C
Hybridization Buffer (2x) (Gene expression analysis)	8.3ml 12xMES 17.7ml 5M NaCl 4.0ml 0.5M EDTA 0.1ml 10% Tween-20 19.9ml H_2O store in the dark at 4°C

Nick-Translation (10x Buffer):	500mM Tris-HCl pH 7.2 100mM $MgSO_4$ 1mM DTT
1xPBS:	1:10 dilution of 10xPBS (see stock solutions)
Pepsin-Solution:	100ml 0.01M HCl 5mg Pepsin (prepare freshly)
Sörensen-Buffer:	3,6g KH_2PO_4 4,14g Na_2HPO_4 ad 2l ddH_2O
2xSSC:	1:10 dilution of 20xSSC (see stock solutions)
SSC-Wash-Buffer:	95ml H2O 2ml 20xSSC 300 µl NP-40 pH 7.0-7.5 (prepare freshly)
Target Retrieval Buffer	DAKO, pH 6.1
TE-Buffer	1.21g Tris 0.37g EDTA ad 1l ddH_2O adjust to pH 9.0 store at RT

TNB Blocking Buffer:	0,5 g Blocking Reagent (Roche) 10 ml 10 x TN Buffer ad 100 ml ddH_2O solve while heating store at 4°C/long time storage at -20°C
TNT-Wash-Buffer:	50ml 10xTN-Buffer 250µl Tween20 ad 500ml dd H_2O (prepare freshly)
0.5M Tris (pH 10.0)	303g Tris ad 5l ddH_2O pH 10.0 store at RT
0.1M Tris-Buffer (pH 7.6)	12.1g Tris Ultrapure 90.0g NaCl ad 1l ddH_2O adjust to pH 7.6 with 37% HCL
Trypsin-Solution	50mg Trypsin 100ml PBS

WASH A
(SNP/Expression analysis)

Non-Stringent Wash Buffer	300ml 20x SSPE
	1.0ml 10% Tween-20
	699ml H_2O (Lonza)
	Filter through a 0.2µm filter
	store at 4°C or RT

WASH B (SNP analysis)

Stringent Wash Buffer	30ml 20x SSPE
	1.0ml 10% Tween-20
	969ml H_2O (Lonza)
	pH 8.0, filter through a 0.2µm filter
	store at 4°C or RT

WASH B
(Expression analysis)

Stringent Wash Buffer	83.3ml 12xMES (for expression analysis)
	5.2ml 5M NaCl
	1.0ml 10%Tween
	910.5ml H_2O (Lonza)
	filter through a 0.2µm filter
	store in the dark at 4°C

WASH 1 (CGH):	20ml 20xSSC
	950ml ddH2O
	3ml NP-40
	dissolve for 90 seconds in microwave and stir for 5 minutes
	adjust to pH 7.0

WASH 2 (CGH):	100ml 20xSSC 850ml ddH2O 1ml NP-40 stir for 5 minutes adjust to pH 7.0

*5.4 **Culture Medium***

LB-Broth	25 g LB-Broth adjust to 1 l H_2O autoclave for 20 minutes at 121°C and 103 kPa
LB-Agar	40 g LB-Agar in 1 l H_2O autoclave for 20 minutes at 121°C and 103 kPa Chloramphenicol was added after medium was cooled down to ~60°C. Agar was poured in culture plates which were stored at 4°C.
RPMI 1640+GlutaMAX	Medium + 10% FCS + 1% penicillin/streptomycin
RPMI 1640 without L-Glutamine	Medium + 10% FCS + 1% Gentamycine

5.5 Cell Lines

KE-37	human T-cell leukemia (DSMZ, German Collection of Microorganisms and cell Cultures, Braunschweig, Germany)[1]
MOLT-3	human T-cell leukemia (DSMZ)[1]
HSB-2	human T-cell leukemia (DSMZ)[1]

5.6 Primer Combinations for PCR and Genescan Analysis

5.6.1 Detection of BCL2 Breakpoints

1) MBR 5' CAGCCTTGAAACATTGATGG 3', mcr 5' CGTGCTGGTACCACTCCTG 3', J_H 5' ACCTGAGGAGACGGTGACC 3'. [45]

2) MBR 5' TATGGTGGTTTGACCTTTAG 3', mcr 5' GGACCTTCCTTGGTGTGTTG 3' and J_H ACCAGGGTCCCTTGGCCCCA 3'.[45]

5.6.2 Detection of Clonal Rearrangements

FR1-J_H (InVivoScribe Technologies, La Ciotat, France)

FR2 (5' TGG(AG)TCCG(AC)CAG(GC)C(AGCT)GG 3')

FR3 (5' ACACGGC(C/T)(G/C)TGTATTACTGT 3')[46]

LJ_H (5' TGAGGAGACGGTGACC 3')

VLJ_H (5'GTGACCAGGGTNCCTTGGCCCCAG 3')[46,47]

Vκ-Jκ (InVivoScribe Technologies, La Ciotat, France)

Vκ-Kde+intron-Kde (InVivoScribe Technologies, La Ciotat, France)

5.6.3 Primers for Sequencing Analysis

M13F (5'-TGT AAA ACG ACG GCC AGT-3')[48]

M13R (5'-GAG CGG ATA ACA ATT TCA CAC AGG-3')[48]

5.7 Laboratory Equipment/Material

Autoclave	MM Vakulab S3000
	H+P Labortechnik Varioklav 75S
Balance	Ohans, Adventurer
Centrifuges	Eppendorf 5415R/5417R/5415D
	Heraeus Sepatech Biofuge 15R
Cell Strainer	BD Falcon, 70µm Nylon,
	BD Biosciences, Bedford
Confocal Microscope	Leica, TCS SP2
Cryostat	Medim Universal Micratome Cryostat DDM-P500
Counting Chamber	
(0.0025 mm^2)	Neubauer improved, Marienfeld
Fluorescense Microscope	Zeiss, Axioskop2 fluorescence microscope
	Leica, Leitz DMRBE
Gel-documentation	Herolab UVT-28 SE
Gel electrophoresis chamber	Biorad
	Roth
	Mitsubishi P91
Heatblock/Thermomixer	HLC Haep Labor Consult HBT 130
	Eppendorf Thermomixer comfort
	SciGene, Hybex Microsample Incubator
	Eppendorf, ThermoStatplus
Heating Plate	Medax
Hybridization Oven	Heraeus thermiconP®
	Affymetrix, GeneChip Hybridization Oven 640

Hybridizer	Dako Cytomation, StatSpin
Hood	Heraeus, Hera, Safe
Homogenizer	Medimachine, DAKO, Glostrup, Denmark
Incubator	New Brunswick Scientific, Co. INC, Model G25
	Incubator Shaker/ innova 4230 Refrigerated
	Incubator Shaker
	Hettich, Universal/K25
	Beckman, J2-HS
Light Microscope	Olympus, Color View, BX50
Micropipettors	Eppendorf
	Gilson
Microwave	Panasonic
Nanodrop, Spectrophotometer	peQLab, Biotechnology GmbH, ND-1000
pH-Electrode	inolab, WTW, series
Parafilm	Roth
Pipetaid	Brand Accu-Jet®
Precision Balance	Ohaus Adventurer™
Scanner	Affymetrix, GeneChip Scanner 7G
Seal & Sample	
(Aluminium Foil Lids)	Beckman, Biomek
Sequencer	Applied Biosystems ABI Prism® 3130 –
	Avant Genetic Analyzer
Photometer	Amersham Biosciences GeneQuant pro
Tissue Arrayer	Beecher Instruments Micro-Array Technology
Tissue Culture flasks	Saarstedt, Newton, USA
Tissue Homogenizer	Medimachine, DAKO, Glostrup, Gemrany
Thermocycler	Eppendorf Mastercycler personal
	Eppendorf Mastercycler gradient
	Applied Biosystems,
	GeneAmp PCR System 9700
	with gold-plated block
Drying Oven	Memmer, Drying Oven
Vaccum Manifold	KNF Lab, Laboport

Vacuum Regulator	Qiagen
Vortexer	Scientific Industries, Vortex Genie2
Fluidics Station	Affymetrix, GeneChip Fluidics Station 450/450DX
Waterbath	Heinse-Ziller GFL 1086
	Köttermann Labortechnik
	Memmert

5.8 ***Databases and Software***

BRB (Biometric Research Branch) array tools

http://linus.nci.nih.gov/BRB-ArrayTools.html

BioEdit

http://www.mbio.ncsu.edu/BioEdit/BioEdit.html

Biocarta

http://www.biocarta.com/genes/index.asp

Cluster and TreeView software

http://rana.lbl.gov/EisenSoftware.htm

CNAGv.3.0 (Copy number analyzer for gene chip)

http://www.genome.umin.jp/

GTYPE (Gene Chip Genotyping Analysis Software)

https://www.affymetrix.com/support/technical/other/gtype.affx

ISIS (The Imaging Science and Information Systems)

http://www.metasystems.de/

GCOS (Gene Chip Operating Software)

http://www.affymetrix.com/support/technical/software_patches/gcos.affx

GeneMapper v3.7

https://products.appliedbiosystems.com/ab/en/US/adirect/ab?cmd=catNavigate2&catID=600798

GSEA (Gene Set Enrichment Analysis)

http://www.broad.mit.edu/gsea/

GSEA/MsigDB annotation platform

http://www.broad.mit.edu/gsea/msigdb/annotate.jsp

IdeogramBrowser

http://www.informatik.uni-ulm.de/ni/staff/HKestler/ideo/

iHOP (Information Hyperlinked over Proteins)

http://www.ihop-net.org/UniPub/iHOP/

imaGenes

http://www.imagenes-bio.de/

IMGT (ImMunoGeneTics)

http://www.imgt.org/

Leica, Confocal Software

http://www.leica-microsystems.com/

NCBI-IgBLAST

http://www.ncbi.nlm.nih.gov/igblast/

NCBI MapViewer

http://www.ncbi.nlm.nih.gov/mapview/maps.cgi

NCBI SKY/M-FISH & CGH datbase

http://www.ncbi.nlm.nih.gov/sky/

KEGG PATHWAY database

http://www.genome.jp/kegg/pathway.html

Reactome

http://reactome.org/

Signature Database

http://lymphochip.nih.gov/signaturedb/

SPSS (Statistical Package for the Social Science software) version 15.0 for windows

http://www.spss.com/statistics/

UCSC Genome Browser

http://genome.ucsc.edu/cgi-bin/hgTracks?org=human

VBASE2

http://www.vbase2.org/

5.9 ***Methods***

5.9.1 Tissue Samples

Formalin-fixed and paraffin-embedded (FFPE) tissue of 247 mature T-cell lymphomas including 64 peripheral T-cell lymphomas, not otherwise specified (PTCL (NOS)), 41 systemic anaplastic large cell lymphomas (ALCL, 14 ALK-positive and 27 ALK-negative cases), seven primary cutaneous ALCL, 29 angioimmunoblastic T-cell lymphomas (AITL), 86 intestinal (enteropathy-associated) T-cell lymphomas (EATCL) and 20 cases of T-cell prolymphocytic leukemia (T-PLL), 84 FL cases of an independent validation set (80 FL grade 1 and 2, 4 FL grade 3A) as well as FFPE or fresh frozen tissue of 35 predominantly diffuse FL cases were selected for this study. These cases were derived from the Department of Pathology, University of Wuerzburg, Germany, the Department of Pathology, University of Vienna, Austria, from the Department of Pathology, Caritas-Krankenhaus Bad Mergentheim, Germany and from the Department of Clinical Pathology, Robert-Bosch-Krankenhaus, Stuttgart, Germany and were all classified according to the WHO criteria[27].

Slides were cut from formalin-fixed and paraffin-embedded (FFPE) tissues and stained with Hematoxylin and Eosin (HE), Giemsa, and periodic acid-Schiff (PAS). Moreover, DNA was available from fresh frozen tissue of 184 previously published FL cases (151 FL grade 1 and 2, 32 FL grade 3A, 1 FL (no grade available).[25]

Ethics approvals for the entire study were obtained from the local Ethics Committees.

5.9.2 *Clinical Data*

Clinical data of all 35 patients with diffuse FL were retrieved from treating physicians according to clinical records, and treatment information was obtained from 22 patients. 34/35 (97%) of the specimens represented initial diagnostic biopsies. One patient had already been treated by the time the biopsy was performed. Clinical data from the 184 FL cases was available from a previous publication[25].

5.9.3 *Tissue Microarray Assembly (TMA)*

Tumor tissue areas of paraffin embedded tissue blocks were pre-selected based on the tumor cell content which was microscopically evaluated using the matched hematoxilin/eosin staining. With a „Manual tissue puncher“ (Beecher Instruments, Silver Spring, Maryland, USA) at least three 0.6 mm thick punches with 1.0 mm in diameter were taken from the selected regions of a donor tissue block for each case and inserted in an acceptor block with a distance of 1.5mm between the punches of the same case and 3 mm between the punches of different cases. A microtome was used to prepare 1 µm thick tissue slices from the acceptor block which were brought to 3-aminopropyltriethoxysilane (APES) coated microscope slides and dried for one week at 56°C in a drying oven to avoid the floating of the tissue slices during the staining procedure.

5.9.4 Cell Culture

All cell lines were maintained in the CO_2 incubator at 37°C in 5% carbon dioxide and were cultured in RPMI 1640 medium with L-glutamine (PAA Laboratories GmbH, Pasching, Austria), 1% penicillin/streptomycin (10,000 units/ml penicillin and 10 mg/ml streptomycin) and 10% FCS as recommended by the DSMZ (German Collection of Microorganisms and Cell Cultures).

5.9.4.1 Freezing and Defrosting Cells

Non adherent cells, cultured in 75 cm^2 culturing flasks, were harvested under optimal growing conditions and pelleted by centrifugation at 200 x g for 10 minutes at 4°C. All cell pellets were resuspended in 2ml RPMI culture medium (10% FCS, 1% penicillin/streptomycin), respectively and afterwards unified in a single falcon tube. Cells were diluted in an appropriate amount of freezing medium (RPMI 1640 with 20% FCS, 1% penicillin/streptomycin, 10% DMSO) to obtain a concentration of $1x10^7$ cells/ml according to the counting results using a Neubauer Chamber. Aliquots of 1 ml cell suspension were then subjected to the following freezing cascade: -20°C over night→ -80°C over night → -196°C.

For defrosting, cells were thawed quickly at 37°C under sterile conditions and were added immediately to a 50 ml Falcon tube filled with RPMI medium. To remove DMSO cells were pelleted by centrifugation at 200 x g for 10 minutes at RT and resuspended in fresh culture medium.

5.9.5 Disaggregation of Cells from FFPE Tissue

In 29/35 diffuse FL cases nuclei were isolated from paraffin blocks according to previously described methods[49-52] with minor modifications. Briefly, two to five sections (35 µm thick) were cut and paraffin was dissolved by adding 8 ml xylene at 37°C. After 30-60 minutes the xylene was discarded and the procedure was repeated three times. Afterwards, the tissue was rehydrated by incubation with 8ml of 100%, 70% and 50% ethanol for 30 minutes at 37°C. After washing two times with 8 ml distilled water for 30 minutes at 37°C, and 30 minutes incubation with 8 ml 37°C pre-warmed digestion buffer (3.4mM tri-sodium citrate, 0.1% NP-40, and 0.5mM Tris, pH 7.6), the tissue was mechanically disaggregated using Medimachine (DAKO, Glostrup; Denmark). The resulting cell suspension was furthermore subjected to an enzymatic digestion using 0.5% trypsin (Serva GmbH, Heidelberg, Germany) for 2 hours at 37°C. The isolated nuclei were harvested after centrifugation at 1000 rpm for 10 minutes and three additional washings with 10 ml PBS solution. By constantly vortexing, the remaining nuclei were fixed in cold Carnoy`s fixative (methanol: acetic glacial acid = 3:1, stored at -20°C) and dropped onto APES coated slides after 24 hours incubation at -70°C.

5.9.6 Classical Cytogenetic Banding Analysis

Classical cytogenetic studies were carried out following established protocols.[53] Briefly, unstimulated and/or–stimulated (phorbol-12,13-dibutyrate (substance P)[54]) cell cultures with 1-2x10^6 cells per ml RPMI medium[55] were set up after mechanical disaggregation of the specimens using a cell strainer and a plunger. The cells were then directly processed or allowed to grow overnight.

For metaphase preparation, 100µl colcemid was added to the cell culture followed by a 30 minute incubation period at 37°C. Afterwards cells were exposed to a hypotonic solution of 0.075 M KCl for 20 minutes at 37°C, fixed in methanol/acetic glacial acid (3:1), and finally dropped onto glass slides. The slides were dried for three to five days at 56°C.

The metaphases were stained using a trypsin-Giemsa standard technique. Briefly, slides were incubated five to 30 seconds (depending on cell material and RT) in a trypsin solution (0.05%), washed in PBS and afterwards stained for six minutes in a Giemsa solution. After washing the slides in distilled water and drying the slides at RT the metaphases were evaluated according to the guidelines of the International System for Human Cytogenetic Nomenclature (ISCN).[56] A chromosomal aberration was regarded as clonal, if two or more metaphases of one case harbored the same structural alteration or chromosomal gain, or if a loss of a whole chromosome was found in at least three different metaphases.

Images were captured with a Zeiss Axioskop2 microscope (ZEISS, Jena, Germany) and evaluated using the IKAROS imaging system (MetaSystems, Altlussheim, Germany).

5.9.7 Fluorescence In Situ Hybridization (FISH) Analysis

FISH was performed on metaphase preparations and cell suspensions as well as on FFPE tissue either available as whole tissue slides or arranged in a TMA format according to former protocols.[57,58] Cases were hybridized with a broad panel of probes to detect different structural aberrations (**Table 1**).[1,59] For evaluation of the signal distribution 200 cells were analyzed randomly. An aberrant clone was defined according to the cut-off level evaluated for each probe in control studies with reactive neutral buffered formalin embedded lymph node specimens calculating the mean prevalence of a given signal in at least 200 cells plus three standard deviations (**Table 1**). Illustrations were performed on a Zeiss Axioskop2 microscope (Zeiss, Jena, Germany) using the ISIS imaging system software (MetaSystems, Altlussheim, Germany).

5.9.8 Probe Design and Probe Labeling

The genomic location of the FISH probes (**Table 1**) was determined using the NCBI Map Viewer and the UCSC Genome Browser (**Table1**). BAC clones flanking the *TCR* loci *TCR*α/δ, *TCR*β, *TCR*γ (**Fig.5**) and the *BCL11b* loci[1] as well as the locus specific YAC and BAC clones for the chromosomal regions 1p36, 1p22 and 1q32[1,59] were purchased from RZPD. The combination of BACs RP11-725G5, RP11-164H13, RP11-185P18 flanking and partly spanning the TCL cluster[9] was kindly provided by R. Siebert (Institute of Human Genetics, Kiel, Germany). *E.coli* cultures with the according BACs were plated on agar plates containing chloramphenicol (12.5 µg/µl) and grown over night. Single clones were picked, cultured and the isolated plasmid DNA (Nucleobond Kit, Machery Nagel, Germany) was labelled with either Dig-dUTP (Roche Diagnostics, Mannheim, Germany) or Bio-dATP by standard nick translation (Invitrogen, Karlsruhe, Germany) according to the manufacturers instructions. Each labelled probe was tested on CGH Target Slides (Abbot Molecular, Wiesbaden, Germany) for specific binding.

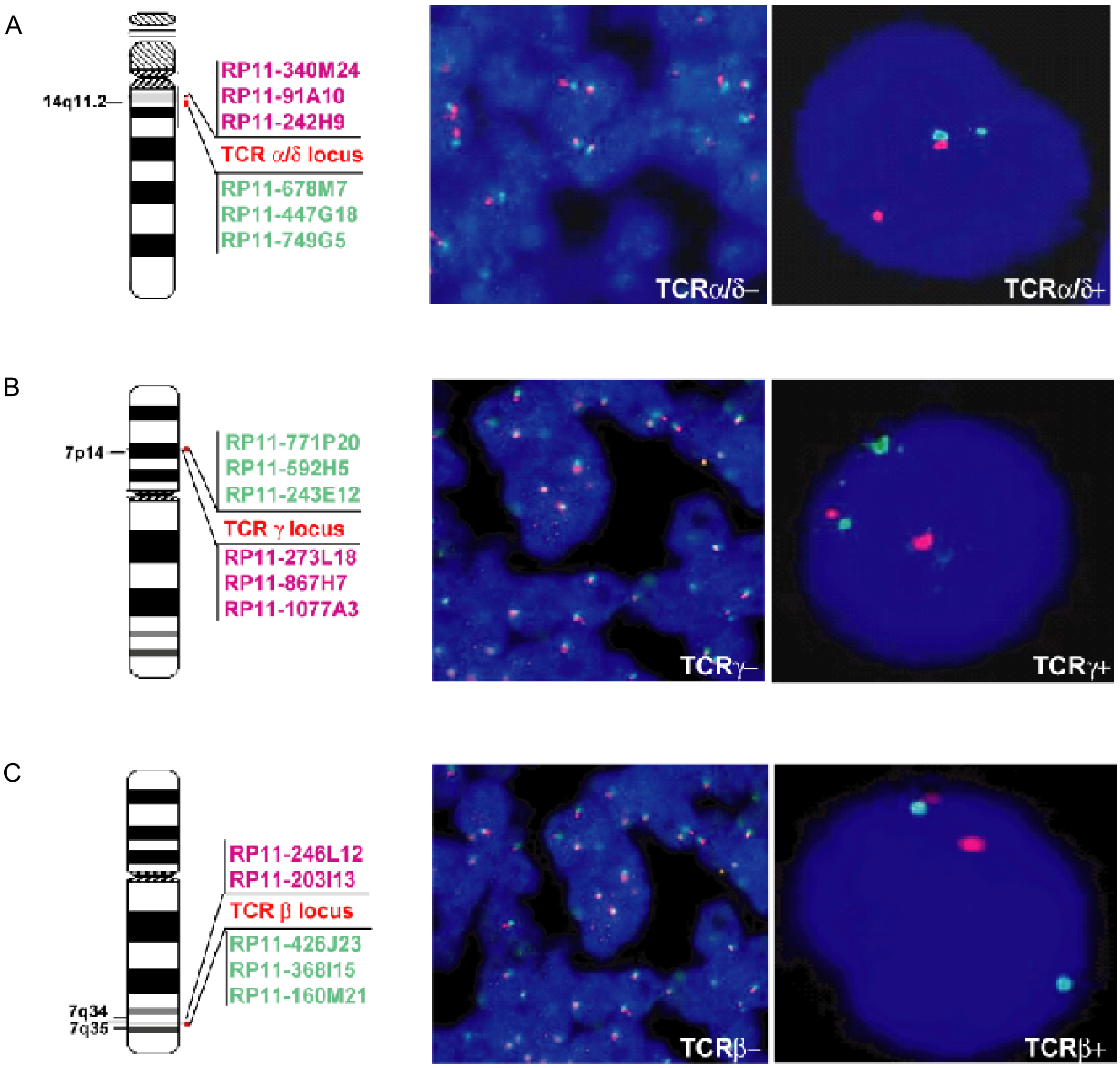

Figure 5: Design of the breakapart FISH assays for the detection of breakpoints in the *TCR* loci and control hybridizations. (**A**) Probe set for the *TCR*α/δ locus, negative FFPE tissue control, T-PLL as positive control. (**B**) Probe set for the *TCR*γ locus, negative FFPE tissue control, precursor T-cell lymphoblastic leukemia/lymphoma as positive control. (**C**) Probe set for the *TCRβ* locus, negative FFPE tissue control, cell line HSB-2 as positive control.

5.9.9 Positive Controls for FISH Segregation Assays

To test our FISH segregation assays for the detection of breakpoints in one of the *TCR* loci, three human T-cell lymphoblastic lymphoma derived cell lines (HSB-2, MOLT-3 and KE-37) and 21 primary lymphoma samples were selected. KE-37 is affected by a chromosomal breakpoint at the 14q11 locus, HSB-2 carries a translocation t(1;7)(p34;q35) and MOLT-3 is cytogenetically characterized by the translocation t(7;7)(p15;q11). Moreover three of 20 cases of T-cell prolymphocytic leukemia (T-PLL) carried an inv(14)(q11q32) based on previous karyotypic analysis. A precursor T-cell lymphoblastic leukemia/lymphoma that was previously shown to harbour a chromosomal break in the TCRγ locus was kindly provided by R. Siebert (Institute of Human Genetics, Kiel, Germany). [9]

Table 1 BAC clones and commercially available probes used for this thesis

Clones/Probes	Location of probes	Gene locus	Resource	Cut-off
RPCI11-242H9 RPCI11-91A10 RPCI11-340M24 RPCI11-447G18 RPCI11-678M7 RPCI11-749G5	Centromeric Telomeric	*TCR*α/δ	RZPD	12.2%
RPCI11-246L12 RPCI11-203I13 RPCI11-426J23 RPCI11-368I15 RPCI11-160M21	Centromeric Telomeric	*TCR*β	RZPD	10.2%
RPCI11-273L18 RPCI11-867H7 RPCI11-1077A3 RPCI11-243E12 RPCI11-592H9 RPCI11-771P20	Centromeric Telomeric	*TCR*γ	RZPD	9.9%
RPCI11-1127D7 RPCI11-1088A3 RPCI11-543C4 RPCI11-860P2	Centromeric Telomeric	*BCL11b*	RZPD	10%
RPCI11-725G5 RPCI11-164H13 RPCI11-185P18	Centromeric Telomeric/Spanning	*TCL1*	RZPD	4%
RP4- 755G5	Locus specific	1p36	RZPD	5%
YAC 968g8	Locus specific	1p22	RZPD	5%
YAC 958e1	Locus specific	1q32	RZPD	6%
Break-apart probe	Flanking	*BCL3*	Dako, Denmark	9%
Break-apart probe	Flanking	*HOX11A/ TLX1*	Dako, Denmark	7%
Break-apart probe	Flanking	*IgH*	Abott, Germany	9%
Break-apart probe	Flanking	*MYC*	Abott, Germany	9%
Break-apart probe	Flanking	*BCL2*	Abott, Germany	8%
Break-apart probe	Flanking	*BCL6*	Abott, Germany	8%
Fusion-probe	Flanking	*IGH/BCL2*	Abott, Germany	16%
Centromeric probe	Spanning	*CEP7*	Abott, Germany	5%
Centromeric probe	Spanning	*CEP1*	Abott, Germany	5%

RPCI11: RZPD, Deutsches Ressourcenzentrum für Genomforschung (http://www.imagenes-bio.de/)

5.9.10 *Fluorescence Immunophenotyping and Interphase Cytogenetics as a Tool for the Investigation of Neoplasms (FICTION)*

FICTION analysis allows the parallel detection of surface proteins and chromosomal changes in a single cell. The procedure is based on common FISH protocols[57,58] with minor modifications. Shortly, fresh cells were dropped onto APES coated slides and fixed in acetone for ten minutes at 4°C. After drying for 15 minutes at RT, cells were washed two times for seven minutes in tris buffer (pH 7.6) and were than stepwise dehydrated in 70%, 80% and 100% ethanol followed by a two hour drying step at RT. Notably, cells were not digested with pepsin since this was found to destroy the surface proteins. Completely dried cells were incubated for 10 minutes at 80°C on a heating plate using probes for *TCR*α/δ and *IgH*. After overnight incubation at 37°C in a hybridization chamber, slides were washed three times for five minutes in 0.2 SSC at 65°C and then incubated in antibody diluent for 15 minutes (Dako, Glostrup, Denmark). The detection of CD3 and CD79 was performed, using the following antibodies. 1. anti-CD3 (rab., 1:400, Dako, Glostrup, Denmark)/anti-CD79A (rab., 1:50, Lab Vision, UK), 2. anti-rab.-Cy5 (donkey, 1:100, Jackson ImmunoResearch, Europe). In between the cells were washed three times for five minutes in tris-buffer (pH 7,6). Afterwards the slides were embedded in Vectashield Mounting Medium (Axxora, Lörrach, Germany) with 4, 6-diamidino-2-phenylindole (DAPI).

Illustrations were performed on a Leica-DMRE (Leica Microsystems, Wetzlar, Germany) using the Leica Confocal Software. Further evaluations were performed on a Zeiss Axioskop2 microscope (Zeiss, Jena, Germany). At least 200 well hybridized cells were analyzed randomly.

5.9.11 Comparative Genomic Hybridization (CGH) Analysis

Conventional CGH was performed as previously described in another study[60] using the CGH Nick Translation Kit from Vysis (Abbot Molecular, Wiesbaden, Germany). Shortly, DNA was isolated from fresh frozen tissue, labeled with spectrum red and spectrum green dNTPs by nick translation (Abbot Molecular) and cohybridized with normal DNA from healthy individuals to metaphase spreads (Abbot Molecular). After counterstaining with DAPI the metaphases were visualized and analyzed using the Cytovision Ultra Workstation (Applied, Imaging, Sunderland, UK). For graphical representation of the CGH data in a karyotype format the imaging options provided by the SKY/M-FISH&CGH database were used. Complete CGH data are available at http://www.ncbi.nlm.nih.gov/sky/.

5.9.12 Immunohistochemistry (IHC)

Immunostaining was performed according to standard protocols[43] using either whole tissue sections or TMAs. For diagnostic purposes, immunostaining was performed on whole paraffin sections using the B-cell markers CD20 (Clone L26, DAKO, Glostrup, Denmark, 1:1000, Citrate-Buffer, pH6) and CD23 (Clone 1B12, NOVOCASTRA, Newcastle upon Tyne, United Kingdom, 1:80, target retrieval (TR)-Buffer, pH 6.1) and the T-cell markers CD3 (NOVOCASTRA, 1:80, Citrate-Buffer, pH6) and CD5 (Clone 4C7, NOVOCASTRA, 1:40, Citrate-Buffer, pH6).

Further stainings with antibodies against BCL2 (Clone 124, DAKO, 1:400, Citrate-Buffer, pH 6.0), CD10/MME (NCL-CD10 270, NOVOCASTRA, 1:100, Citrate-Buffer, pH 7.0), IRF8/ ICSBP1 (polyclonal, Santa Cruz Biotechnology (California, USA),1:200, Citrate-Buffer, pH 6.0), IRF4/MUM1 (MUM-1p, DAKO, 1:800, TR-

Buffer, pH 6.1), GZMB/GZMB (GrB-7, Monosan (Uden, Netherlands), 1:80, Citrate-Buffer, pH 6.0), FOXP3 (1:50, TR-Buffer (DAKO), pH 6.1, kindly provided by G. Roncador, Spanish National Cancer Research Centre Madrid, Spain), CD57 (BD Biosciences (New Jersey, USA), 1:800, Citrate-Buffer, pH 6.0) and BCL6 (Clone pG/B6p, DAKO, 1:20, Citrate-Buffer, pH 6.0) were performed on whole FFPE tissue slides or TMAs. Proliferation indices (PI) were recorded after staining with the MIB1 antibody (MIB-1, DAKO, 1:800, Citrate-Buffer, pH 6.0) detecting the Ki67 antigen. The presence of follicular dendritic cell (FDC) meshworks was evaluated either by staining for CD23 (Clone 1B12, NOVOCASTRA, 1:80, Citrate-Buffer, pH6) or CD21 (Clone 1F8, DAKO, 1:200, TR-Buffer, pH6.1). All immunohistochemical reactions were performed after antigen retrieval by pressure cooking using the peroxidase anti-peroxidase (PAP) method.

5.9.13 Polymerase Chain Reaction (PCR) for the Detection of BCL2 Breakpoints

DNA from fresh frozen tissue of 184 FL cases was isolated and PCR was performed at both the major breakpoint region (Mbr) and the minor cluster region (mcr) of *BCL2* according to a standard protocol.[45]

5.9.14 Gene Expression Analysis and Statistical Evaluation

Gene expression studies were performed using the HG U133 A and U133 B gene expression arrays from Affymetrix (Affymetrix, Santa Clara, CA, USA). RNA was isolated from frozen tissue samples using the ALLPrep DNA/RNA Mini Extraction Kit from Qiagen (Qiagen, Hilden, Germany), following the manufacturer's instructions. The data was normalized to 500 arbitrary units using the MAS5 algorithm by the Gene Chip Operating Software (GCOS) from Affymetrix.

To compare the gene expression profiles, a two sided t-test and gene set enrichment analysis (GSEA) (http://www.broad.mit.edu/gsea) was performed as described (**Fig.6)**,[61,62] using either 81 previously published[63] lymphoma associated gene signatures from the signature database of the Staudt laboratory http://lymphochip.nih.gov/signaturedb/, or 836 regulative motifs gene sets (c3) from the Molecular Signatures Database (MSigDB).[61] GSEA allows the ranking of genes based on their difference in expression among two phenotypes and wants to determine if the genes of a given geneset are randomly distributed or if they are primarily found at the top or the bottom of the ranked gene list. The more genes of a given signature/geneset appear at the top or the bottom of a ranking list, the higher is the possibility that the given signature/geneset is significantly enriched for one phenotype.

If the nominal p-value and the tail-FDR (tail-false discovery rate) were 0.05 and 0.25 or less, the corresponding gene set was assessed as significantly enriched for the stated phenotype. The tail-FDR provides an estimate of the probability that a gene set/signature with a given normalized enrichment score represents a false positive finding.[64] A GSEA integrated leading edge analysis was performed using the significantly enriched gene sets to extract the genes which account for the enrichment score.

For the correlation of gene expression data and CGH results chromosomal regions showing alterations in at least five FL cases were considered (S1) and cases were coded as normal or altered. Probesets from the Affymetrix HG U133 A and U133 B gene expression arrays and positional gene sets (c1) from the MsigDB, mapping to these regions, were selected and tested for association with a t-test and a GSEA approach, respectively. To account for multiple comparisons, local FDR (for the t-test) and tail-FDR (for analysis with GSEA) were calculated for significant p-values respectively, and those with a locFDR ≤ 0.01 or a tail-FDR ≤ 0.25 were considered truly statistically significant. According to the results of the t-test, chromosomal regions that showed an excess of probes significantly associated with expression were determined by comparison of observed to expected associations using a Poisson model. Annotations to gene families were done using the Broad Institute annotation platform which is based on the MSigDB database.

Moreover, data were analyzed using the Statistical Package for the Social Science software (SPSS, version 15.0 for Windows). To evaluate the difference in survival analysis was performed according to the method described by Kaplan and Meier, and the curves were compared by the log-rank test. Frequencies in different parameters were compared and analyzed using Fishers exact test. All p-values were two-sided and p-values <0.05 were considered significant.

For cluster analysis and visualization of the data the Cluster and TreeView software packages provided by M. Eisen (http://rana.lbl.gov/EisenSoftware.htm, M. Eisen, Berkeley, CA, USA) were used.

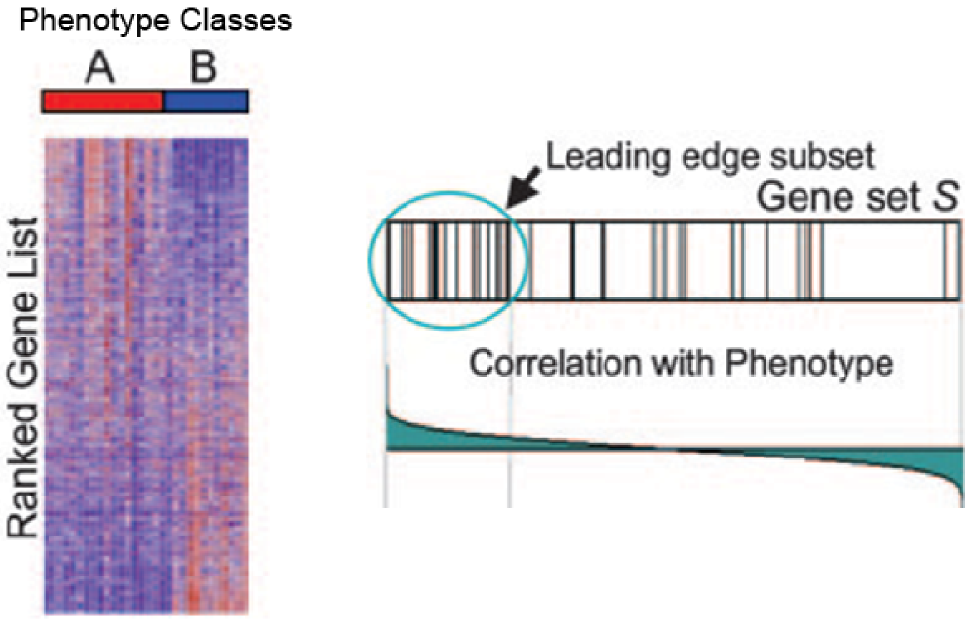

Figure 6: Overview of the GSEA method according to the publication of Subramanian et al., 2005.[61] A heatmap showing the ranked genes of a gene expression dataset according to their correlation with one of the phenotypes and a plot that depicts the enrichment of genes of a given signature/geneset that is correlated with one of the phenotypes. The more genes of a given signature appear at the top or the bottom of a ranking list, the higher is the possibility that the given signature/geneset is significantly enriched for one of the phenotypes. The leading edge subset represents the significantly enriched genes that account for the significant enrichment of a signature/geneset.

5.9.15 High Density Single Nucleotide Polymorphism (SNP) Array Analysis

Single nucleotide polymorphism (SNP) array studies were performed using the 250k NSP subarray from the 500k array set (Affymetrix, Santa Clara, CA, USA) according to the manufacturer's instruction. Data files were generated with the GCOS and the GTYPE software from Affymetrix using the Dynamic Modeling (DM) algorithm (threshold setting = 0.33). Unpaired analysis using an independent reference set of 16 lab internal controls and 15 additional controls provided by

Affymetrix/the HapMap project (www.affymetrix.com/www.hapmap.org) was performed. The results were visually analyzed using CNATv4.0 (Affymetrix) and CNAGv3.0 applying the AsCNAR algorithm (Genome Laboratory, Tokyo University). Only alterations with more than 20 consecutive SNPs were counted. If two similarly altered segments were separated by a gap which was smaller than 0.5 Mb and shorter in length than both altered segments, the gap was closed and the alterations were counted as one.

5.9.16 Clonality Analysis (Genescan)

Clonality analysis of the variable heavy chain (V_H) and variable light chain (V_L) rearrangements of 17 t(14;18)-positive and 17 t(14;18)-negative FL cases was performed by Genescan analysis using consensus primers for the framework region 2 (V_H-FR2) and framework region 3 (V_H-FR3) together with HEX/FAM labelled consensus primers for the joining region (LJ_H/VLJ_H) (**Fig.7**). For amplification of the FR3 a single step protocol was used (10' 95°C, 30'' 95°C, 45'' 60°C, 45'' 72°C (go to step 2, repeat 34 times), 10' 72°C, 8°C hold), while a semi-nested approach was followed for the amplification of the FR2 (first round: 10' 95°C, 30'' 95°C, 45'' 60°C, 45'' 72°C (go to step 2, repeat 34 times), 10' 72°C, 8°C hold); second round: 5' 95°C, 30'' 95°C, 30'' 65°C, 1' 72°C (go to step step2, repeat 5 times) 30'' 95°C, 30'' 64°C, 1' 72°C (go to step 5, repeat 5 times), 30'' 95°C, 30'' 63°C, 1' 72°C (go to step 8, repeat 18 times), 10' 72°C, 8°C hold).

Cases which revealed no monoclonal result were additionally investigated by FAM-labelled Biomed-2 primer mixes from InVivoScribe (InVivoScribe Technologies, La Ciotat, France). First a primer mix was applied containing family specific V_H-FR1 primer together with a J_H consensus primer and second cases with no proven monoclonal Ig_H rearrangement were investigated using the family specific $V\kappa$-primers together with either a $J\kappa$ or an intragenic Kde primer. The PCR products were analyzed with an ABI Prism 3130-Avant Genetic Analyzer (Applied Biosystems, Foster City, CA) and visualized by the GeneMapper 3.7 software.

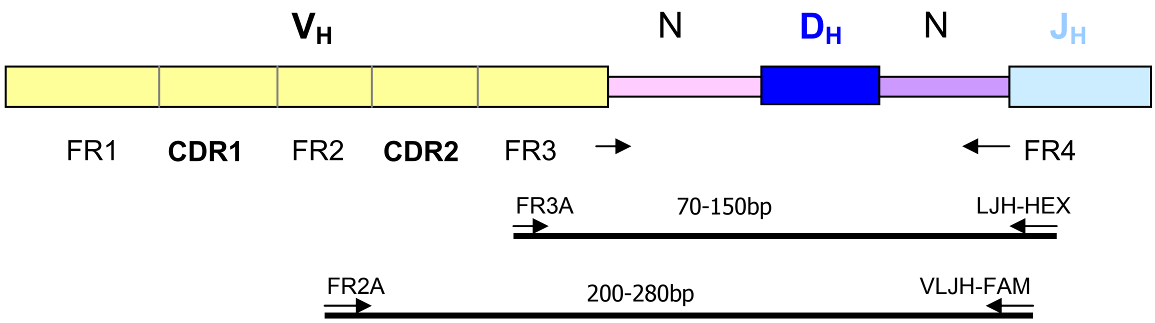

Figure 7: Schematic presentation of the V-D-J-region of a *IgH* gene locus and the aligned primer combinations FR3-LJH and FR2-LJH/VLJH that were used for Genescan analysis.

5.9.17 Analysis of Ongoing Somatic Hypermutation (SHM)

To study ongoing SHM the DNA of selected cases with a proven clonal immunoglobulin variable heavy chain (IgV_H) rearrangement was amplified in a seminested approach using the primer combination FR2A-LJH/VLJH. PCR was performed according to the conditions used for Genescan analysis. PCR products were separated on 1.5% agarose gels, excised and gel purified using the gel extraction kit from Marligen (Marligen Biosciences, Urbana-Pike, MD). Purified PCR products were subcloned using the TOPO TA Cloning Kit from Invitrogen (Invitrogen, Karlsruhe, Germany) following the manufacturer's instructions. Plasmid-DNA was isolated from 10-15 subclones (Jet prep kit, Genomed, Germany) and sequenced by automated fluorescent sequencing with an ABI Prism 3130-Avant Genetic Analyzer (Applied Biosystems, Foster City, CA) using M13-forward and M13-reverse primers. Sequences were analyzed using the NCBI-IgBLAST and VBASE2 software and evaluated manually mainly according to the criteria as previously described.[65,66] Shortly, the V_H gene sequences were compared with the germ line genes and somatic mutations were determined disregarding the somatic mutations which were identical for all subclones. Only mutations which were observed more than once in the subclones from the same tumor specimen (confirmed mutation) were considered as an evidence for ongoing SHM.

Silent mutations which occurred in a base triplet with a replacement mutation were not counted and two replacement mutations in one base triplet were counted only once.

6 Results

6.1 *Establishment of TMA-Based FISH Assays Using Paraffin Embedded Material of Peripheral T-Cell Lymphomas*

6.1.1 TCR Breakpoint Analysis in Mature T-Cell Lymphomas

The cut-offs for the *TCR* probes were set at 12.2% for the *TCRα/δ,* 10.2% for the *TCRβ* and 9.9% for *TCRγ* probes, following the hybridization of two reactive lymph nodes and ten B-cell lymphoma cases. Furthermore, split signals for the *TCRα/δ* locus were observed in the cell line KE-37 and in 13 of 19 T-PLL cases. A breakpoint in the *TCRγ* locus was detected in a case of precursor T-cell lymphoblastic leukemia/lymphoma with reported *TCRγ–* translocation and the HSB-2 cell line carried a split signal when hybridized with the probes for the *TCRβ* locus (**Fig.5**).[1]

According to our FISH analysis that was performed on 227 paraffin embedded mature T-cell lymphomas (64 PTCL (NOS), 41 ALCL (14 ALK-positive and 27 ALK-negative cases), seven primary cutaneous ALCL, 29 AITL and 86 EATCL) arranged in a TMA format, only two cases (0.9%) showed evidence of a chromosomal breakpoint affecting the *TCRα/δ* locus (14q11), whereas no alterations were observed in the *TCRβ* (7q35) and/or *TCRγ* (7p14-p15) loci. One case showed a break in the *TCRα/δ* locus and another break slightly telomeric of the *BCL3* (19q13) gene suggesting a translocation event between these loci (**Fig.8**).[1] The other case seemed to be affected by an inversion between the *TCRα/δ* locus at 14q11 and the *IgH* locus at 14q32.3 which was proven by co-hybridization approaches on metaphase spreads of this case. A FICTION approach furthermore showed that only T-cells and not B-cells were affected by this inversion (**Fig.8**).[1]

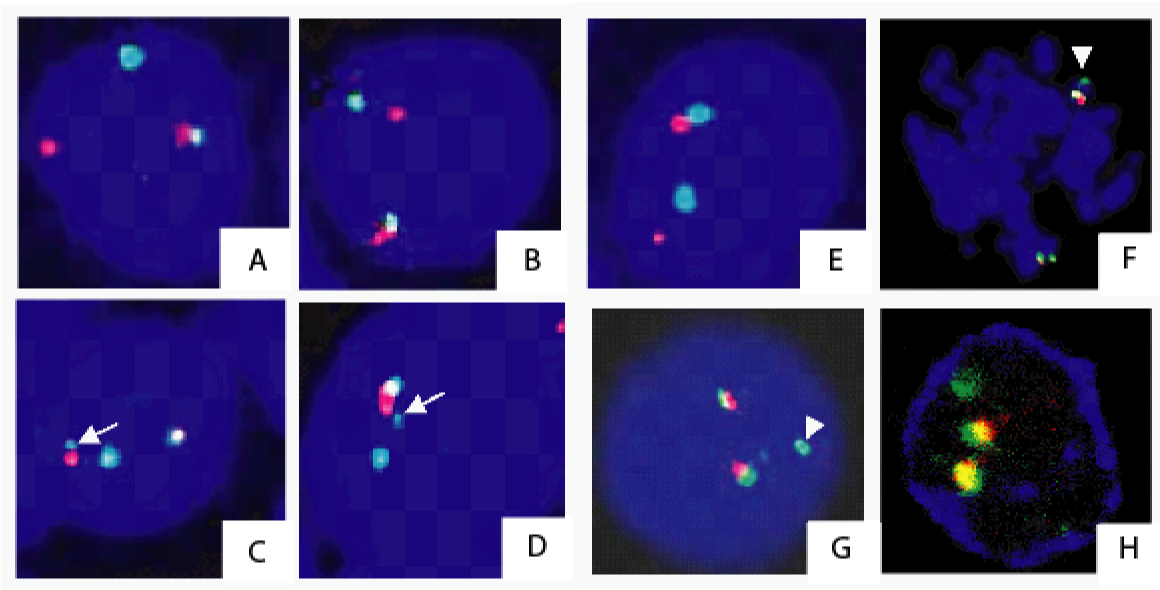

Figure 8: (**A,B**) Interphase FISH indicating a breakpoint in the *TCR*α/δ locus (14q11). **(C,D**) Interphase FISH using a *BCL3* (19q13) break-apart probe. Arrows indicate an additional split of the green/telomeric signal.
(**E**) Interphase FISH indicating a breakpoint in the *TCR*α/δ locus. (**F,G**) Tumor metaphase and interphase nucleus hybridized with a *IgH* (14q32.3) break-apart probe. Note a separate green signal (arrowhead). (**H**) FICTION demonstrating the presence of an *IgH* break in CD3-positive tumor cells.

6.2 Molecular Characterization of "Classic" FL Grades 1-3A

6.2.1 Genetic Alterations in FL and Their Correlation with Survival

A total of 180 of 184 "classic" FL cases grades 1-3A, previously studied by gene expression profiling[25] were successfully hybridized by our CGH approach. Chromosomal gains and losses could be detected in 127/180 FL. The hereby obtained results show recurrent gains and losses such as gains in 1q, 2p, 7, 8q, 12q, 18q and X as well as losses in 6q, 10q and 13q (**Fig.9A**). The presence of amplifications of 18q21 correlated with inferior outcome when correlating the minimally altered chromosomal regions (MCR) with overall survival of FL patients. Only four tumors, however, carried this alteration and all four patients died in less than five years (*P*=0.002, FDRq=0.08).

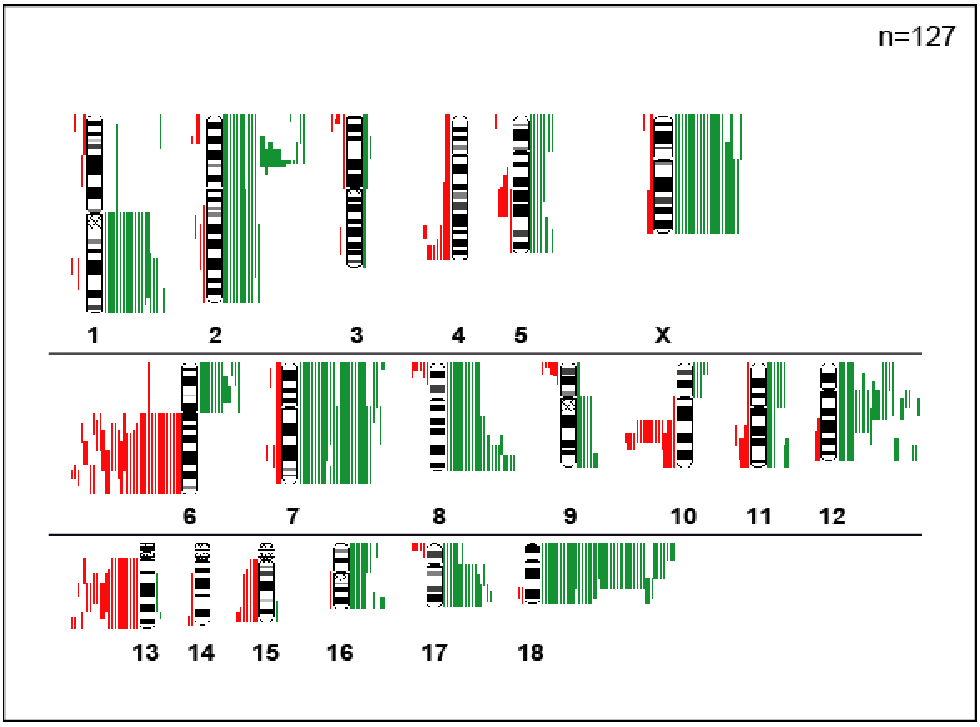

Figure 9A: Comparative genomic hybridization (CGH) in follicular lymphom (FL). Chromosomal gains and losses in 127 FL showing altered karyotypes by CGH. Gains are displayed in green bars and losses are displayed in red bars.

6.2.2 Correlation of Genetic Alterations with Gene Expression

For the analysis of association between distinct chromosomal alterations revealed by CGH and gene expression[25] 195 chromosomal regions were selected that were altered in at least five cases (**S_Table1**). A t-test approach revealed a total of 2465 probesets that were significantly associated with alterations of a distinct chromosomal region having a local FDR of smaller than 0.01. With few exceptions, chromosomal gains were associated with increased expression and chromosomal losses were associated with decreased expression. The significant probesets revealed by our t-test approach could be subjected to the 195 altered chromosomal bands whereas a significant excess of associations was observed for only 41 of these chromosomal bands according to a Poisson model (**S_Table2**). Annotation of the significant genes by the gene families "oncogenes", "tumor suppressor genes", "transcription factors", "translocated genes", "cytokines" and "kinases" using the Broad Institute annotation platform revealed, amongst many others, genes such as the transcription factors *BCL11A* and *REL* whose expression correlated with gains/amplifications of 2p16 (**Fig.9B, S_Table3A and B, S_Fig.1A-M**). Furthermore, increased expression of the kinases *CDK4* and *TBK1* that are both assigned to the chromosomal band 12q14 was associated with chromosomal gains in this region. In 18q21, the transcription factors *MBD1*, *MBD2*, *SMAD2*, *SMAD4* and *TCF4* and the anti-apoptotic oncogene *BCL2* showed increased expression in FL cases with a genomic gain in this region. Conversely, reduced expression of the transcription factors *FOXO3A* and *PLAGL1* and the kinases *MAP3K7*and *CDC2L6* as well as a reduced expression of the tumor suppressor gene *PTEN* correlated with losses in 6q and 10q23, respectively (**Fig.9B, S_Table2B, S_Fig.1A-M**). Comparable results were obtained by our

GSEA approach thus validating these findings (data not shown). Next, we analyzed whether any of the minimal chromosomal regions (MCRs) was associated with the expression level of the prognostically relevant bystander signatures IR1 and IR2.[25] Each MCR was found to be uniformly associated with a lower expression of the IR1 signature with almost half of the MCRs having a p-value of less than 0.05 for this quantity, whereas no MCR was found to be significantly correlated with the IR2 signature.

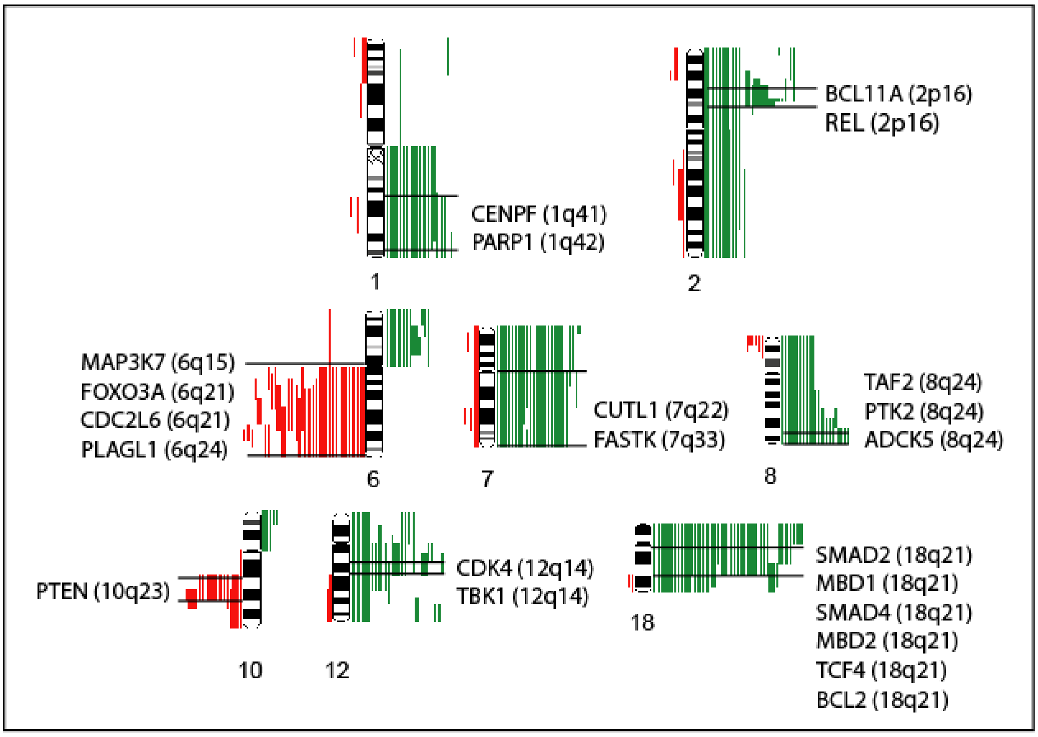

Figure 9B: Selected genes that show upregulation in FL with gains in the chromosomal regions 1q, 2p, 7q, 8q, 12q and 18q or downregulation in FL with losses in the chromosomal regions 6q and 10q.

6.3 ***Characterization of t(14;18)-Negative FL***

6.3.1 Study Cohorts

PCR analysis to detect BCL2 rearrangements was performed in all 184 FL cases and revealed clonal bands in 90 cases. Of the remaining 94 FL, 74 had FFPE tissue available that were subjected to FISH analysis, resulting in 57 samples with t(14;18) and 17 samples without detectable t(14;18). Thus, information on the t(14;18) status was available in 164 FL (147 FL with and 17 FL without t(14;18)). All 17 t(14;18)-negative cases and 17 randomly selected t(14;18)-positive cases were investigated by Genescan analysis, and the SHM status was evaluated in a subset of cases. SNP array analysis could be performed in 11 FL without t(14;18). The study set with both CGH data and information on the t(14;18) status comprised 102 FL with and ten cases without t(14;18).

The validation set for IHC experiments consisted of 84 additional, preselected FL (42 FL with and 42 FL without t(14;18)).

6.3.2 Definition of the Subgroups Based on BCL2-Breakpoint and BCL2-Protein Status

As detailed above, of 164 FL with available information 147 cases presented with the translocation t(14;18), whereas it was lacking in 17 cases. Performing BCL2 staining by IHC, the t(14;18)-negative cases were furthermore divided into six cases with and eleven cases without BCL2 expression (**Fig.10B**). The incidence of t(14;18) was almost equal among cases which were assigned to different grades (1-3A) with FL grade 1 and 2 showing t(14;18) in 90% of cases and FL grade 3A showing t(14;18) in 86% of cases.

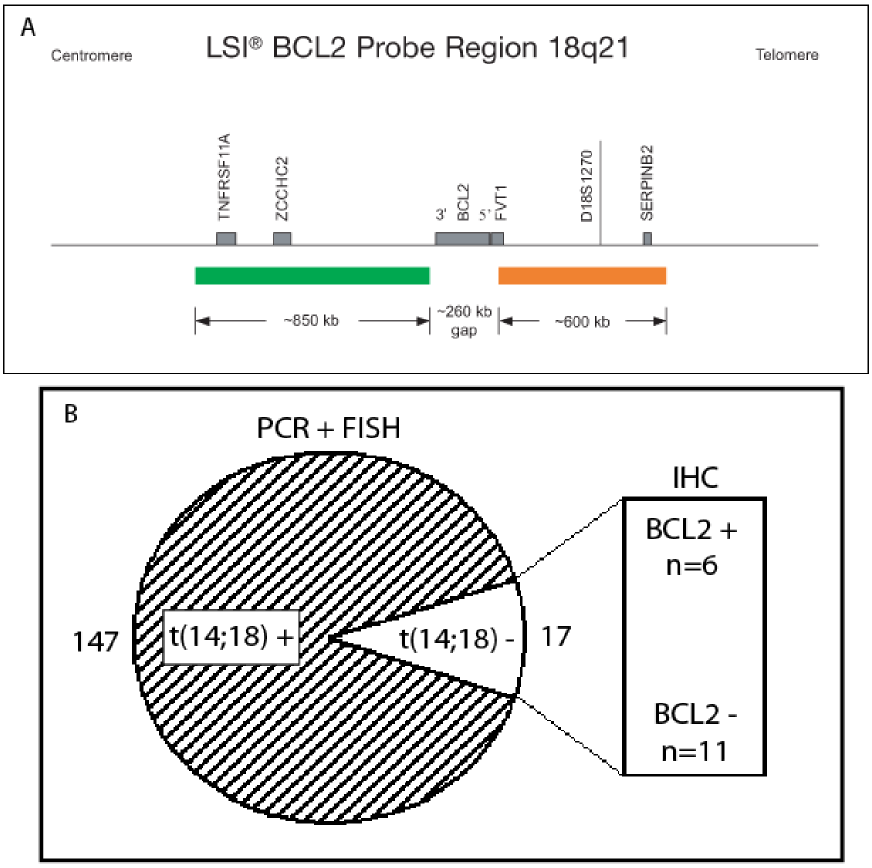

Figure 10A,B: Definition of FL subgroups with and without translocation t(14;18). (**A**) Schematic presentation of the BCL2 breakapart probe from Vysis. (**B**) 147 FL showed evidence of the t(14;18) by PCR or FISH techniques, whereas 17 FL were t(14;18)-negative. By IHC the t(14;18)-negative subgroup could be furthermore divided in six cases with and eleven cases without BCL2 expression.

6.3.3 Clonality Analysis

Genescan analysis revealed clonality in all 17 t(14;18)-negative and a comparable control group of 17 t(14;18)-positive cases using the primer combinations V_H-FR1+J_H-FAM, V_H-FR2-LJ_H-HEX/VLJ_H-FAM, V_H-FR3+LJ_H-FAM, V_K+J_K-FAM and V_K+Kde-FAM (Table 2). A clonal rearrangement of the V_H chain was detected in 94% of cases with t(14;18) but only in 65% of t(14;18)-negative cases (p=0.085). However, all remaining cases were affected by a clonal rearrangement of the V_κ

chain (**Table 2, Fig.11**). Using the primer combination V_H-FR2-LJ_H/VLJ_H all of the five tested monoclonal t(14;18)-negative FL and all of the three tested monoclonal t(14;18)-positive FL cases showed somatically mutated *IgV_H* genes without statistical difference in mutational rate between the two groups and all cases had evidence of ongoing SHM by subcloning and sequencing.

Table 2: Genescan analysis of 17 t(14;18)-positive and 17 t(14;18)-negative FL cases.

Clonality IGH_IGK	***t(14;18) +***		***t(14;18) -***		***t(14;18) -+***		***t(14;18) --***	
	No.	**%**	**No.**	**%**	**No.**	**%**	**No.**	**%**
IGH (FR1/FR2/FR3)								
monoclonal/biclonal	16/17	**94**	11/17	**65**	5/6	**83**	6/11	**54.5**
polyclonal	1/17	**6**	6/17	**35**	1/6	**17**	5/11	**45**
IGK								
monoclonal/biclonal	1/1	**100**	6/6	**100**	1/1	**100**	5/5	**100**
polyclonal	0/1	**0**	0/6	**0**	0/1	**0**	0/5	**0**

IGH=Immunoglobulin heavy chain, IGK=Immunoglobulin kappa chain, FR1A=Framework region 1, FR2=Framework region 2, FR3=Framework region 3, No= Number of cases, t(14;18) += t(14;18)-positive, t(14;18) -= t(14;18)-negative, t(14;18) - +=t(14;18)-negative but BCL2 positive, t(14;18) - -= t(14;18)-negative and BCL2-negative.

A

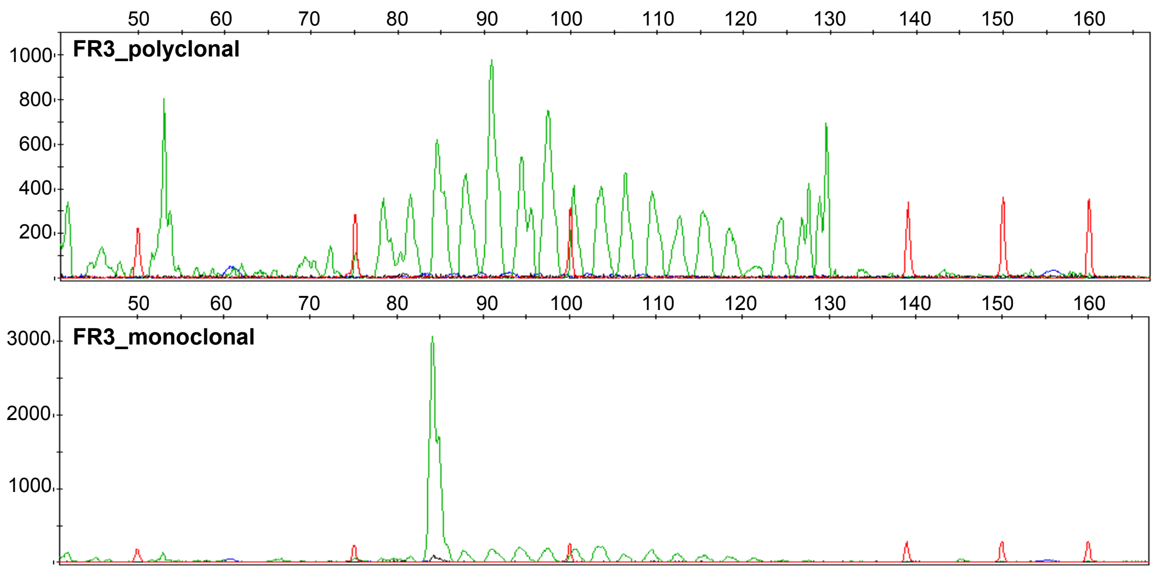

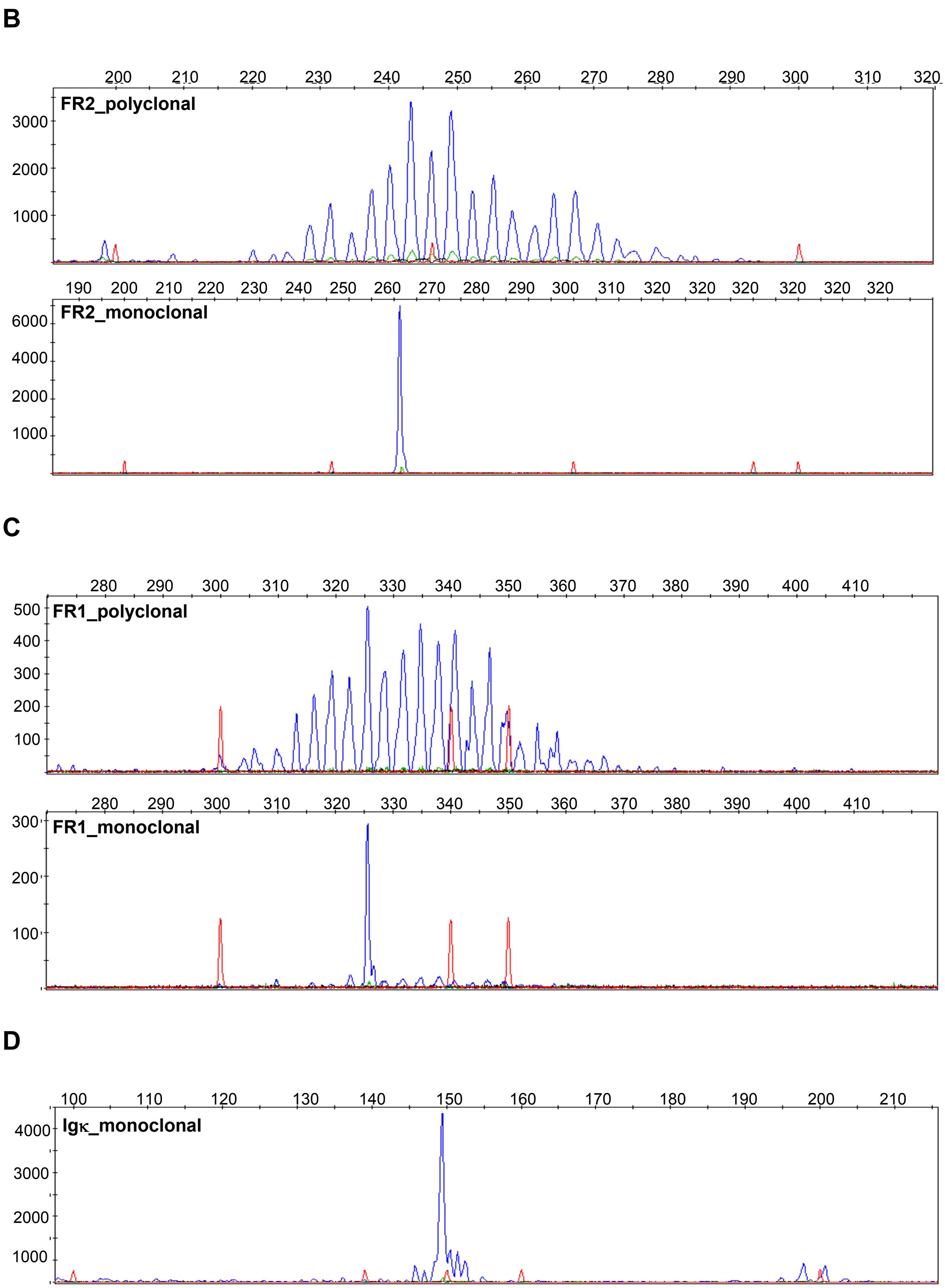

Figure 11: Genescan analysis. Polyclonal and monoclonal rearrangements were detected using the primer combinations (A) FR3-LJ$_H$ (B) FR2-LJ$_H$/VLJ$_H$, (C) FR1-J$_H$ and (D) Igκ-Jκ for the detection of *IgV$_H$* (A-C) and *IgVκ* (D) rearrangements.

6.3.4 FL Cases with and without Translocation t(14;18) Differ in Gains/Amplifications of the Chromosomal Region 18q11-q21

By CGH, various genetic alterations were observed which appeared in different frequencies among 102 t(14;18)-positive and ten t(14;18)-negative FL cases such as gains in chromosome 7 (19.5% versus 0%), 8q (16% versus 0%) and X (13.5% versus 0%) as well as deletions in 13q (14% versus 0%) and 10q (12.5% versus 0%) (**Fig.12 A, B**). A gain/amplification in 18q (18q11-q21) that was present in 32% of t(14;18)-positive but in none of the t(14;18)-negative cases was found to be the only significant alteration distinguishing FL cases with and without t(14;18) (p=0.032). We did not observe a gain of chromosomal material at this region by neither CGH nor by FISH analysis in any of the t(14;18)-negative FL cases, irrespective of their BCL2 expression status (**Fig.13**).

By CGH a higher percentage of t(14;18)-positive FL cases showed genetic alterations compared to cases without t(14;18), although this difference did not reach statistical significance (70% versus 47%, p=0.1). No genetic alterations were found which were solely restricted to t(14;18)-negative FL cases. With respect to previous findings[38-40,44] we furthermore investigated the frequency of 3q27/*BCL6* rearrangements in 15 t(14;18)-negative and 39 t(14;18)-positive cases by FISH using a BCL6 breakapart probe. The frequency did not differ significantly between the two phenotypes (18% versus 27%, p=0.475, data not shown).

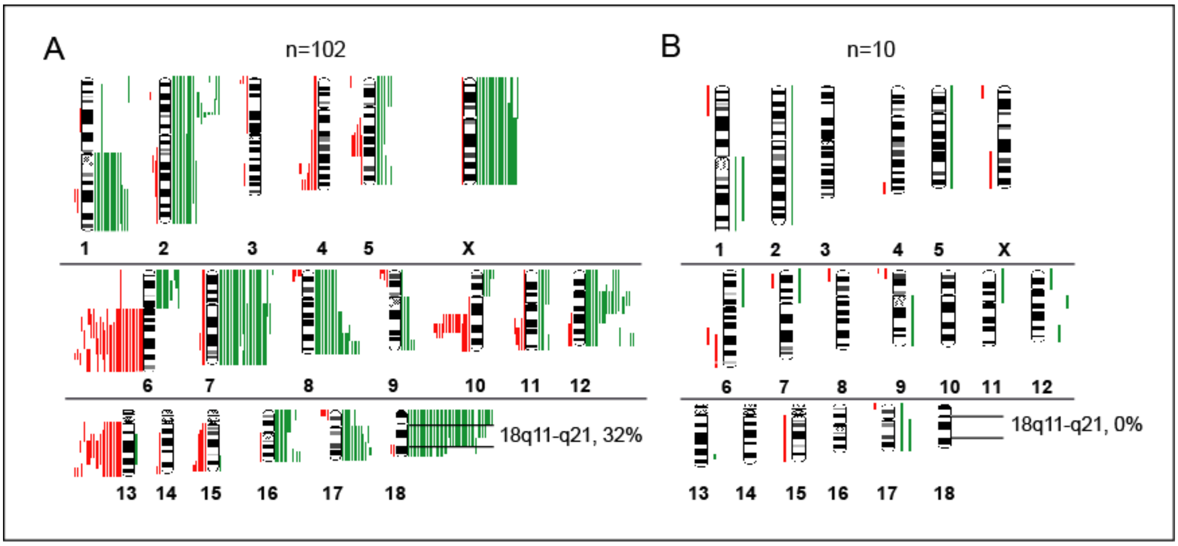

Figure 12A,B: Chromosomal gains and losses in FL with and without translocation t(14;18) detected by CGH. (A) Gains (green bars) and losses (red bars). n=number of cases

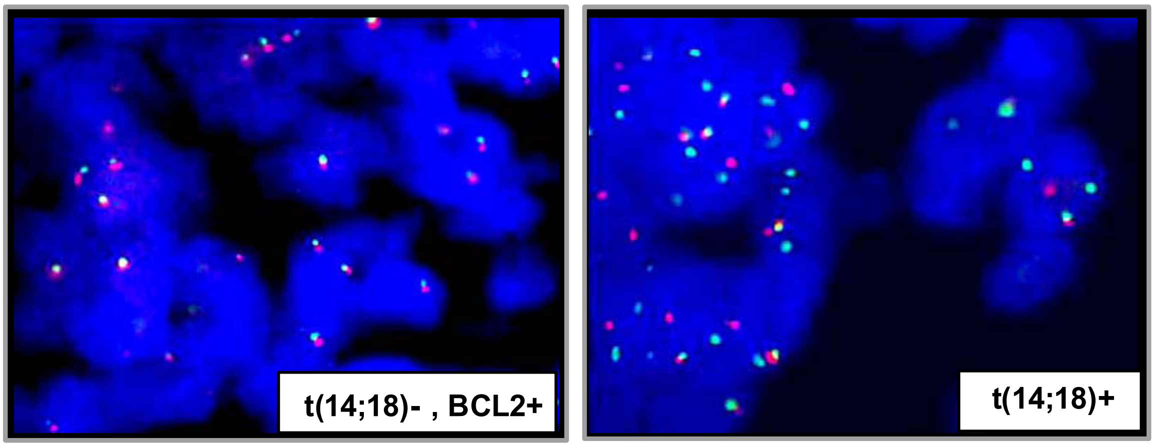

Figure 13: Representatitve FISH results of a FL case with t(14;18) and a BCL2 expressing FL case without t(14;18). Separated red and green signals indicate a breakpoint in the chromosomal region 18q21.3, whereas fused signals indicate a t(14;18)-negative situation.

6.3.5 *Genetic Assessment of FL Cases without t(14;18) Using High Density SNP Arrays*

To define genetic alterations of the t(14;18)-negative FL cases at higher resolution we studied eleven cases (three with and eight without BCL2 expression) using 250K (NSP) SNP arrays. This approach confirmed the results revealed by CGH with some minor exceptions (**Fig.12 A, B** and **Fig.14**). In addition a couple of further alterations such as frequent gains of 2p and gains in 3q as well as sporadic amplifications in 2p16.1, 8q, 12q and 17q were revealed by our SNP approach (**Fig.14**). Four of the t(14;18)-negative FL showed small gains/amplifications in the chromosomal region 2p16.1 including the *BCL11A* and *REL* locus which was not evident by conventional CGH analysis. Gains/amplifications in 18q11-q21 that affected 32% of t(14;18)-positive but none of the t(14;18)-negative cases by CGH was observed in only one FL case without t(14;18) by SNP array analysis. This gain did not include the *BCL2* locus and the case showed no evident BCL2 expression by IHC. Finally, we did not observe frequent alterations specific for cases without t(14;18) by this high resolution approach.

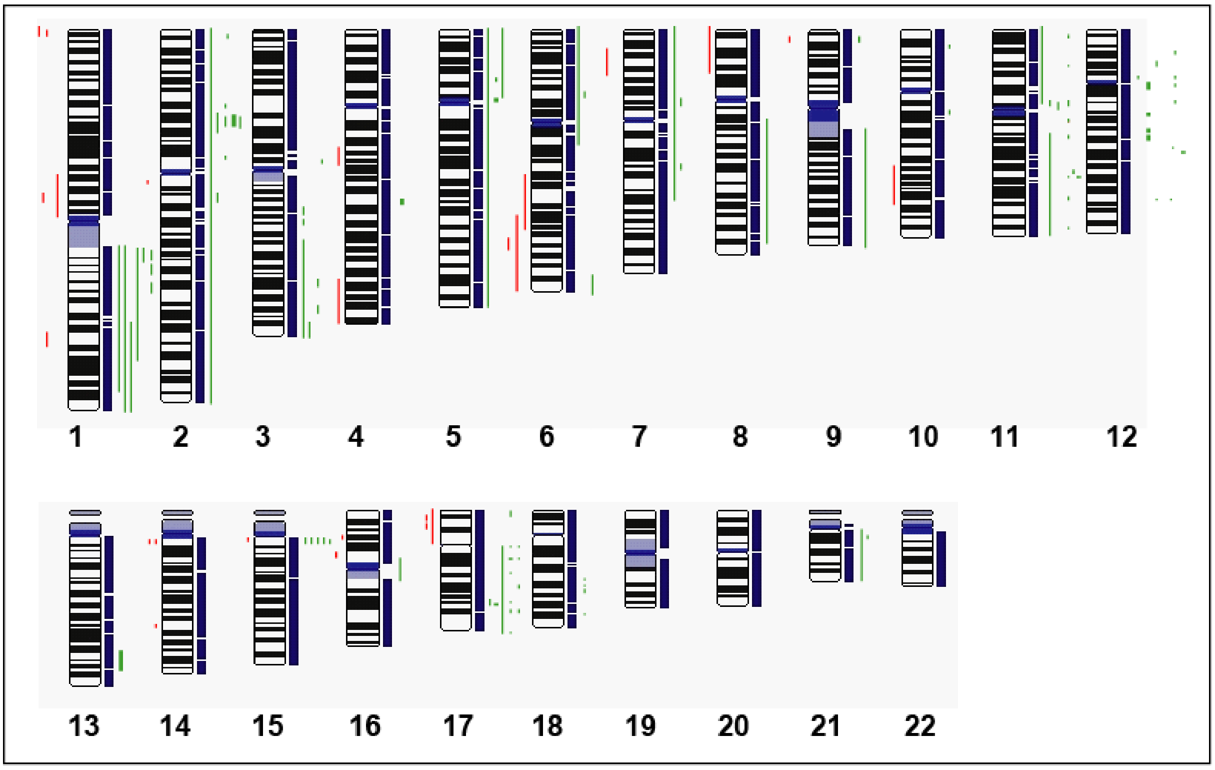

Figure 14: High density SNP array profiling in t(14;18)-negative FL. Schematic presentation of copy number gains/amplifications (green bars) and losses (red bars) in eleven t(14;18)-negative FL determined by high resolution 250K SNP array analysis.

6.3.6 FL Cases with and without Translocation t(14;18) Differ in Gene Expression Profiles

A two-sided t-test showed that the global gene expression is highly different between FL cases with and without t(14;18). 1562 probesets of the HG U133 plus 2.0 gene expression array were differentially expressed between the two study groups ($p \leq 0.001$). The oncogene *BCL2* was the most differentially expressed gene between the two groups ($p<0.0001$, data not shown), with a higher expression in t(14;18)-positive cases.

Subsequent GSEA analysis with lymphoma associated gene expression signatures[63] revealed major differences between t(14;18)-positive and t(14;18)-negative FL cases. In particular, an enrichment of GCB-cell-signatures was observed in the group of t(14;18)-positive cases (n=147) whereas an enrichment of ABC-, NFKB-, post-GCB-, T-cell, cell cycle-, proliferation- and interferon-signatures was observed in the group of t(14;18)-negative cases (n=17) (**Table 3**). Importantly, the IR1 signature that had been previously shown to be associated with improved survival times in FL was significantly enriched among t(14;18)-negative FL, whereas the IR2 signature was not significantly enriched in one of the two subgroups.

Table 3: Gene set enrichment analysis (GSEA) with 81 lymphoma associated signatures[63] in 147 t(14;18)-positive and 17 t(14;18)-negative FL cases.

Signatures	*Enriched in t(14;18)+*	*Enriched in t(14;18)-*	*p-value*	*FDR q-value*
GCB *Rosenwald et al., 2002*[67] *Dave et al., 2006*[68]	YES	NO	0.01	<0.1
ABC *Wright et al., 2003*[69]	NO	YES	0.02	<0.1
NFKB *Lam et al., 2005*[70]	NO	YES	≤0.02	≤0.1
POST-GCB *Shaffer et al. 2002*[71] *Weller et al., 2004*[72] *Wright et al., 2003*[69]	NO	YES	0.02	<0.1
IR1 *Dave et al., 2004*[25]	NO	YES	0.03	<0.1
T-CELL *McHugh et al., 2002*[73] *Kovanen et al., 2003*[74]	NO	YES	<0.01	0.14
CELL-CYCLE *Shaffer et al., 2001*[75]	NO	YES	<0.01	0.2
PROLIFERATION *Su et al., 2004*[76] *Rosenwald et al., 2003*[77]	NO	YES	≤0.02	≤0.1
Interferon *Baechler et al., 2003*[78]	NO	YES	<0.01	<0.1

FDR=False discovery rate, GCB=Germinal center B-cell, ABC= Activated B-cell, IR1=Immuneresponse 1, t(14;18)+=t(14;18)-positive, t(14;18)-=t(14;18)-negative

In agreement with these findings, an enrichment of genesets corresponding to a PAX5-regulatory motif was observed by GSEA analysis in t(14;18)-positive cases whereas an enrichment of the regulatory motif genesets MYC/MAX and NFKB was observed in t(14;18)-negative FL cases (**Table 4**). Notably, very similar results were obtained when FL cases grade 3A were excluded from the analysis.

In a further comparison between FL cases with t(14;18) (n=147) and those without t(14;18) but evident BCL2 expression (n=6), we also revealed an enrichment of GCB-signatures in t(14;18)-positive cases and an enrichment of ABC-, NFKB-, marginal-zone B-cell- and cell-cycle/proliferation signatures in t(14;18)-negative FL cases (data not shown).

Table 4: Gene set enrichment analysis (GSEA) with regulatory-motif sets (C3) in 147 t(14;18)-positive and 17 t(14;18)-negative FL cases.

Regulatory Motifs	***Function upon TF binding***	***Enriched in t(14;18) +***	***Enriched in t(14;18) -***
PAX5	Inhibits plasma cell differentiation	yes	no
E2F/1/4	Cell cycle control	no	yes
MYC and/or MAX	Cell cycle regulation, proliferation, growth, differentiation and metabolism	no	yes
NFKB/65	Regulators of the immune, inflammatory, stress, proliferative and apoptotic responses of a cell to a very large number of different stimuli	no	yes
USF/2	Key regulatory elements of the transcriptional machinery	no	yes
AML1	Critical regulator of hematopoietic development	no	yes
SRF	Cellular migration and normal actin cytoskeleton and contractile biology.	no	yes
PEA3	Key role in metastasis, regulates transcription of matrix metalloproteinases (MMP)	no	yes

TF=Transcription factor, t(14;18)+=t(14;18)-positive, t(14;18)-=t(14;18)-negative

6.3.7 *Differences in Clinical Parameters Between FL Cases with and without t(14;18)*

The clinical variables age, Eastern Cooperative Oncology Group (ECOG) performance status, gender, tumor grade, stage, extranodal sites, B symptoms and lactate dehydrogenase (LDH) levels of FL with and without t(14;18) are provided in **Table 5**. Patients with t(14;18)-negative FL presented more frequently with lower stage of disease (62% versus 27% in t(14;18)-positive FL; *P*=0.008), whereas no differences were observed between the two groups regarding the other clinical variables and overall survival (**Table 5, Figure 15**).

Table 5: Differences in clinical parameters between t(14;18)-positive and t(14;18)-negative FL cases.

Clinical Variable		t(14;18) +		t(14;18) -		P-Value
		No.	%	No.	%	
AGE	≤60	97/146	66.4	10/16	62.5	n.s.
	>60	49/146	33.6	6/16	37.5	
ECOG	<2	106/123	86.2	14/14	100	n.s.
	≥2	17/123	13.8	0/14	0	
GENDER	MALE	76/146	52	7/16	44	n.s.
	FEMALE	70/146	48	8/16	56	
TUMOR GRADE	1 or 2	123/147	83.7	13/17	76.5	n.s.
	3	24/147	16.3	4/17	23.5	
STAGE	I or II	38/141	27	10/16	62.5	0.008
	III or IV	103/141	73	6/16	37.5	
EXTRANODAL SITES	<2	119/139	85.6	15/15	100	n.s.
	≥2	20/139	14.4	0/15	0	
B-SYMPTOMS	ABSENT	116/146	79.5	15/16	93.75	n.s.
	PRESENT	30/146	20.5	1/16	6.25	
LDH	NORMAL	71/133	53.4	9/15	60	n.s.
	> NORMAL	62/133	46.6	6/15	40	

ECOG=Eastern Cooperative Oncology Group performance status, LDH=Lactate dehydrogenase, n.s.=not significant, t(14;18)+=t(14;18)-positive, t(14;18)-=t(14;18)-negative

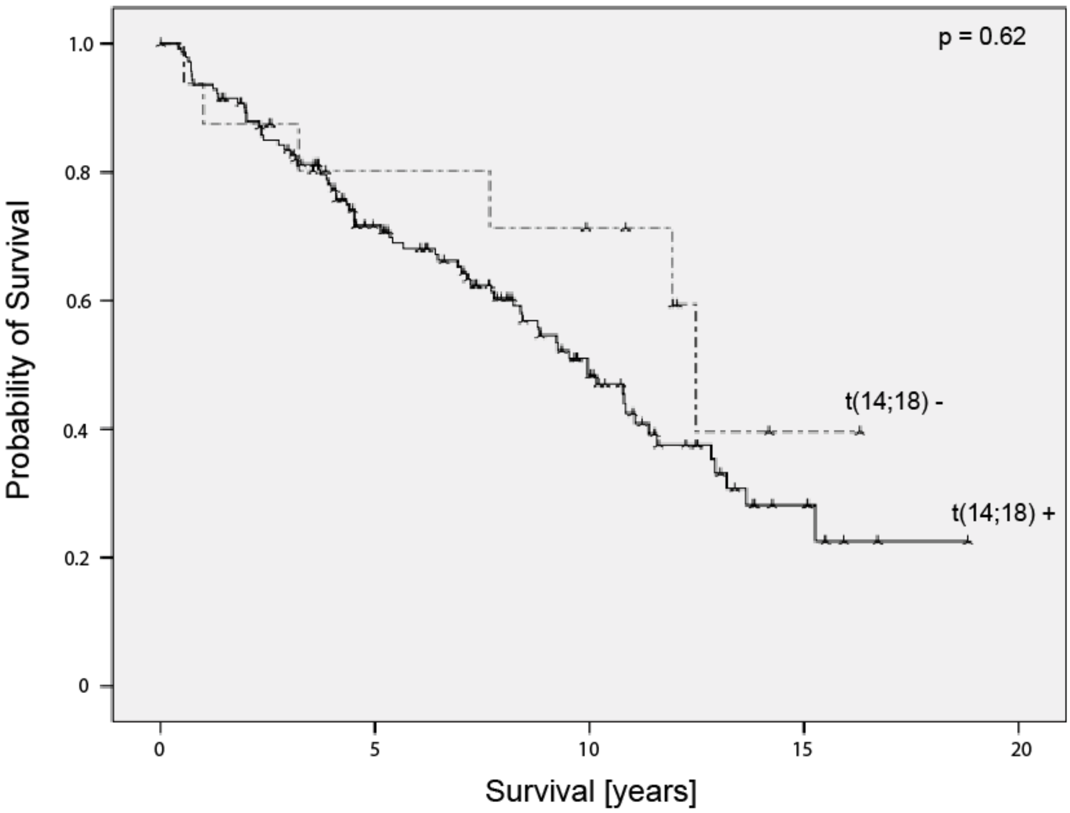

Figure 15: Overall survival of FL patients with and without t(14;18). Kaplan Meier survival plot for FL patients with and without t(14;18). Survival differences were not statistically significant (*p*=0.62) (log rank test).

6.3.8 Validation of Gene Expression Data by IHC Analysis on FL Cases of an Independent Test Set

To validate the results from the comparison of gene expression profiles between FL cases with and without t(14;18) by GSEA, IHC was performed on 42 selected t(14;18)-positive and 42 selected t(14;18)-negative low grade FL cases of an independent test set using antibodies against the proliferation marker Ki67/MIB1, the post-germinal center marker and NFKB target IRF4/MUM1, the GC markers CD10/MME, BCL6 and IRF8, the cytotoxic T-cell marker GZMB, the T-regulatory cell marker FOXP3 and the follicular T-cell marker CD57.

Table 6: Immunohistochemical results in a validation set of 84 FL including 42 t(14;18)-positive and 42 t(14;18)-negative FL

ANTIBODIES (IHC)		t(14;18)+		t(14;18)-		P-Value
		No.	%	No.	%	
CD10	positive	42/42	100	26/38	68.4	<0.01
	negative	0/42	0	12/38	31.6	
BCL6	positive	40/40	100	38/38	100	-
IRF4/MUM1	>10%	0/0	0	4/35	11.4	0.039
	≤10%	42/42	100	31/35	88.6	
IRF8	positive	36/39	92.3	37/38	97.4	n.s.
	negative	3/39	7.7	1/38	2.6	
Ki67	>25%	24/41	58.5	30/33	90.9	<0.01
	≤25%	17/41	41.5	3/33	9.1	
GZMB	>3%	7/36	19.4	19/35	54.3	<0.01
	≤3%	29/36	80.6	16/35	45.7	
FOXP3	>5%	21/40	52.5	25/36	69.4	n.s.
	≤5%	19/40	47.5	11/36	30.55	
CD57	>15%	7/40	17.5	2/37	5.4	n.s.
	≤15%	33/40	82.5	35/37	94.6	

n.s.=not significant, t(14;18)+=t(14;18)-positive, t(14;18)-=t(14;18)-negative, IHC=Immunohistochemistry, No=number of cases

Statistically significant differences were observed for the markers CD10, IRF4, Ki67 and GZMB (**Table 6**). While a strong CD10 expression could be detected in 100% of t(14;18)-positive cases it was lacking or only very weakly expressed in approximately 30% of cases without t(14;18). A low or absent CD10 expression was restricted to t(14;18)-negative cases which showed no BCL2 expression whereas all t(14;18)-negative cases with BCL2 expression were strongly positive. By contrast, IRF4, Ki67 and GZMB expression was higher in t(14;18)-negative cases (**Table 6, Fig.16**). No significant differences in expression were detected for BCL6, CD57, IRF8 and FOXP3 between the two FL subgroups (**Table 6**).

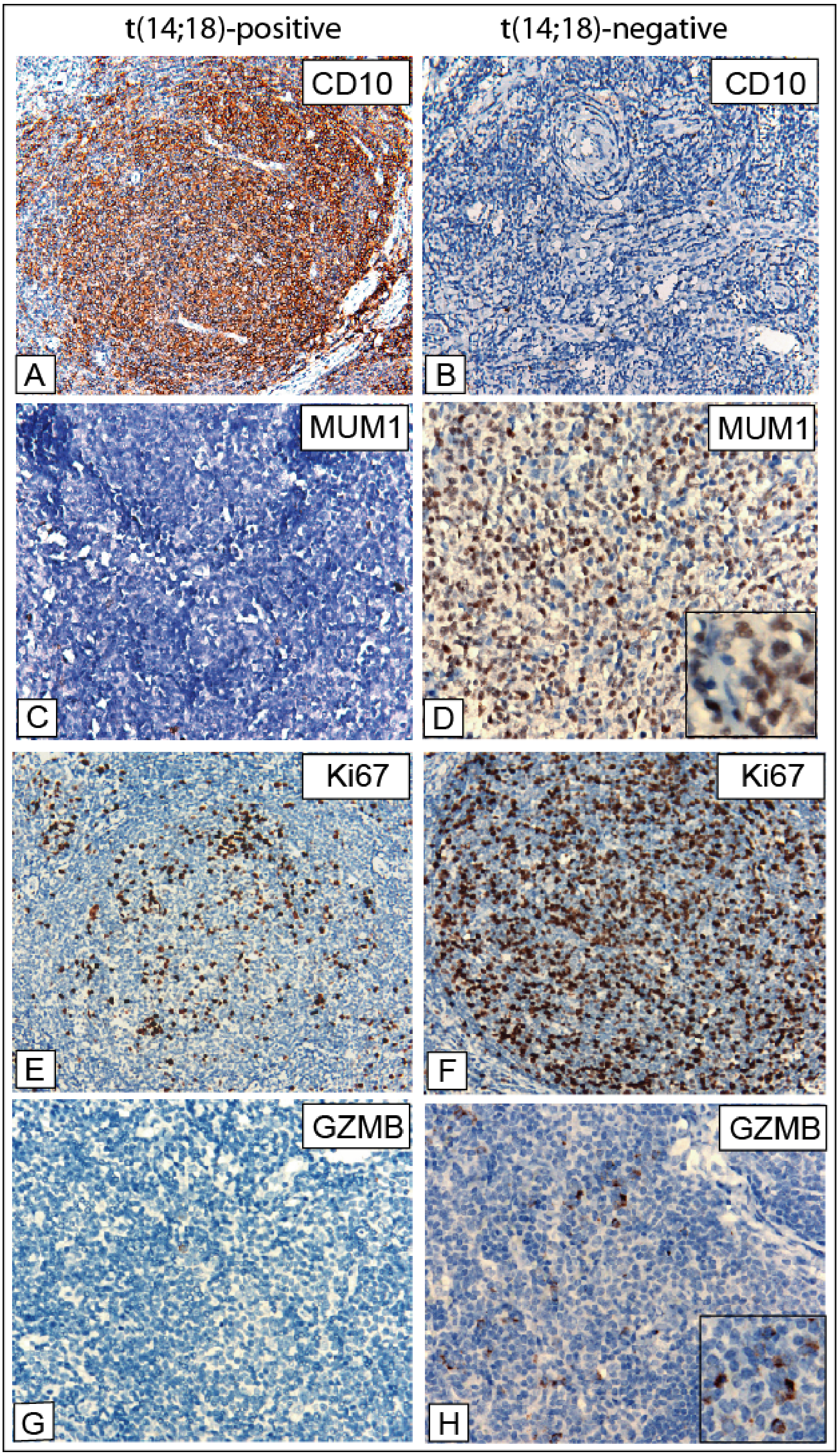

Figure 16: Immunohistochemistry in FL with and without t(14;18). Representative stainings for CD10, IRF4/MUM1, Ki67 and GZMB in t(14;18)-

positive (A, C, E, G) and t(14;18)-negative (B, D, F, H) FL grades 1-2. Images A and B were captured at 200x magnification and images C-H at 400x magnification using an Olympus, Color View, BX50 microscope, the Color View digital camera and the analysis work soft imaging system (all Olympus, Tokyo, Japan).

6.4 ***Characterization of a Specific Morphological Variant of t(14;18)-Negative Diffuse FL***

6.4.1 Immunophenotypic and Clinical Features of FL with an Unusual Predominantly Diffuse Growth Pattern

All 35 FL cases (12 grade 1 and 23 grade 2) of an independent FL study set with an unusual predominantly diffuse growth pattern that were investigated by our group displayed similar clinical and morphological features. Clinically, the tumor presented in the inguinal region in 29/35 cases. In all cases the total area of follicular infiltrates consisting of a mixture of -distinctly prevailing- centrocytes and some intermingled centroblasts was less than 25% (**Fig.17 A-C**). The vast majority of tissue, however, was diffusely infiltrated by the tumor with small centrocyte-like or round cells. In contrast to FL cases most, tumors presented with a low clinical stage (8/20 stage I, 7/20 stage II, 5/20 stage III or IV). Moreover, complete remission was achieved in 15 of 16 patients with available follow-up information.

The infiltrating neoplastic cells showed positivity for CD20 (**Fig.17 D**), the follicles stained positive for CD10 and BCL6 consistent with a GC B-cell phenotype (**Fig.17 G, I**) and BCL2 was expressed in the diffuse areas (**Fig.17 K-L**). BCL2 expression in the neoplastic follicles varied considerably between cases and ranged from entirely negative to moderately strong in most of the GC B-cells. Moreover, CD3+ and CD5+ T-cells were found to be densely intermingled, especially in the diffuse parts (**Fig.17 E**). The diffusely infiltrated areas showed CD10 expression in 30/35 cases with some B-cells in this area showing BCL6 expression (**Fig.17 G, I (Inset)**). Co-expression of CD23 on the neoplastic B-cells, especially the ones in the diffuse areas, was observed in 27/35 cases (**Fig.17 H**) while CD21 expression was solely restricted to the FDCs of the neoplastic follicles (**Fig.17 J**). The proliferation rate as indicated by a Ki67 staining ranged from 15%-45% and was slightly higher in the atypical follicles. However, no zonation phenomenon was observed (**Fig.17 F**).[59]

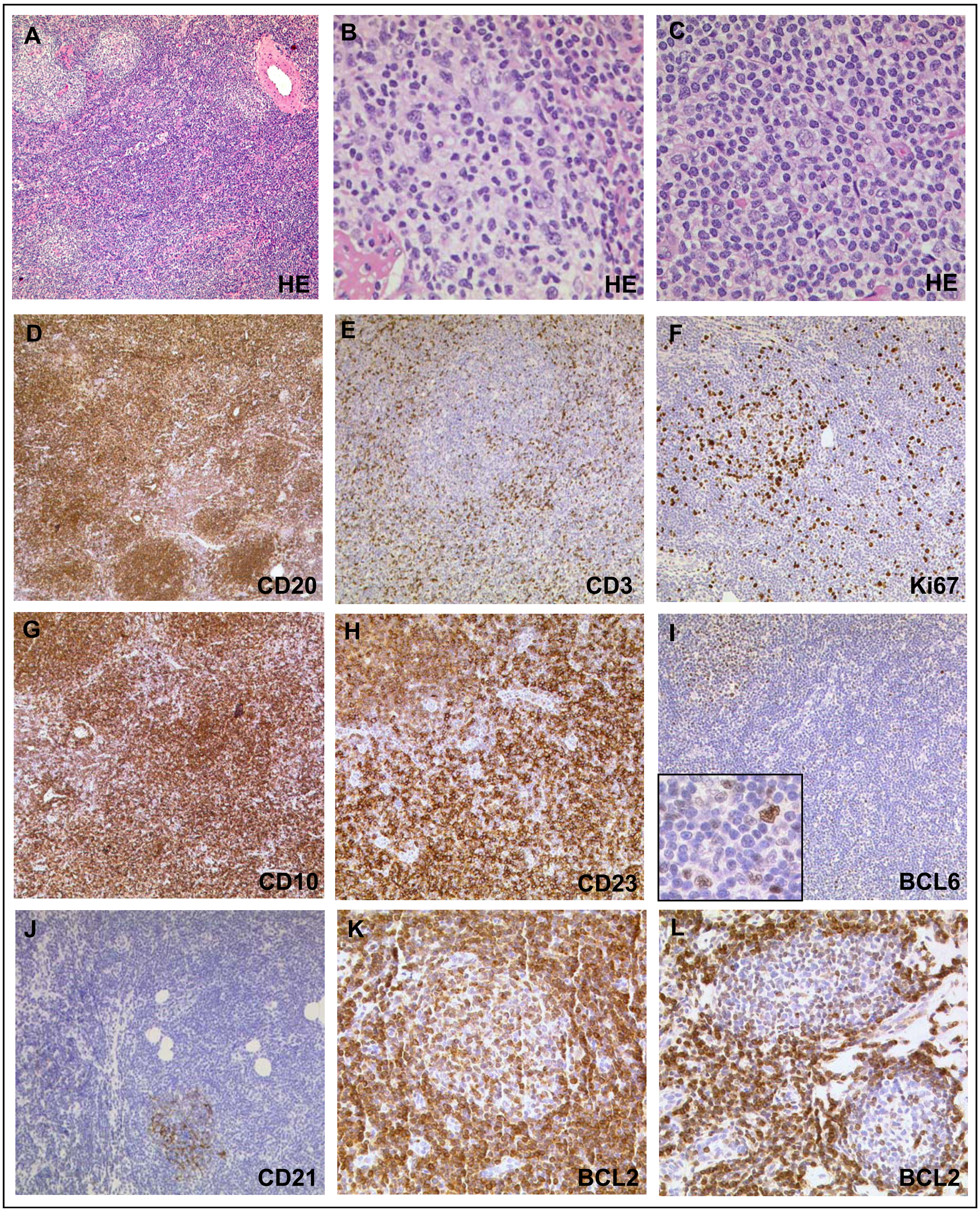

Figure 17: Morphological and immunohistochemical features of predominantly diffuse FL. A diffuse infiltration pattern, with only few intermingled atypical follicles (200x) **(A)**. Neoplastic follicles dominated by centrocytic cells (400x) **(B)**. In the diffuse areas tumor cells present with rounder nuclear contours (400x) **(C)**. Tumor cells express CD20 (200x) **(D)** and reactive T-cells (CD3) are prominent in diffuse areas (200x) **(E)**. The proliferative activity (Ki-67) is centered

more in the atypical follicular structures and less in the diffuse infiltrates (200x) **(F)**. CD10 is expressed in atypical follicles and diffusely infiltrated areas in the majority of cases (200x) **(G)**, as is CD23 (400x) **(H)**. BCL6 expression can be observed in all atypical follicles and in the nuclei of some interspersed B-cells in the diffuse infiltrates (200x) (Inset, 400x) **(I)**. CD21 stain follicular dendritic cells (FDC) in the atypical follicle whereas no CD21 staining is observed in the diffuse infiltrate (200x) **(J)**. BCL2 expression varies between different cases and among different areas of the same case (400x) **(K, L)**. Images were taken using the Olympus, Color View, BX50 microscope, the Color View digital camera and the analysis work soft imaging system (all Olympus, Tokyo, Japan).

6.4.2 Conventional Cytogenetic Characterization of FL with an Unusual Predominantly Diffuse Growth Pattern

Neither karyotyping nor FISH analysis using a BCL2/IgH dual colour dual fusion probe revealed the presence of the translocation t(14;18) in 28/29 (97%) successfully hybridized diffuse FL. Vice versa, the translocation t(14;18) was absent in only one of six typical FL cases (**Fig.18**). However, no signal distribution was observed that would indicate an amplification of the *BCL2* locus in diffuse FL cases without t(14;18).

In contrast, a deletion in 1p was observed in 27/29 cases using the locus specific FISH probe for 1p36.3, whereas the chromosomal band 1p22 was conserved in all cases with 1p36.3 deletion (**Fig.18**). Furthermore, using a locus specific probe for 1q32 and a centromeric probe for chromosome 1, all but one case showed a disomic signal constellation.[59]

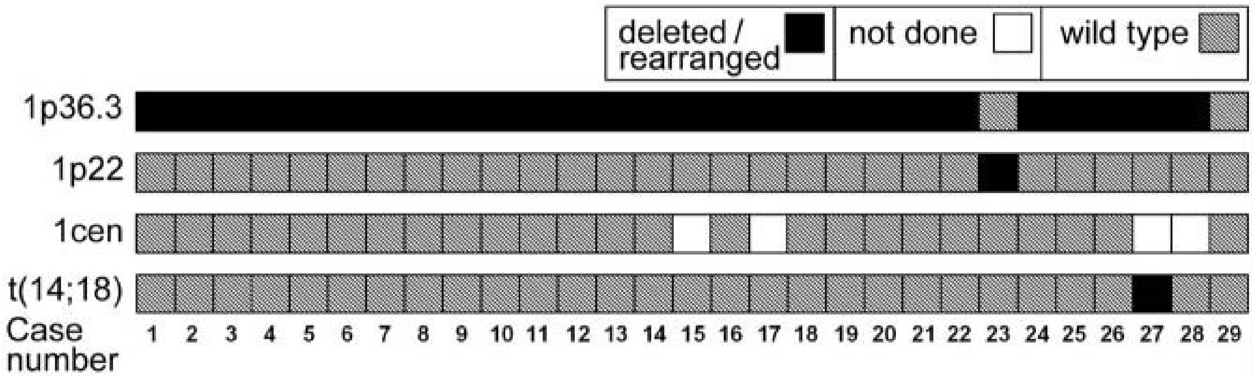

Figure 18: Fluorescence in situ hybridization (FISH) in 29 FL with predominantly diffuse growth pattern. FISH results are provided for the chromosomal regions 1p36.3, 1p22, the centromeric region of chromosome 1 and for the translocation t(14;18) status.

6.4.3 Gene Expression Profiling of Predominantly Diffuse FL

A cluster analysis approach including the gene expression profiles of four predominantly diffuse FL cases and 150 typical FL cases[25] showed that FL with a predominantly diffuse growth pattern fit in the FL cluster, but nevertheless represent a distinct subgroup (**Fig.19**). A two sided t-test revealed 3000 probe sets of the HG U133 A gene expression array with a significant difference in expression between the two FL groups (p-value < 0.0001). In a GSEA approach with lymphoma associated gene expression signatures[63], we found a significant enrichment of GCB cell-, proliferation-, cell cycle- and B-cell signatures in the FL cases, whereas we found an enrichment of several T-cell-, NK-cell- and two DC subset signatures (BDCA1-positive DC derived from blood and CD123-positive DC derived from tonsils) in predominantly diffuse FL cases (**Table 7**).[59]

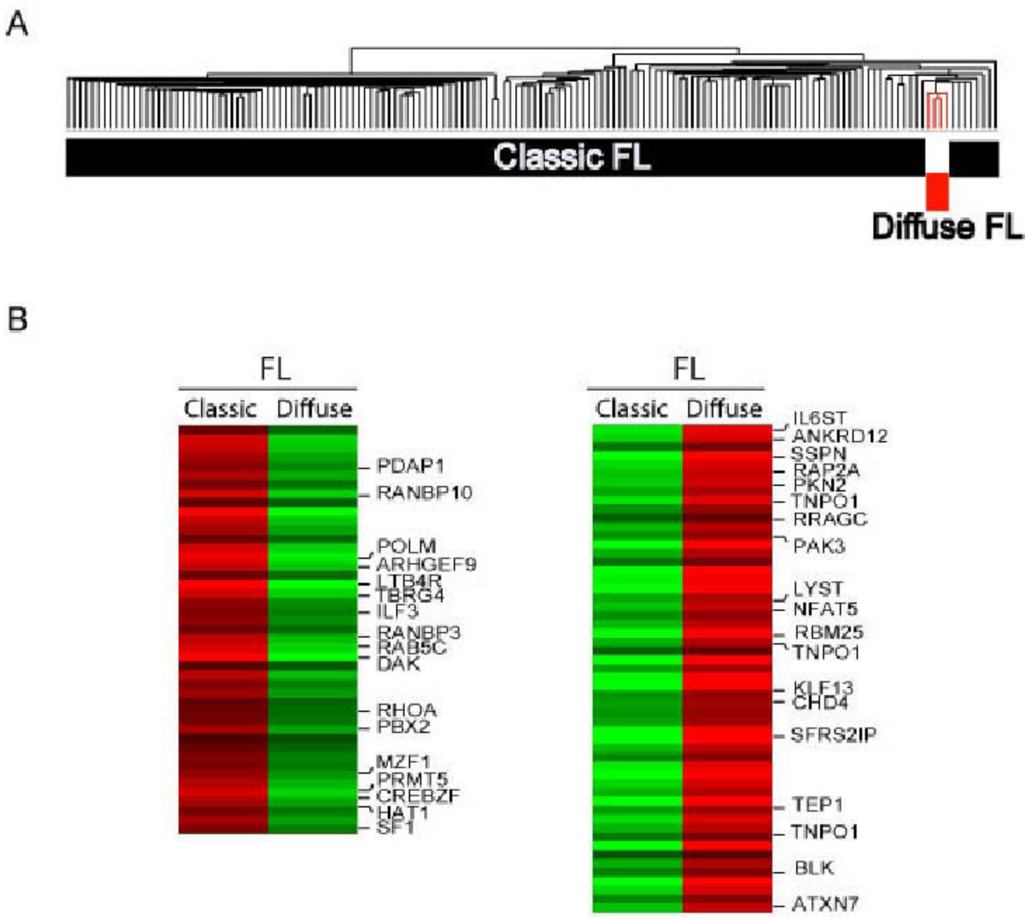

Figure 19: Gene expression profiling of predominantly diffuse follicular lymphoma cases. (A) Hierarchical clustering shows that the gene expression profile of diffuse FL cases fall into the spectrum of FL, but is nevertheless characterised by a distinct gene expression signature. **(B)** Top 100 probe sets that are differentially expressed between FL and diffuse FL (according to the results of a t-test between the groups).

Table 7: Gene set enrichment analysis (GSEA) with 81 lymphoma associated signatures[63] in 150 'Classic' and four predominantely diffuse FL cases.

SIGNATURES	*ENRICHED IN ‚Classic' FL*	*ENRICHED IN ‚Diffuse' FL*	*P-VALUE*	*FDRQ*
GCB *Rosenwald A et al., 2002*[67]	**YES**	**NO**	**<0.01**	**≤0.1**
Proliferation *Su AI et al., 2004*[76] *Rosenwald A. et al., 2002*[67]	**YES**	**NO**	**<0.01**	**<0.05**
Cell Cycle *Liu D et al., 2004*[79] *Whitfield ML et al., 2002*[80] *Cho RJ et al., 2001*[81]	**YES**	**NO**	**<0.01**	**<0.05**
B-Cell *Basso K et al., 2004*[82] *Su AI et al., 2004*[76] *Shaffer AL et al., 2002*[71]	**YES**	**NO**	**<0.05**	**<0.1**
T/NK-CELL *Kovanen PE et al., 2003*[74] *Su AI et al., 2004*[76]	**NO**	**YES**	**<0.05**	**<0.2**
Dendritic Cell *Lindstedt M et al., 2005*[83]	**NO**	**YES**	**<0.05**	**<0.25**
IR1 *Dave SS et al., 2004*[25]	**NO**	**YES**	**<0.01**	**0.1**

FDR=False discovery rate, GCB=Germinal center B-cell, ABC= Activated B-cell, IR1=Immuneresponse 1

7 Discussion

Non Hodgkin lymphoma (NHL) is a neoplasm derived from lymphocytes and involves most frequently lymph nodes, spleen, and other organs of the immune system. Approximately 90% of NHLs are B-cell lymphomas whereas the occurrence of T-cell and NK-cell lymphomas as well as immunodeficiency-associated lymphoproliferative disorders is very low. Compared to other neoplasias such as carcinomas lymphomas occur rarely, however, the incidence has been rising over the last 40-50 years. Many patients with aggressive NHL can be cured whereas indolent forms are not currently curable. Several treatment regimens reaching from multi agent chemotherapy to more specific biologic, targeted therapies are currently available. However, not all patients can be properly diagnosed and not all respond to the current treatment regimens.

7.1 Mature T-cell Lymphomas are Only Rarely Affected by Breakpoints in the TCR Gene Loci

Mature T-cell lymphoma is a very rare disease and only little information exists on the molecular events that contribute to the pathogenesis of these tumors.[2] Whereas chromosomal translocations involving the *TCR*α/δ, *TCR*β and *TCR*γ loci were initially thought to be absent in mature T-NHL other than T-PLL which are affected by the inversion inv(14)(q11q32) in approximately 80% of cases, recent data suggest that occasional cases of PTCL (NOS) and AILT do carry breakpoints in one of the *TCR* loci.[9] To evaluate the exact frequency of breakpoints in the *TCR* loci of mature T-cell NHL we developed an improved FISH assay for the detection of breakpoints within the *TCR* loci of 227 paraffin embedded mature T-cell lymphoma specimens, arranged in a TMA format. While previous studies were performed on cytogenetic suspensions in smaller series of cases,[9,10] our FISH assay is applicable to FFPE tissue and allows for an unbiased selection of a large number of cases.[1] Only two of the mature T-cell lymphoma cases, namely one Lennert lymphoma and one AITL, harbored a translocation of the *TCR*α/δ locus, whereas no chromosomal translocation of the *TCR*β and *TCR*γ loci was detected. In the one case with Lennert lymphoma we furthermore detected a breakpoint slightly telomeric of *BCL3* indicative of a translocation t(14;19)(q11;q13). BCL3 overexpression that promotes cell survival in B- and T-cells,[84] was reported to be a regular feature of Hodgkin lymphoma, ALCL and PTCL NOS.[85] However, our data is in line with previous findings [9] indicating that BCL3 upregulation is only rarely resulting from the t(14;19) involving the *TCR*α/δ locus. The AILT case was found to carry the inversion inv(14)(q11q32) that is commonly known to involve the *TCL* or *BCL11B* gene loci.[2] However, we could clearly demonstrate a breakpoint in the Ig_H locus in this case. Interestingly, the inv(14)(q11q32) was detected in a primary as well as in a relapse sample taken five years later, a finding which points to an early event in tumorigenesis and a selection of tumor cells carrying the *TCR*α/δ*/IgH*. Since AITL is often associated with an EBV-associated B-cell proliferation (as present in our case), the possibility had to be excluded that proliferating B-cells rather than tumor T-cells were affected by the inv(14)(q11q32). However, FICTION analysis clearly proved that the presence of the inv(14)(q11q32) was restricted to the CD3-positive T-cells, but could not be detected in the non tumoral CD79-positive B-cells that surround the tumor.

According to our results, the frequency of breakpoints in one of the *TCR* loci is a rare but recurrent event in mature T-NHL other than T-PLL,[1] which was also confirmed by a subsequent study that showed an involvement of the *TCR*α/δ or *TCR*β loci in 3/102 (3%) and 1/80 (1%) of PTCL cases, respectively.[8] Since T-cells, in contrast to GC B-cells, do not undergo a second genetic recombination at a mature developmental stage these low frequencies may be anticipated. However, many of the translocations present in B-NHL such as the t(11;14) in MCL and the t(14;18) in FL are believed to occur at an early developmental stage (during VDJ recombination) as well,[86] but nevertheless, the tumor cells reach a mature phenotype, analogous to T-PLL.[2] Presently it is not clear why T-cell neoplasias with an early oncogenic hit in the *TCR* loci are only rarely capable of developing to a mature stage.

In summary, the results of this study show that mature T-cell lymphomas are only rarely affected by breakpoints in their *TCR* loci suggesting other molecular mechanisms that may be responsible for tumor pathogenesis in these neoplasms.

*7.2 **The Follicular Lymphoma Dataset of This Study is Representative and Shows Characteristic Molecular Features***

Follicular Lymphoma (FL) is the second most common mature B-cell neoplasm making up 20-30% of all NHL. FL is characterized by the hallmark translocation t(14;18) leading to an overexpression of the anti-apoptotic BCL2 oncogene.[2] Although BCL2 is thought to play a major role in FL pathogenesis, many studies provided evidence that BCL2 expression alone is not sufficient to develop frank lymphoma.[34,35] This theory was supported by the findings that secondary alterations occur in almost 100% of t(14;18)-positive FL cases.[31]

In this study gains and losses were detected by CGH in 127/180 low grade FL cases that were previously described to be characteristic for FL such as gains in 1q, 2p, 7, 8q, 12q, 18q and X as well as losses in 6q, 10q and 13q.[26,31,87]

With few exceptions, chromosomal gains were associated with increased gene expression and, chromosomal losses were associated with decreased gene expression, suggesting that the changes observed in expression are direct results of the chromosomal alterations rather than indirect effects due to regulation. As an example, an increased expression of the kinases *CDK4* and *TBK1* that can be both assigned to the chromosomal band 12q14 was significantly associated with chromosomal gains in this region. Interestingly, amplification of *CDK4* and its deregulated expression was already described in the context of FL transformation[88] and a gain in 12q that includes the *CDK4* locus was furthermore described in a recent array-CGH study with 128 FL cases.[87] Similarly to our approach that revealed a significant correlation between gains in 18q21 and an increased expression of the transcription factors *MBD1*, *MBD2*, *SMAD2*, *SMAD4 and TCF4* as well as the oncogene *BCL2*, this array-CGH study also described an amplification in 18q21 that included *MBD2* and *TCF4,* gains in 18q that covered the *BCL2* locus and gains in the *SMAD2* locus that correlated significantly with gene expression.[87] Moreover, a reduced expression of the transcription factors *FOXO3A* and the kinases *MAP3K7* and *CDC2L6* was observed in FL cases with losses in 6q which is also in line with previous findings.[87] Finally, losses in 10q23 correlated with a reduced expression of the tumor suppressor gene *PTEN*. Notably, a deletion of *PTEN* was also described in other FL studies,[87,89] however detailed sequencing studies could not reveal inactivating mutations in the second allele of cases with evident *PTEN* deletion.[89]

7.3 *Follicular Lymphomas Lacking the Translocation t(14;18) Belong to the Spectrum of "Classic" FL But Show Distinct Clinical and Molecular Features*

Approximately 90% of FL cases are characterized by the translocation t(14;18) that results in BCL2 overexpression.[39,90] However, approximately 10% of FL cases lack this genetic hallmark, and, in the majority of cases, also BCL2 expression. Although gene expression profiling and cytogenetic studies in FL so far allowed to divide cases, based on the composition of the tumor microenvironment, in a good prognosis and a bad prognosis group[25] and to unravel the mechanisms of FL pathogenesis, especially the transformation to DLBCL,[17,19,91] only little is known about the pathogenesis in cases lacking the t(14;18). Therefore, we compared low grade FL cases with and without t(14;18) by gene expression profiling, CGH analysis, SNP analysis and by IHC and our results suggest that t(14;18)-negative FL differ in many molecular aspects, however still seem to belong to the spectrum of FL cases. In contrast to the majority of other FL studies, we specifically excluded FL cases grade 3B, based on the accumulating evidence that these cases are molecularly different from FL cases 1-3A.[43,44]

As already mentioned, our CGH approach revealed characteristic recurrent gains and losses as they were previously described for FL by the literature, such as gains in 1q, 2p, 12q and 18q as well as losses in 6q and 10q, indicating that this entity is well represented by this study set.[26,31,87]

In line with previous findings, we detected the t(14;18) in 147 of 164 (90%) of FL cases,[39,90] whereas the remaining 17 FL cases without t(14;18) were furthermore divided by IHC in six cases with and eleven cases without BCL2 expression. As expected from the literature, we could also not detect BCL2 expression in all cases with t(14;18) which may be due to somatic mutations in the *BCL2* gene leading to crippled epitopes that are not detectable by conventional antibodies.[92]

By CGH, various differences among t(14;18)-positive and t(14;18)-negative FL were observed which were all restricted to FL cases with t(14;18) such as gains in 18q, 7, 8q and X as well as losses in 10q and 13q. However, gains or amplifications in 18q11-q21 were the only significant difference between the two groups. In contrast to previous findings reporting a frequent gain of chromosomal material of 18q in t(14;18)-negative but BCL2-positive FL cases,[39] we did not observe a gain of chromosomal material by neither CGH nor by FISH analysis in any of the t(14;18)-negative cases of this FL series, irrespective of their BCL2 expression status. Moreover, SNP analysis of eleven t(14;18)-negative FL cases using high resolution 250K NSP arrays did confirm these results with the exception of one single t(14;18)-negative showing a small gain in 18q, however excluding the *BCL2* locus. These results suggest that alternative mechanisms for BCL2 expression may exist, such as deregulated promoter usage which may be due to overexpression of transcriptional regulatory elements or the modification of the corresponding binding sites by histone acetylation[93,94] in cases lacking the t(14;18). Furthermore, SNP analysis also validated the other results revealed by CGH analysis with only few exceptions and uncovered additional genetic alterations such as gains or amplifications in 2p16.1 (including the *REL* locus) which were found in four additional cases compared to the results revealed by CGH in those cases. However, no frequent alterations were found allowing to discriminate cases with and without t(14;18) on the genetic level. Moreover, we were unable to confirm a frequent occurrence of trisomy 3 or a gain/amplification of 3q27 in our series of t(14;18)-negative FL cases which is not in line with other studies.[42,95] This discrepancy might be either due to the absence of FL grade 3B in our series or may be due to differences in the genetic constitution of FL cases in Asia and western countries.

Similar explanations might be also true for our finding that cases with the translocation t(14;18) tended to have a higher load of genetic alterations compared to cases without t(14;18) which differs from previous findings.[96] Again, the other study included FL cases grade 3B which were frequently described to lack the t(14;18) in the majority of cases and to have a higher karyotypic complexity.[39,43,44]

The comparison of gene expression profiles between t(14;18)-positive and t(14;18)-negative FL cases grades 1-3A by GSEA using lymphoma associated gene expression signatures[63] indicate differences in the maturation stage of the neoplastic B-cells, the composition of the microenvironment and the usage of oncogenic pathways.

Specifically, the enrichment of GCB-cell-signatures and PAX5 regulatory motifs in cases with t(14;18) and the enrichment of ABC-, and post-GC signatures in cases without t(14;18) suggest that FL cases with t(14;18) are closer related to a GC B-cell phenotype whereas FL cases without t(14;18) may correspond to a post GC stage of B-cell differentiation similar to the situation in DLBCL where the cases are subdivided in GCB and ABC subtypes.[67,97]

However, the findings of our IgV_H mutational analysis argue against this hypothesis. Notably, ongoing SHM, a feature of GC B-cells, was observed in all of five tested t(14;18)-negative cases. This argues against completely differentiated

B-cells as normal counterparts in t(14;18)-negative FL cases and rather favours the hypothesis of a late GC B-cell phenotype.

This idea is supported by our IHC stainings on 84 preselected FL cases of a validation series including 42 selected cases with and 42 selected cases without t(14;18) which revealed a strong expression of the GC marker CD10 in 100% of t(14;18)-positive cases, while this staining was weak or absent in ~32% of t(14;18)-negative cases. Interestingly, CD10 staining was only weak or absent in cases lacking both the t(14;18) and BCL2 expression while all cases with BCL2 expression showed a strong CD10 staining. In line with these findings IRF4/MUM1, a marker of late or post GC B-cells was more frequently expressed by cases without t(14;18) (0% versus ~11%). GSEA analysis also identified an enrichment of proliferation signatures in FL cases without t(14;18), a finding that could be also confirmed immunohistochemically by staining with the proliferation marker Ki67 in our validation series. Whereas expression of Ki67 affected more than 25% of the cells in 91% of t(14;18)-negative cases, it was detected in less than 25% of cells in 41% of t(14;18)-positive FL cases. As is known from the literature, high grade FL cases usually have a higher proliferation index and show a higher incidence of cases with a CD10-/IRF4/MUM1+ phenotype.[98] Interestingly, our validation set contains only four cases of FL grade 3A, two of which are t(14;18)-positive. FL grade 1,2 and FL grade 3 were equally distributed between the groups. Thus, it is unlikely that the composition of the two FL subgroups account for the differences in the proliferation rate and rather suggests that a higher proliferation rate is a biological feature of t(14;18)-negative FL. The absence of FL grade 3B and the low amount of FL cases grade 3A might also explain why we did not observe a significant association between a higher Ki67 staining and an increased expression of IRF4/MUM1 as well as no inverse correlation between CD10 and IRF4/MUM1 expression or between the expression of BCL6 and IRF4/MUM1 in our series, as was previously reported by other authors.[98] However, although expression of IRF4/MUM1 and BCL6 is mutually exclusive in normal GC B-cells, a coexpression of both proteins was previously observed in a subset of neoplastic GC B-cells suggesting that expression of these proteins may be deregulated in some tumors.[99] The enrichment of NFKB signatures in FL without t(14;18) by GSEA as well as the increased expression of well known NFKB target genes in this subgroup furthermore point to an increased NFKB activity in cases lacking the t(14;18). IHC assays with antibodies for the NFkB subunit p65 and the NFkB target gene c-FLIP unfortunately failed. In addition, the composition of the microenvironment, an important biologic and prognostic feature in FL,[25] appears to be different between FL cases with and without t(14;18), as evidenced by an enrichment of the IR1 and T-cell signatures in t(14;18)-negative FL. Moreover, GZMB, a cytotoxic molecule, was more highly expressed in the t(14;18)-negative FL subgroup, a finding that could be validated immunohistochemically demonstrating an increased number of cytotoxic cells expressing GZMB in t(14;18)-negative FL.

Interestingly, a comparison between FL carrying the translocation t(14;18) and the FL subgroup that expresses BCL2 but lack the translocation t(14;18) also revealed an enrichment of GCB-signatures in t(14;18)-positive cases and an enrichment of ABC-, NFKB-, marginal-zone B-cell- and cell-cycle/proliferation signatures in t(14;18)-negative but BCL2 expressing FL cases. This result suggests that the presence of the translocation t(14;18) has a different effect on the gene expression pattern of these cases than BCL2 expression alone.

In principle, the question arises if FL cases lacking both the t(14;18) and CD10 expression might be misclassified marginal zone B-cell lymphoma (MZBL) cases or reactive hyperplasias rather than 'true' FL cases. However, there are many specific morphological and molecular features which strongly suggest that the t(14;18)-negative cases of our series belong to the spectrum of 'true' FL cases. From a morphological point of view, these cases present with a predominance of centrocytes and only few intermingled transformed blasts and a prominent proliferation in the marginal zones was not obvious.[2] On a molecular level, these cases strongly express the GC B-cell markers BCL6 and IRF8[100] and show gains or amplifications of the *REL* locus in 2p16.1 in five of 17 t(14;18)-negative cases. In particular, a gain or amplification of *REL* was described to be a frequent finding in t(14;18)-positive FL cases and in the GCB subtype of DLBCL.[67] The absence of characteristic genetic alterations of MZBL such as trisomies 3, 7 and 18 in our cases furthermore supports the diagnoses of FL.[2] Finally, Genescan analysis revealed a clonal rearrangement in all 17 t(14;18)-negative FL cases of either the V_H or the $V\kappa$ chain gene locus which strongly suggests a neoplastic background rather than a reactive condition.

Besides the differences in gene expression and underlying genetic alterations, no difference in overall survival was observed between the t(14;18)-positive and t(14;18)-negative FL subgroups which also held true for other clinical parameters (ECOG performance status, gender, involvement of extranodal sites, B-symptoms or LDH). One potential exception might be the more frequently observed low disease stage among t(14;18)-negative FL which, however, needs to be validated in larger and more homogeneously treated cohorts.

It is important to note that FL subsets that frequently lack the t(14;18) and show distinct genetic and clinical features were not included in this study. Specifically, pediatric follicular lymphomas, cutaneous follicle center lymphomas and the recently described FL subgroup with a predominantly diffuse growth pattern and frequent deletions in the chromosomal region 1p36[101], that will be discussed in the following section, were excluded from these investigations, for which only FL with a predominantly follicular growth pattern were selected.

In summary, this study suggests that FL cases lacking the translocation t(14;18) belong to the biological spectrum of FL, but show distinct molecular features as well as evidence of a different composition of the tumor microenvironment.

7.4 ***Definition of a New t(14;18)-Negative FL Subset that Shows an Unusual Predominantly Diffuse Growth Pattern and a Chromosomal Deletion in 1p36***

In the course of this thesis we also described a new subtype of t(14;18)-negative FL characterized by a predominantly diffuse growth pattern, frequent clinical presentation with large, localized tumors in the inguinal region, a particularly indolent clinical course and a unifying chromosomal deletion in 1p36. Notably, these FL cases are distinct from the 17 “classic” t(14;18)-negative FL that were described in the previous part of this thesis.

Predominantly diffuse FL are characterized by a strikingly diffuse growth pattern of centrocytes and centroblasts with less than 25% follicularity.[2] Here, we describe

35 FL cases that are characterized by a predominantly diffuse growth pattern, consistent with the diagnosis of predominantly diffuse FL. Immunohistochemically, these cases are well in line with FL and consistent with a derivation from a germinal center B-cell. All cases were found to be CD5 negative and display reactivity for CD10 and BCL6 in the neoplastic follicles. Moreover, CD23 expression was evident in these cases, especially in the diffuse parts of the infiltrate, combined with co-reactivity of CD10 in a substantial number of cases. In line with these features, gene expression profiling of diffuse FL revealed a phenotype that falls into the spectrum of FL, but nevertheless shows distinct features.

In particular by GSEA an enrichment of GCB cell-, proliferation-, B-cell-, and cell-cycle-signatures was observed in FL, consistent with the observation that the Ki67 labelling is relatively low within the diffuse areas, that BCL-6 expression is downregulated, and that CD10 expression is strongly reduced in some diffuse FL. In contrast, an enrichment of T-cell-, NK-cell- and DC-signatures were found in diffuse FL cases, pointing to a higher amount of non-malignant bystander cells which is also supported by morphological and immunohistochemical observations. Whether the increased number of bystander cells in diffuse FL replace the germinal center micro-milieu of FL cases and may support the growth of the tumor cells, is presently unclear. It is noteworthy that the enrichment of both DC signatures (blood-derived BDCA1-positive DC and tonsillar CD123-positive DC)[83] in diffuse FL was predominantly based on genes (e.g. *IL13RA1*, *PTCRA*, *IL27RA* and *IL3RA*) that are also widely expressed by other cells of the immune system, such as T- and NK cells[102-105] rather than of markers of follicular DC such as

CD21, CD23 or CD35. Therefore it is unclear, if increased numbers of specific DC subsets account for the enrichment of these two gene expression signatures.

One of the most surprising findings in this study was that, in spite of the presence of atypical follicles, only 1 of 33 diffuse FL tested turned out to harbor the translocation t(14;18). In this context one should mention that also the site of origin itself may predict for the t(14;18) status in FL as can be seen from primary cutaneous FL that are *BCL2* rearranged in less than 50% of cases.[106,107]

Ideally, malignancies with similar features regarding morphology, immunophenotype and clinical presentations also display similar genetic features. In this study, we found that del(1p36) which was detected in 28 of 29 cases (97%) is a recurring genetic aberration in predominantly diffuse FL and suggest that this alteration may constitute a primary aberration in this particular tumor type.

A recent study on 58 FACS-sorted FL samples using SNP arrays revealed loss of heterozygosity (LOH) and, especially, copy-neutral LOH (uniparental disomy) in 1p36 in 50% of the samples, making this chromosomal region the second most frequently altered region in FL.[108] Various putative tumor suppressors have been mapped to this chromosomal region including *TP73*,[109] *RUNX3*,[110] *TNFR2*,[111] *ID3*,[112] *PAX7*,[113] *DAN*,[114] and *CDC2L1*,[115] however, no tumor suppressor of potential importance for the pathogenesis of diffuse FL has been identified so far.

It is interesting to note that in our series only one case exhibited a del(1p36) together with the t(14;18), while the vast majority of deletions in this region are associated with a *BCL2* rearrangement and occur in FL. This may point to a different target gene in FL and diffuse FL or to the biological importance of the t(14;18) that, in case of its presence, leads to the phenotype of classical (predominantly follicular) FL irrespective of an additional deletion in 1p36.

In summary, we here described a new subtype of FL with a predominantly diffuse growth pattern, frequent clinical presentation in the inguinal region and characteristic genetic features including a lack of the t(14;18) and a deletion in 1p36.

8 Future Perspectives

Future studies on FL without t(14;18) will have to address the question whether the molecular differences of this subgroup have impact on clinical parameters, the clinical course and/or the response to current treatment regimens.
Furthermore, it will be essential to identify the gene(s) in 1p36 whose deletion may be crucial in the pathogenesis of predominantly diffuse t(14;18)-negative FL and future studies will have to address the clinical behaviour of these cases in the context of clinical trials.

Gene expression profiling of FL cases with and without t(14;18) in our study revealed –among other findings- a significant higher expression of well known anti-apoptotic markers and NFKB targets such as *c-FLIP*, *TNF*α or *BCL2A1* in t(14;18)-negative FL cases suggesting a different oncogenic pathway in this subset. These results, however, have to be confirmed on an independent test set and functional studies are essential to provide more evidence on the role of these genes in the pathogenesis of FL.

Since our CGH and SNP-array approaches could not confirm a gain of chromosomal material in 18q in cases without t(14;18) but evident BCL2 expression as observed in another study,[39] it might be also interesting to investigate the alternative mechanisms of BCL2 overexpression in t(14;18)-negative FL.

Finally, it might be worthwile to investigate t(14;18)-negative FL by high throughput "Tumor Resequencing"[116,117] in order to identify cancer relevant somatic mutations. In addition, it might also be interesting to study these cases for their miRNA- and methylation profiles.

9 Supplements

Supplemental Table 1:

Chromosomal regions that were selected for the analysis of associations between distinct chromosomal alterations that were present in at least five cases and the expression levels of genes localized in each of these regions.

Chromosomal Region	*Chromosomal Changes*	*No. of Cases*
1q21	gain	15
1q22	gain	15
1q23	gain	15
1q24	gain	15
1q25	gain	16
1q31	gain	18
1q32	gain	18
1q41	gain	19
1q42	gain	18
1q43	gain	17
1q44	gain	17
2p11	gain	10
2p12	gain	10
2p13	gain	11
2p14	gain	21
2p15	gain	21
2p16	gain	20
2p21	gain	15
2p22	gain	14
2p23	gain	12
2p24	gain	13
2p25	gain	13
2q11	gain	11
2q12	gain	11
2q13	gain	11
2q14	gain	11
2q21	gain	11
2q22	gain	12
2q23	gain	12
2q24	gain	12
2q31	gain	12
2q32	gain	12
2q33	gain	12
2q34	gain	11
2q35	gain	11
2q36	gain	11
2q37	gain	11
4q31	loss	5
4q32	loss	5
4q33	loss	8
4q34	loss	8
4q35	loss	8

5p12	gain	7
5p13	gain	7
5p14	gain	7
5p15	gain	7
5q11	gain	5
5q12	gain	5
5q13	gain	5
5q14	gain	5
5q15	gain	5
5q21	loss	5
5q22	loss	5
5q23	loss	5
5q31	gain	5
5q32	gain	6
5q33	gain	6
5q34	gain	6
5q35	gain	6
6p11	gain	9
6p12	gain	9
6p21	gain	12
6p22	gain	11
6p23	gain	11
6p24	gain	11
6p25	gain	11
6q11	loss	17
6q12	loss	17
6q13	loss	18
6q14	loss	22
6q15	loss	25
6q16	loss	26
6q21	loss	28
6q22	loss	28
6q23	loss	29
6q24	loss	27
6q25	loss	24
6q26	loss	23
6q27	loss	23
7p11	gain	23
7p12	gain	23
7p13	gain	23
7p14	gain	23
7p15	gain	23
7p21	gain	24
7p22	gain	24
7q11	gain	26
7q21	gain	25
7q22	gain	25
7q31	gain	23
7q32	gain	22
7q33	gain	23
7q34	gain	23
7q35	gain	23
7q36	gain	23

8p11	gain	11
8p12	gain	11
8p21	gain	11
8p22	gain	11
8p23	gain	11
8q11	gain	11
8q12	gain	11
8q13	gain	11
8q21	gain	13
8q22	gain	15
8q23	gain	18
8q24	gain	21
9p23	loss	6
9p24	loss	6
9q12	gain	5
9q13	gain	5
9q21	gain	5
9q22	gain	5
9q31	gain	5
9q32	gain	5
9q33	gain	5
9q34	gain	7
10p13	gain	5
10p14	gain	5
10p15	gain	5
10q22	loss	12
10q23	loss	17
10q24	loss	8
11p11	gain	6
11p12	gain	6
11p13	gain	6
11p14	gain	6
11p15	gain	6
11q22	loss	5
11q23	gain	5
11q24	gain	5
11q25	gain	5
12p11	gain	11
12p12	gain	11
12p13	gain	9
12q12	gain	17
12q13	gain	19
12q14	gain	18
12q15	gain	16
12q21	gain	10
12q22	gain	6
12q23	gain	8
12q24	gain	9
13q12	loss	10
13q13	loss	11
13q14	loss	14
13q21	loss	18
13q22	loss	17

13q31	loss	15
13q32	loss	13
13q33	loss	13
13q34	loss	13
15q15	loss	5
15q21	loss	5
15q22	loss	5
15q23	loss	5
15q24	loss	5
15q25	loss	6
15q26	loss	7
16p11	gain	6
16p12	gain	6
16p13	gain	7
16q22	gain	5
16q23	gain	7
16q24	gain	7
17p11	gain	6
17p12	gain	6
17p13	loss	5
17q11	gain	12
17q12	gain	12
17q21	gain	13
17q22	gain	14
17q23	gain	15
17q24	gain	15
17q25	gain	13
18p11	gain	39
18q11	gain	36
18q12	gain	36
18q21	gain	33
18q22	gain	18
18q23	gain	16
Xp11	gain	18
Xp21	gain	17
Xp22	gain	16
Xq11	gain	17
Xq12	gain	17
Xq13	gain	17
Xq21	gain	17
Xq22	gain	17
Xq23	gain	17
Xq24	gain	17
Xq25	gain	17
Xq26	gain	17
Xq27	gain	17
Xq28	gain	17

Supplemental Table 2: 195 altered chromosomal bands, 41 (asterisks) of which showed an excess of probes significantly associated with gene expression as determined by a Poisson model.

Chr. Region	*Chr. Changes*	*No. Cases*	*No. Probesets in Chr. Band*	*Significant Expr.Changes*	*%*	*Expected Changes*	*Z-Score*	*Bands with excess of signif. Assoc.*
10p13	gain	5	70	3	4.3	6.1	-1.3	
10p14	gain	5	56	3	5.4	4.9	-0.9	
10p15	gain	5	94	8	8.5	8.2	-0.1	
10q22	loss	12	218	1	0.5	19.1	-4.1	
10q23	loss	17	183	30	16.4	16.0	3.5	*
10q24	loss	8	245	20	8.2	21.5	-0.3	
11p11	gain	6	132	7	5.3	11.6	-1.3	
11p12	gain	6	20	1	5	1.8	-0.6	
11p13	gain	6	122	11	9	10.7	0.1	
11p14	gain	6	45	2	4.4	3.9	-1.0	
11p15	gain	6	483	30	6.2	42.3	-1.9	
11q22	loss	5	104	1	1	9.1	-2.7	
11q23	gain	5	273	11	4	23.9	-2.6	
11q24	gain	5	171	3	1.8	15.0	-3.1	
11q25	gain	5	26	0	0	2.3	-1.5	
12p11	gain	11	98	10	10.2	8.6	0.5	
12p12	gain	11	144	5	3.5	12.6	-2.1	
12p13	gain	9	377	9	2.4	33.1	-4.2	
12q12	gain	17	67	8	11.9	5.9	0.9	
12q13	gain	19	465	50	10.8	40.8	1.4	
12q14	gain	18	100	27	27	8.8	6.2	*
12q15	gain	16	71	18	25.4	6.2	4.7	*
12q21	gain	10	153	14	9.2	13.4	0.2	
12q22	gain	6	59	1	1.7	5.2	-1.8	
12q23	gain	8	171	1	0.6	15.0	-3.6	
12q24	gain	9	501	29	5.8	43.9	-2.3	
13q12	loss	10	182	2	1.1	16.0	-3.5	
13q13	loss	11	94	0	0	8.2	-2.9	
13q14	loss	14	244	17	7	21.4	-0.9	
13q21	loss	18	32	0	0	2.8	-1.7	
13q22	loss	17	52	1	1.9	4.6	-1.7	
13q31	loss	15	51	0	0	4.5	-2.1	
13q32	loss	13	95	1	1.1	8.3	-2.5	
13q33	loss	13	45	0	0	3.9	-2.0	
13q34	loss	13	109	4	3.7	9.6	-1.8	
15q15	loss	5	160	5	3.1	14.0	-2.4	
15q21	loss	5	240	8	3.3	21.0	-2.8	
15q22	loss	5	180	7	3.9	15.8	-2.2	
15q23	loss	5	91	1	1.1	8.0	-2.5	
15q24	loss	5	146	5	3.4	12.8	-2.2	
15q25	loss	6	177	8	4.5	15.5	-1.9	
15q26	loss	7	180	8	4.4	15.8	-2.0	
16p11	gain	6	215	4	1.9	18.8	-3.4	
16p12	gain	6	196	5	2.6	17.2	-2.9	
16p13	gain	7	479	10	2.1	42.0	-4.9	
16q22	gain	5	292	6	2.1	25.6	-3.9	
16q23	gain	7	103	9	8.7	9.0	0.0	
16q24	gain	7	170	11	6.5	14.9	-1.0	
17p11	gain	6	154	1	0.6	13.5	-3.4	
17p12	gain	6	60	0	0	5.3	-2.3	
17p13	loss	5	846	62	7.3	74.2	-1.4	

17q11	gain	12	189	11	5.8	16.6	-1.4	
17q12	gain	12	188	9	4.8	16.5	-1.8	
17q21	gain	13	563	50	8.9	49.4	0.1	
17q22	gain	14	18	0	0	1.6	-1.3	
17q23	gain	15	236	27	11.4	20.7	1.4	
17q24	gain	15	114	5	4.4	10.0	-1.6	
17q25	gain	13	408	31	7.6	35.8	-0.8	
18p11	gain	39	194	48	24.7	17.0	7.5	*
18q11	gain	36	86	11	12.8	7.5	1.3	
18q12	gain	36	149	35	23.5	13.1	6.1	*
18q21	gain	33	220	58	26.4	19.3	8.8	*
18q22	gain	18	62	10	16.1	5.4	2.0	*
18q23	gain	16	54	5	9.3	4.7	0.1	
1q21	gain	15	291	26	8.9	25.5	0.1	
1q22	gain	15	103	11	10.7	9.0	0.7	
1q23	gain	15	314	57	18.2	27.5	5.6	*
1q24	gain	15	124	17	13.7	10.9	1.9	
1q25	gain	16	211	32	15.2	18.5	3.1	*
1q31	gain	18	89	16	18	7.8	2.9	*
1q32	gain	18	315	31	9.8	27.6	0.6	
1q41	gain	19	94	21	22.3	8.2	4.4	*
1q42	gain	18	225	42	18.7	19.7	5.0	*
1q43	gain	17	69	9	13	6.0	1.2	
1q44	gain	17	98	12	12.2	8.6	1.2	
2p11	gain	10	132	10	7.6	11.6	-0.5	
2p12	gain	10	28	0	0	2.5	-1.6	
2p13	gain	11	179	16	8.9	15.7	0.1	
2p14	gain	21	61	10	16.4	5.3	2.0	*
2p15	gain	21	49	11	22.4	4.3	3.2	*
2p16	gain	20	119	22	18.5	10.4	3.6	*
2p21	gain	15	122	13	10.7	10.7	0.7	
2p22	gain	14	126	9	7.1	11.0	-0.6	
2p23	gain	12	182	9	4.9	16.0	-1.7	
2p24	gain	13	75	3	4	6.6	-1.4	
2p25	gain	13	114	6	5.3	10.0	-1.3	
2q11	gain	11	175	12	6.9	15.3	-0.9	
2q12	gain	11	44	4	9.1	3.9	0.1	
2q13	gain	11	108	4	3.7	9.5	-1.8	
2q14	gain	11	135	15	11.1	11.8	0.9	
2q21	gain	11	91	8	8.8	8.0	0.0	
2q22	gain	12	43	2	4.7	3.8	-0.9	
2q23	gain	12	67	11	16.4	5.9	2.1	*
2q24	gain	12	141	4	2.8	12.4	-2.4	
2q31	gain	12	221	25	11.3	19.4	1.3	
2q32	gain	12	122	15	12.3	10.7	1.3	
2q33	gain	12	225	27	12	19.7	1.6	
2q34	gain	11	40	2	5	3.5	-0.8	
2q35	gain	11	141	5	3.5	12.4	-2.1	
2q36	gain	11	103	4	3.9	9.0	-1.7	
2q37	gain	11	240	13	5.4	21.0	-1.8	
4q31	loss	5	196	2	1	17.2	-3.7	
4q32	loss	5	99	1	1	8.7	-2.6	
4q33	loss	8	18	1	5.6	1.6	-0.5	
4q34	loss	8	53	2	3.8	4.6	-1.2	
4q35	loss	8	91	4	4.4	8.0	-1.4	
5p12	gain	7	47	4	8.5	4.1	-0.1	
5p13	gain	7	168	6	3.6	14.7	-2.3	
5p14	gain	7	15	0	0	1.3	-1.1	
5p15	gain	7	165	8	4.8	14.5	-1.7	

5q11	gain	5	81	1	1.2	7.1	-2.3	
5q12	gain	5	90	3	3.3	7.9	-1.7	
5q13	gain	5	149	0	0	13.1	-3.6	
5q14	gain	5	152	2	1.3	13.3	-3.1	
5q15	gain	5	63	0	0	5.5	-2.4	
5q21	loss	5	82	3	3.7	7.2	-1.6	
5q22	loss	5	61	7	11.5	5.3	0.7	
5q23	loss	5	149	7	4.7	13.1	-1.7	
5q31	gain	5	325	3	0.9	28.5	-4.8	
5q32	gain	6	83	1	1.2	7.3	-2.3	
5q33	gain	6	149	0	0	13.1	-3.6	
5q34	gain	6	40	1	2.5	3.5	-1.3	
5q35	gain	6	283	8	2.8	24.8	-3.4	
6p11	gain	9	3	0	0	0.3	-0.5	
6p12	gain	9	128	5	3.9	11.2	-1.9	
6p21	gain	12	647	59	9.1	56.7	0.3	
6p22	gain	11	313	16	5.1	27.4	-2.2	
6p23	gain	11	26	4	15.4	2.3	1.1	
6p24	gain	11	79	11	13.9	6.9	1.5	
6p25	gain	11	88	12	13.6	7.7	1.5	
6q11	loss	17	1	0	0	0.1	-0.3	
6q12	loss	17	17	2	11.8	1.5	0.4	
6q13	loss	18	56	6	10.7	4.9	0.5	
6q14	loss	22	89	19	21.3	7.8	4.0	*
6q15	loss	25	79	19	24.1	6.9	4.6	*
6q16	loss	26	48	13	27.1	4.2	4.3	*
6q21	loss	28	147	42	28.6	12.9	8.1	*
6q22	loss	28	124	23	18.5	10.9	3.7	*
6q23	loss	29	130	19	14.6	11.4	2.3	*
6q24	loss	27	87	22	25.3	7.6	5.2	*
6q25	loss	24	174	33	19	15.3	4.5	*
6q26	loss	23	27	3	11.1	2.4	0.4	
6q27	loss	23	94	19	20.2	8.2	3.7	*
7p11	gain	23	39	7	17.9	3.4	1.9	
7p12	gain	23	33	1	3	2.9	-1.1	
7p13	gain	23	110	21	19.1	9.6	3.7	*
7p14	gain	23	141	26	18.4	12.4	3.9	*
7p15	gain	23	165	19	11.5	14.5	1.2	
7p21	gain	24	95	11	11.6	8.3	0.9	
7p22	gain	24	168	33	19.6	14.7	4.8	*
7q11	gain	26	206	64	31.1	18.1	10.8	*
7q21	gain	25	206	28	13.6	18.1	2.3	*
7q22	gain	25	290	60	20.7	25.4	6.9	*
7q31	gain	23	151	14	9.3	13.2	0.2	
7q32	gain	22	133	22	16.5	11.7	3.0	*
7q33	gain	23	65	12	18.5	5.7	2.6	*
7q34	gain	23	142	17	12	12.4	1.3	
7q35	gain	23	29	0	0	2.5	-1.6	
7q36	gain	23	201	32	15.9	17.6	3.4	*
8p11	gain	11	83	3	3.6	7.3	-1.6	
8p12	gain	11	105	8	7.6	9.2	-0.4	
8p21	gain	11	205	16	7.8	18.0	-0.5	
8p22	gain	11	59	3	5.1	5.2	-1.0	
8p23	gain	11	282	13	4.6	24.7	-2.4	
8q11	gain	11	61	8	13.1	5.3	1.1	
8q13	gain	11	92	9	9.8	8.1	0.3	
8q21	gain	13	156	14	9	13.7	0.1	
8q22	gain	15	159	29	18.2	13.9	4.0	*
8q23	gain	18	49	6	12.2	4.3	0.8	

8q24	gain	21	391	69	17.6	34.3	5.9	*
9p23	loss	6	17	0	0	1.5	-1.2	
9p24	loss	6	102	0	0	8.9	-3.0	
9q12	gain	5	3	0	0	0.3	-0.5	
9q13	gain	5	13	0	0	1.1	-1.1	
9q21	gain	5	172	1	0.6	15.1	-3.6	
9q22	gain	5	178	1	0.6	15.6	-3.7	
9q31	gain	5	147	3	2	12.9	-2.8	
9q32	gain	5	50	0	0	4.4	-2.1	
9q33	gain	5	238	2	0.8	20.9	-4.1	
9q34	gain	7	439	4	0.9	38.5	-5.6	
Xp11	gain	18	298	53	17.8	26.1	5.3	*
Xp21	gain	17	39	0	0	3.4	-1.8	
Xp22	gain	16	235	23	9.8	20.6	0.5	
Xq11	gain	17	11	3	27.3	1.0	2.1	*
Xq12	gain	17	22	3	13.6	1.9	0.8	
Xq13	gain	17	123	16	13	10.8	1.6	
Xq21	gain	17	85	7	8.2	7.5	-0.2	
Xq22	gain	17	132	17	12.9	11.6	1.6	
Xq23	gain	17	49	3	6.1	4.3	-0.6	
Xq24	gain	17	63	20	31.7	5.5	6.2	*
Xq25	gain	17	63	11	17.5	5.5	2.3	*
Xq26	gain	17	78	10	12.8	6.8	1.2	
Xq27	gain	17	31	1	3.2	2.7	-1.0	
Xq28	gain	17	174	30	17.2	15.3	3.8	*
			28118	2465		2465.0	0.0	

Supplemental Table 3A: Annotation of 2465 probe sets that were significantly altered in gene expression in an analysis of association between chromosomal alterations and the expression level of genes localized in each of these regions to the gene families 'oncogenes', 'tumor suppressor genes', 'transcription factors', 'translocated genes', 'cytokines' and 'kinases'.

Cytokines	*Transcription Factors*	*Hox*	*Cell surface Markers*	*Kinases*	*Translocated Genes*	*Oncogenes*	*Tumor Supressor Genes*
	MORF4L1	HOXA1	SHMT2	PFTK1	HSP90AB1	BCL2	NBN
	MYOD1	PHTF2	CD44	NUAK2	NUP98	ARAF	MSH2
	MEF2A		CD24	TBK1	NACA	MDM4	LCMT2
	MORF4L2		CD164	FASTK	FOXO1A	CDK4	SDHD
	CBX3			RPS6KB1	TFEB		SMAD4
	ZXDB			BTK	SET		SMAD2
	TBP			MAP3K7	BCL2		RB1
	CBX1			ACTR2	BCL11A		PTEN
	SART3			MAP3K5	GOPC		BRCA1
	TCEAL1			MAP3K4	TCEA1		FH
	CITED2			ADCK2	MTCP1		
	CNOT4			CLK2	MSN		
	SND1			WNK4	FOXO3A		
	TFB2M			TLK1	ASPSCR1		
	ZNF394			TLK2	CREB1		
	FOXO3A			CSK	CBL		
	TBPL1			CHUK	PIM1		
	GABPB2			ADCK5	AFF3		
	MLL2			IRAK1	TRIM24		
	RCOR3			SRPK2	DDIT3		
	TAF4B			ROCK1	COX6C		
	GTF2IRD2			STK24	SS18		
	MED12			PIM1	NCOA2		
	MECP2			PBK	FCGR2B		
	ZNF7			CDK4	PRCC		
	DDIT3			WEE1	FGFR1OP		
	TRIM37			SRPK1	WHSC1L1		
	ZNF195			RIOK3	ERC1		

BAZ1B	RIPK2
TIMELESS	LRRK2
ABT1	MAP3K12
PIAS2	ACVR1
NFE2L1	NEK2
NFE2L2	BLK
TFB1M	BMPR2
NFKBIE	STK17B
FOXO1A	CHEK1
TFEB	MAPKAPK 2
ATF2	STK17A
PLAGL1	TRRAP
HOXA1	RIOK1
BLOC1S1	MST4
TCF4	UHMK1
TFDP1	PTK2
NKRF	VRK2
TAF2	MAP3K2
YEATS4	PTK2B
KLF8	CDC2L6
TRIP4	DYRK2
TAF6	PDK1
TAF5	GUCY2D
SMAD4	FYN
SUV39H1	ARAF
SMAD2	ULK3
ZFP95	
TULP4	
PHF3	
PSMC5	
CCT4	
HDAC2	
ZNF212	

PSMC2
HIVEP2
ZNF117
GTF3A
ZBTB33
PPARD
COPS5
ZNF532
FOXK2
ZBTB39
ZNF12
ZNF673
WDR39
KIAA0040
HSF1
ZNF407
BRD9
SERTAD2
ZNF281
SP100
BRF2
RING1
LAS1L
RB1
MBD2
MBD1
ZBTB24
GTF2H1
NCOA2
GTF2I
PFDN5
NAB1
JMJD1A
KLHL12

CAND1
ZFP161
BTAF1
BCLAF1
ZNF273
ZNF271
IVNS1ABP
TCF7L2
ZNF174
ZNF706
STAT6
TSC22D3
CHD1L
REL
HAND2
BCL11A
TADA2L
CEBPZ
POU2F1
CHD1
SUPT4H1
GTF3C2
ERCC3
CHD3
GTF3C3
NFATC1
DTX2
SETBP1
CREB1
CRSP3
ZNF24
AFF3
TRIM26
PHF11

TRIM24
ZFP2
ATRX
ILF2
CUTL1
UBTF
YAF2
THRAP4
ZNF259
JMJD4
RNF41
RNF113A
REPIN1

Supplemental_Table 3B: Gene name, gene locus, type of structural alteration, gene family, *P*-value, Bonferroni correction and local FDR for genes depicted in Figure 9B.

Gene	*Locus*	*Structural Alteration*	*Gene Family_GSEA Annotation*	*p-Value*	*Bonferroni*	*Local FDR*
PARP1	1q42	Gain	-	<0.001	1.0	0.0063
CENPF	1q41	Gain	-	<0.00001	0.061	0.00022
BCL11A	2p16	Gain	Transcription Factor, Translocated gene	0.000001	0.061	0.00022
REL	2p16	Gain	Transcription Factor	<0.00001	0.073	0.00026
MAP3K7	6q15	Loss	Kinase	$<1x10^{-6}$	<0.001	$<1x10^{-6}$
FOXO3A	6q21	Loss	Transcription Factor, Translocated gene	$<1x10^{-6}$	0.011	<0.0001
CDC2L6	6q21	Loss	Kinase	$<1x10^{-6}$	$<1x10^{-6}$	$<1x10^{-6}$
PLAGL1	6q24	Loss	Transcription Factor	$<1x10^{-4}$	1.0	0.002091
CUTL1	7q22	Gain	Transcription Factor	$<1x10^{-6}$	0.001	0.00001
FASTK	7q33	Gain	Kinase	<0.0001	1.0	0.0042
TAF2	8q24	Gain	Transcription factor	<0.00001	0.12	<0.001
ADCK5	8q24	Gain	Kinase	<0.0001	0.81	0.0016
PTK2	8q24	Gain	Kinase	$<1x10^{-6}$	0.011	<0.0001
PTEN	10q23	Loss	Tumor Supressor	$<1x10^{-6}$	<0.0001	$<1x10^{-6}$
CDK4	12q14	Gain	Kinase, Oncogene	$<1x10^{-6}$	0.0058	<0.0001
TBK1	12q14	Gain	Kinase	<0.001	1.0	0.0094
MBD1	18q21	Gain	Transcription factor	$<1x10^{-6}$	<0.0001	$<1x10^{-6}$
MBD2	18q21	Gain	Transcription Factor	$<1x10^{-6}$	<0.0001	$<1x10^{-6}$
SMAD4	18q21	Gain	Transcription Factor, Tumor Supressor	0.000001	0.019	0.0001
SMAD2	18q21	Gain	Transcription Factor, Tumor Supressor	$<1x10^{-6}$	<0.0001	$<1x10^{-6}$
BCL2	18q21	Gain	Translocated Gene, Oncogene	<0.0001	0.97	0.0021
TCF4	18q21	Gain	Transcription Factor	$<1x10^{-6}$	<0.0001	$<1x10^{-6}$

Supplemental Figure 1a-m: Diagrams of selected chromosomal regions with genes highlighted whose expression is significantly associated with chromosomal changes at the bands (a) 1q42 (b) 2p16 (c) 6q15 (d) 6q21 (e) 6q24 (f) 7q22 (g) 8q24 (h) 10q23 (i) 12q14 (j) 18p11 (k) 18q11 (l) 18q21 (m) Xq28 according to a t-test (*P*-value < 0.01, local FDR<0.01) and that show a significant excess of association with the chromosomal bands (a) 1q42 (b) 2p16 (c) 6q15 (d) 6q21 (e) 6q24 (f) 7q22 (g) 8q24 (h) 10q23 (i) 12q14 (j) 18p11 (l) 18q21 (m) Xq28 according to a Poisson model (see also Supplemental Table 2).

Fig. 1a

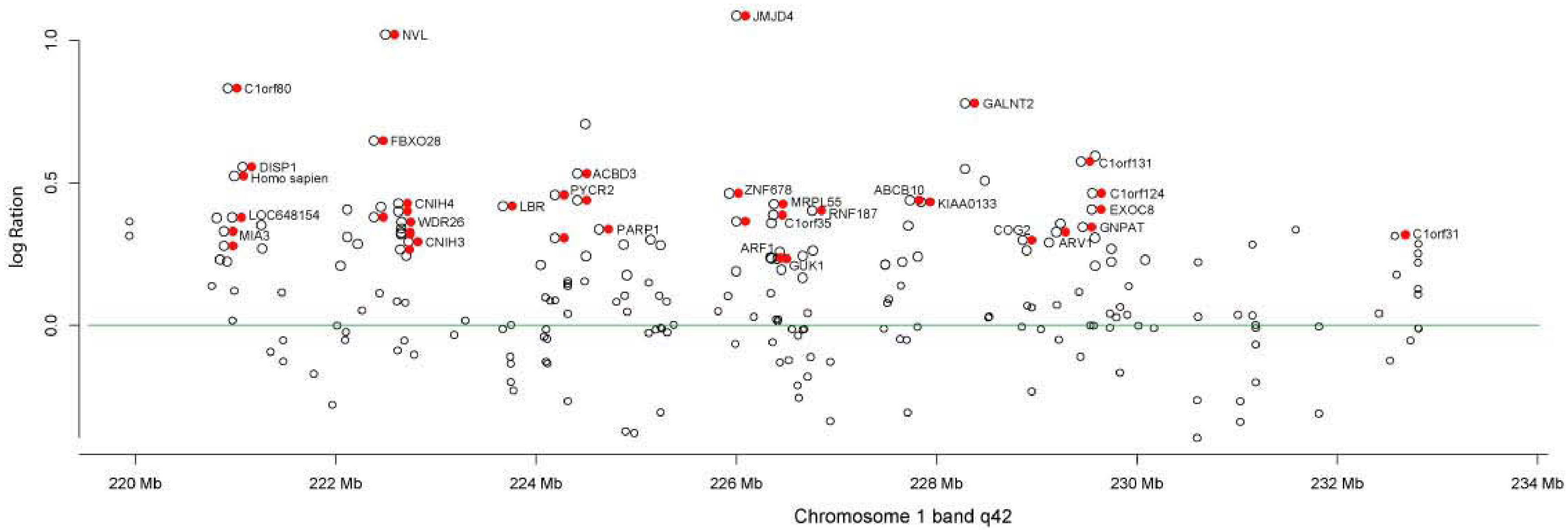

Fig. 1b

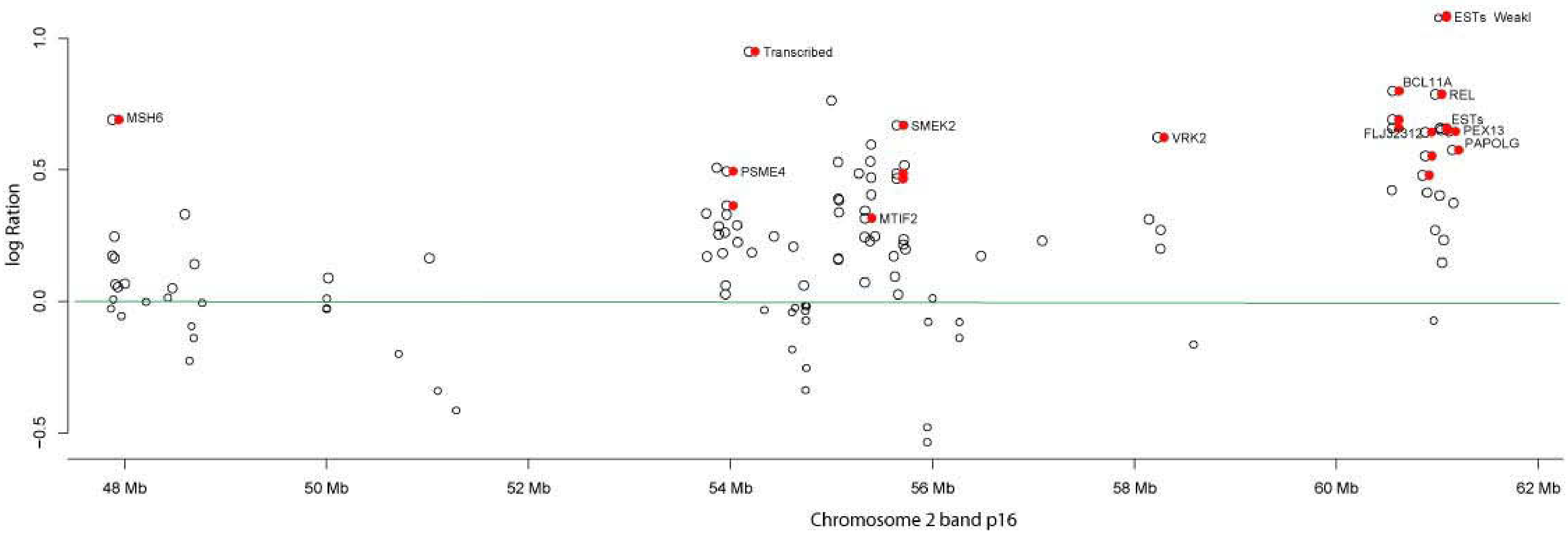

ESTs Weakl
Transcribed
BCL11A
REL
MSH6
SMEK2
ESTs
VRK2
FLJ32312
PEX13
PAPOLG
PSME4
MTIF2
1.0
0.5
0.0
−0.5
log Ration
48 Mb
50 Mb
52 Mb
54 Mb
56 Mb
58 Mb
60 Mb
62 Mb
Chromosome 2 band p16

Fig. 1c

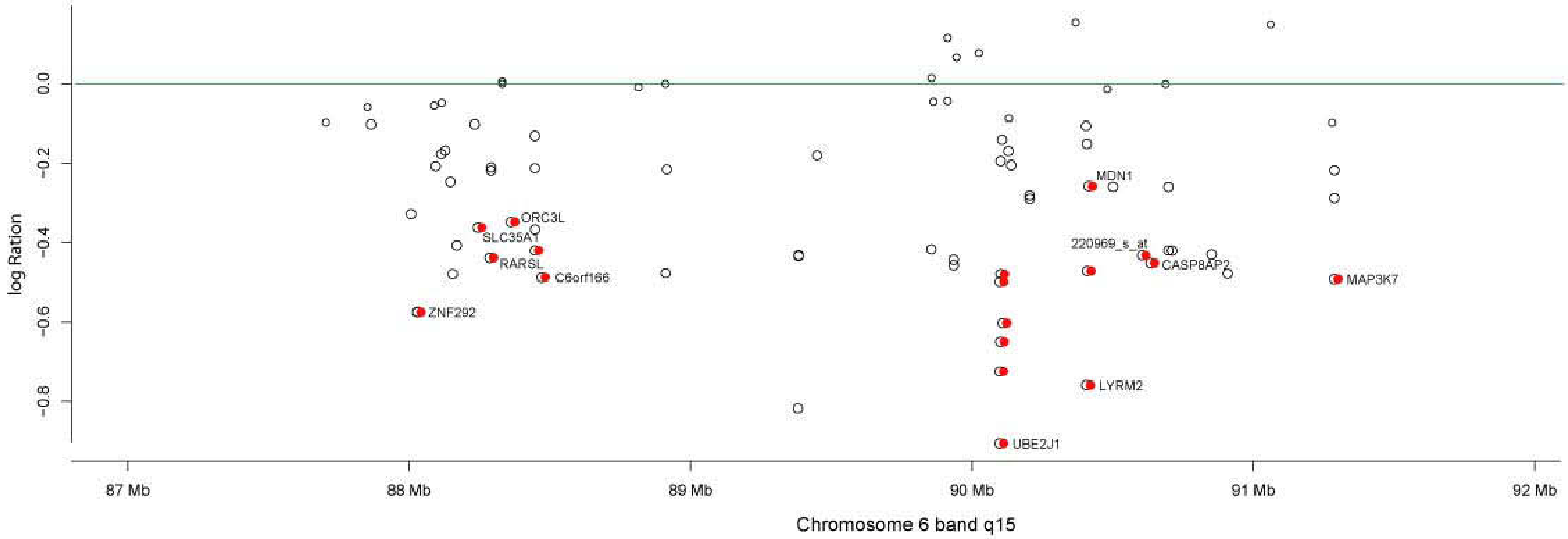

0.0
-0.2
-0.4
-0.6
-0.8
log Ration
MDN1
ORC3L
SLC35A1
220969_s_at
RARSL
CASP8AP2
C6orf166
MAP3K7
ZNF292
LYRM2
UBE2J1
87 Mb
88 Mb
89 Mb
90 Mb
91 Mb
92 Mb
Chromosome 6 band q15

Fig. 1d

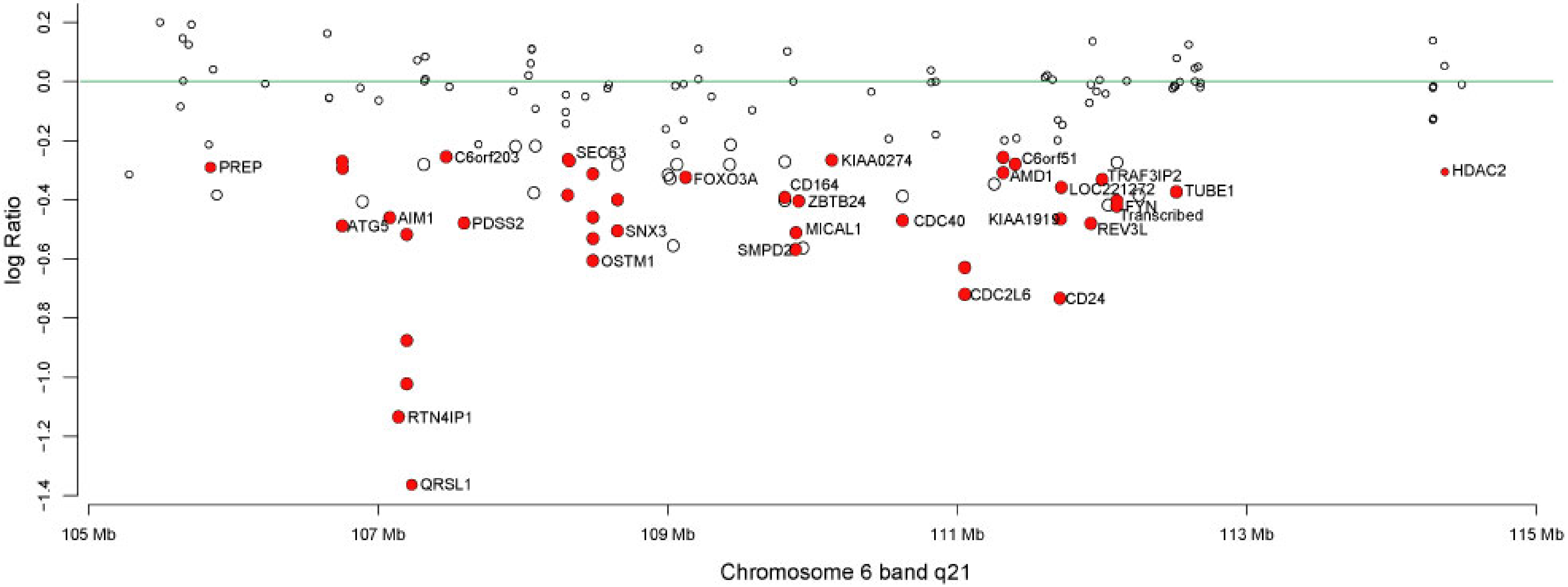

log Ratio
0.2
0.0
-0.2
-0.4
-0.6
-0.8
-1.0
-1.2
-1.4
PREP
ATG5
AIM1
RTN4IP1
QRSL1
C6orf203
PDSS2
SEC63
SNX3
OSTM1
FOXO3A
CD164
ZBTB24
MICAL1
SMPD2
KIAA0274
CDC40
CDC2L6
C6orf51
AMD1
KIAA1919
CD24
LOC221272
TRAF3IP2
FYN
Transcribed
REV3L
TUBE1
HDAC2
105 Mb
107 Mb
109 Mb
111 Mb
113 Mb
115 Mb
Chromosome 6 band q21

Fig. 1e

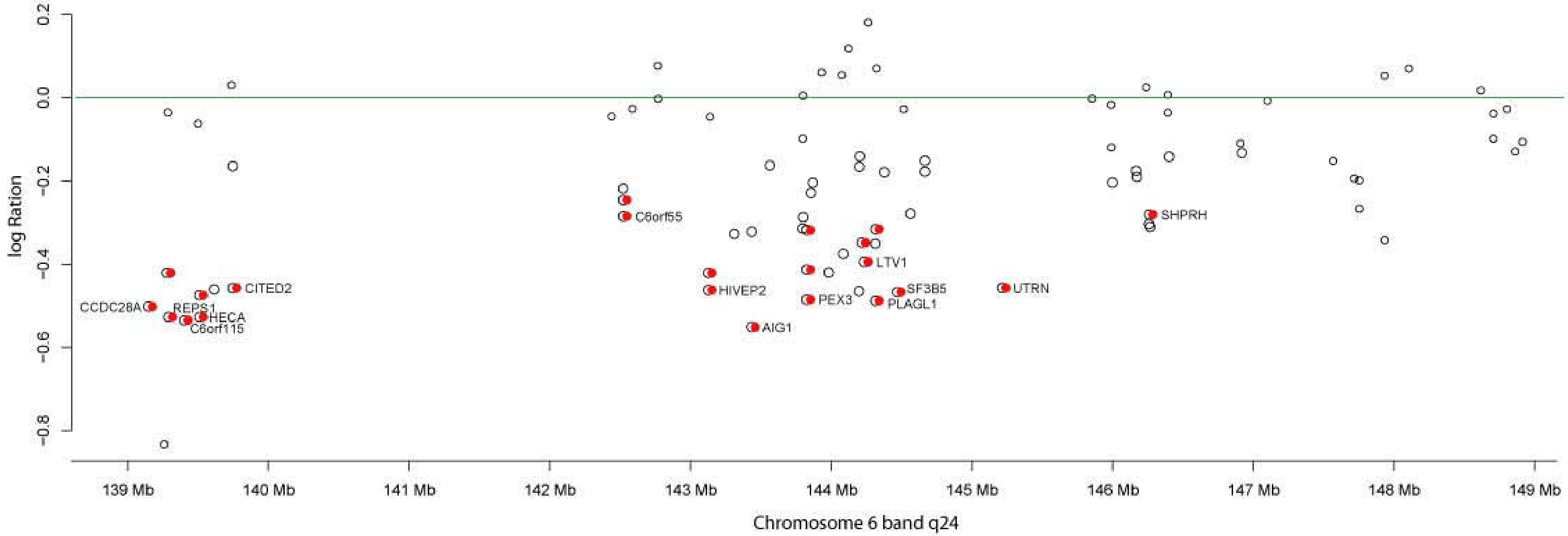

0.2
0.0
-0.2
-0.4
-0.6
-0.8
log Ration
C6orf55
SHPRH
LTV1
CITED2
HIVEP2
SF3B5
UTRN
CCDC28A
REPS1
PEX3
PLAGL1
HECA
C6orf115
AIG1
139 Mb
140 Mb
141 Mb
142 Mb
143 Mb
144 Mb
145 Mb
146 Mb
147 Mb
148 Mb
149 Mb
Chromosome 6 band q24

Fig. 1f

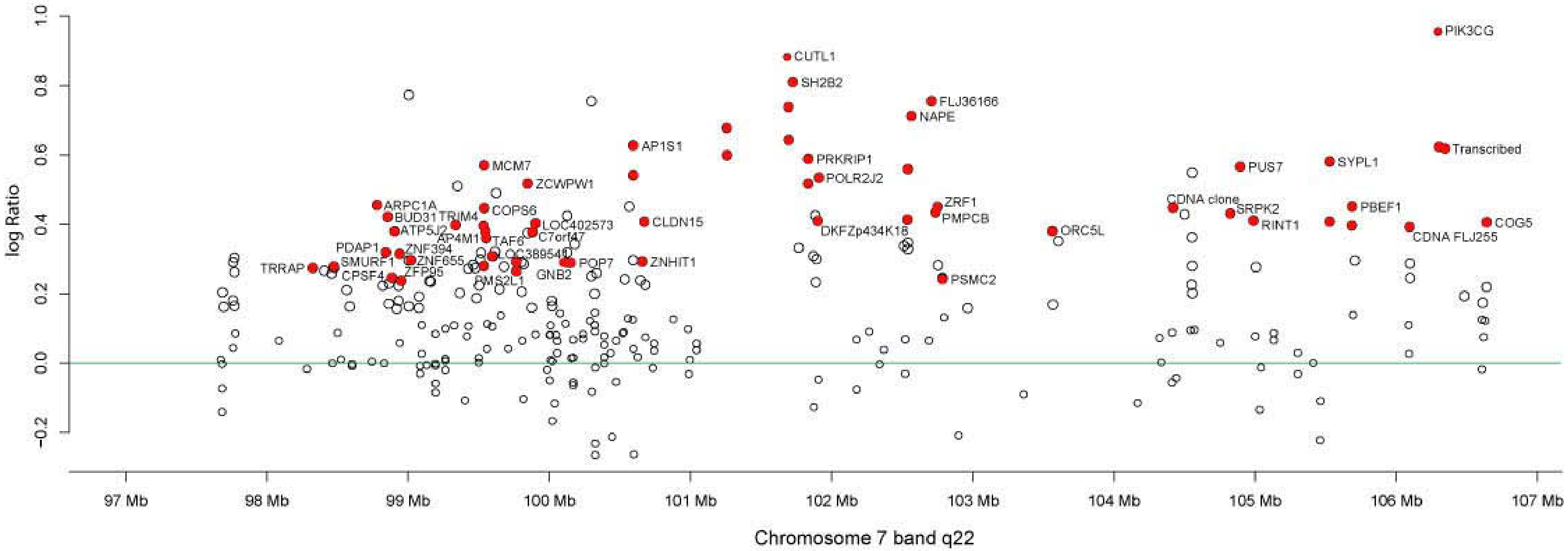

log Ratio
1.0
0.8
0.6
0.4
0.2
0.0
-0.2
97 Mb
98 Mb
99 Mb
100 Mb
101 Mb
102 Mb
103 Mb
104 Mb
105 Mb
106 Mb
107 Mb
Chromosome 7 band q22
PIK3CG
CUTL1
SH2B2
FLJ36166
NAPE
AP1S1
Transcribed
MCM7
PRKRIP1
PUS7
SYPL1
ZCWPW1
POLR2J2
ARPC1A
BUD31
TRIM4
COPS6
CLDN15
ZRF1
PMPCB
CDNA clone
SRPK2
PBEF1
COG5
ATP5J2
LOC402573
AP4M1
TAF6
C7orf47
DKFZp434K18
ORC5L
RINT1
CDNA FLJ255
PDAP1
ZNF394
SMURF1
ZNF655
TRRAP
CPSF4
ZFP95
POP7
ZNHIT1
GNB2
PMS2L1
PSMC2

Fig. 1g

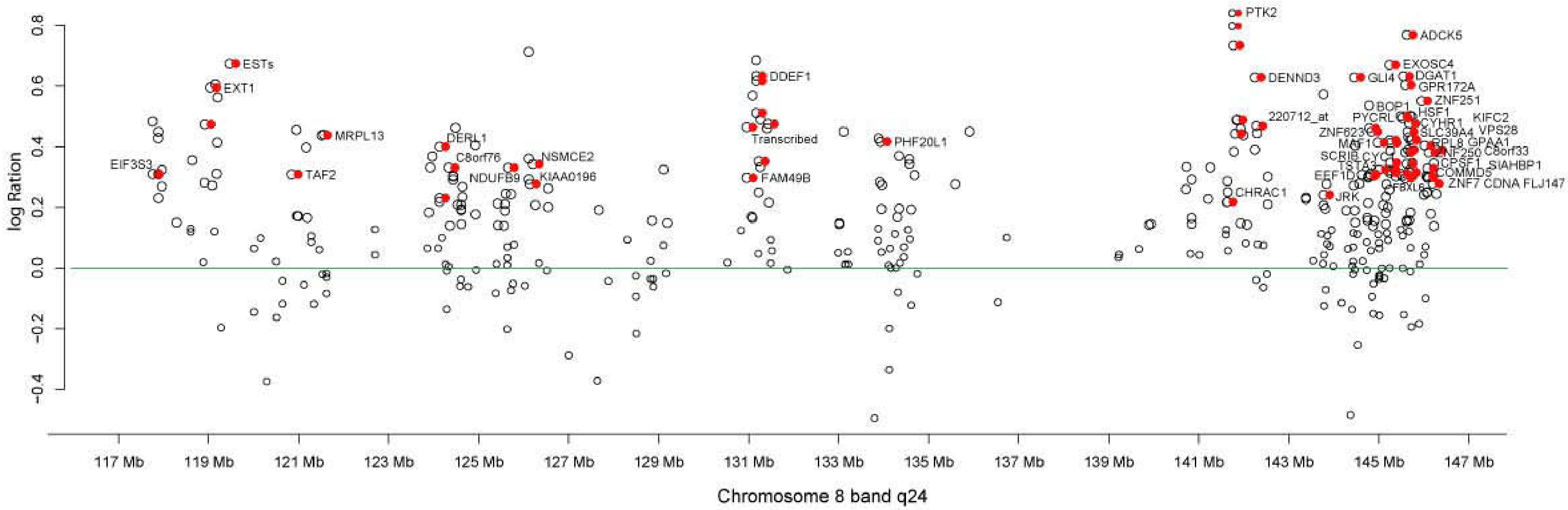
log Ration
Chromosome 8 band q24
117 Mb
119 Mb
121 Mb
123 Mb
125 Mb
127 Mb
129 Mb
131 Mb
133 Mb
135 Mb
137 Mb
139 Mb
141 Mb
143 Mb
145 Mb
147 Mb
PTK2
ADCK5
ESTs
EXT1
DDEF1
DENND3
GLI4
EXOSC4
DGAT1
GPR172A
ZNF251
MRPL13
DERL1
C8orf76
NSMCE2
NDUFB9
KIAA0196
TAF2
EIF3S3
Transcribed
FAM49B
PHF20L1
220712_at
CHRAC1
JRK
KIFC2
VPS28
ZNF7
CDNA FLJ147

Fig. 1h

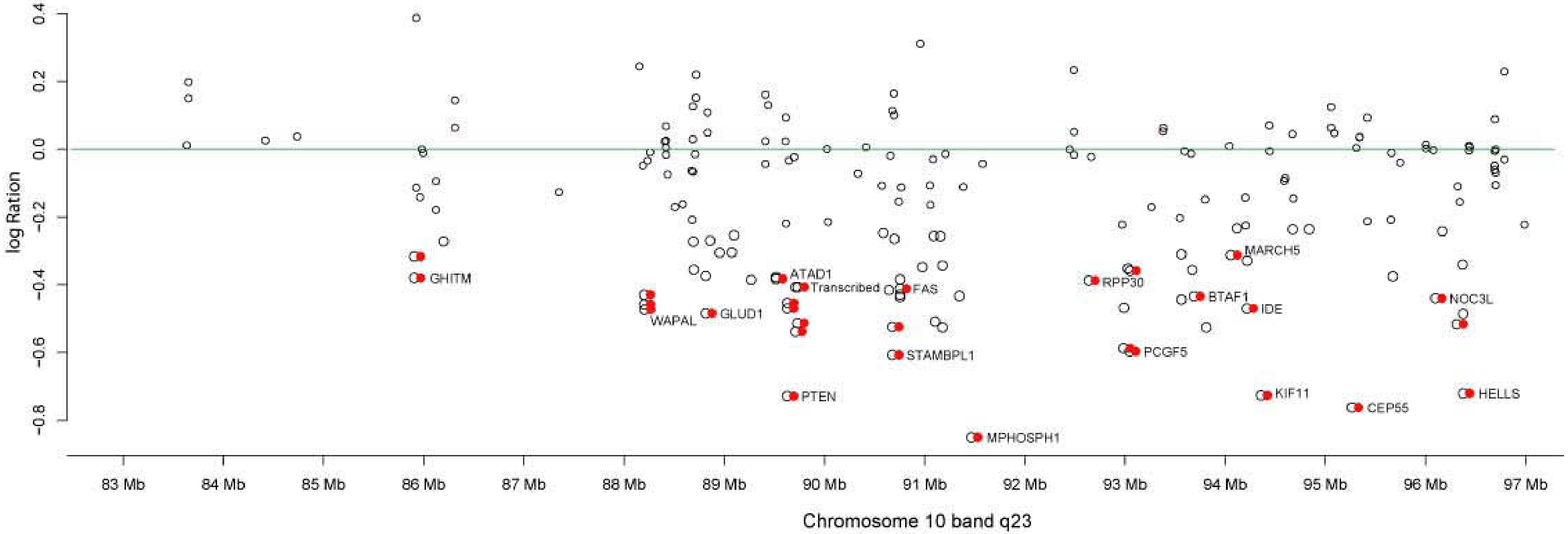

0.4
0.2
0.0
−0.2
−0.4
−0.6
−0.8
log Ration
GHITM
WAPAL
GLUD1
ATAD1
Transcribed
FAS
PTEN
STAMBPL1
MPHOSPH1
RPP30
PCGF5
BTAF1
MARCH5
IDE
KIF11
CEP55
NOC3L
HELLS
83 Mb
84 Mb
85 Mb
86 Mb
87 Mb
88 Mb
89 Mb
90 Mb
91 Mb
92 Mb
93 Mb
94 Mb
95 Mb
96 Mb
97 Mb
Chromosome 10 band q23

Fig. 1i

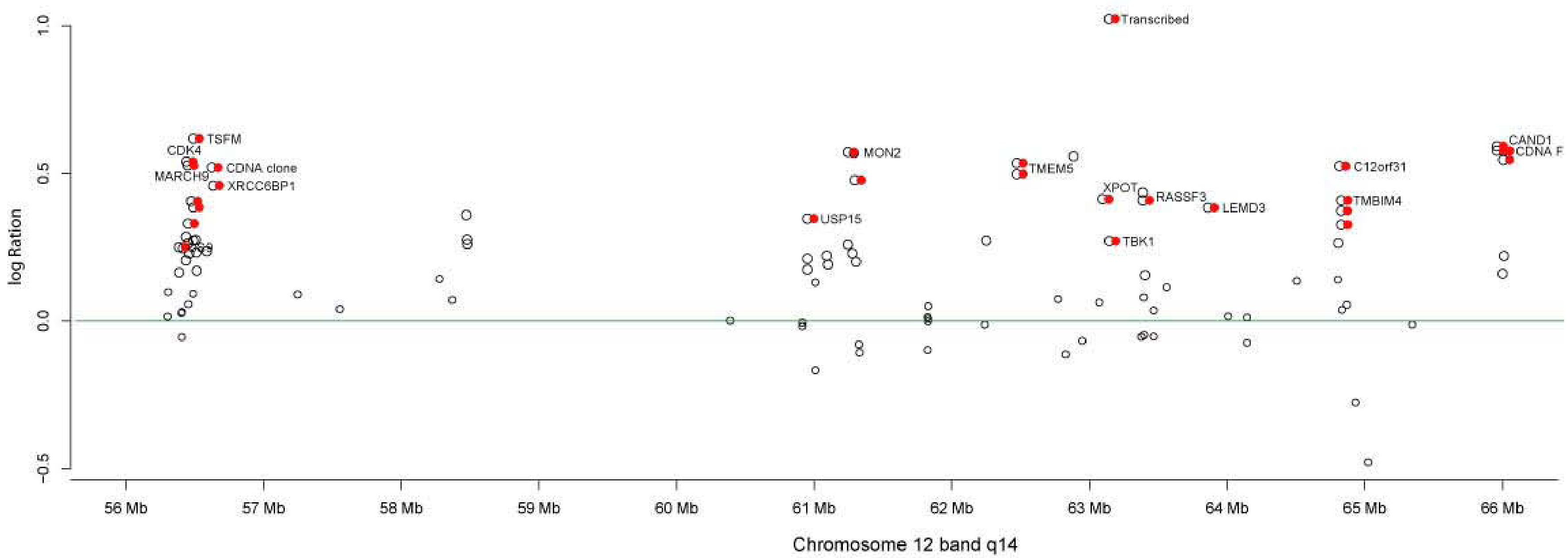
Transcribed
TSFM
CDK4
CDNA clone
MARCH9
XRCC6BP1
MON2
TMEM5
XPOT
RASSF3
LEMD3
USP15
TBK1
C12orf31
TMBIM4
CAND1
CDNA F
log Ration
1.0
0.5
0.0
-0.5
56 Mb
57 Mb
58 Mb
59 Mb
60 Mb
61 Mb
62 Mb
63 Mb
64 Mb
65 Mb
66 Mb
Chromosome 12 band q14

Fig. 1j

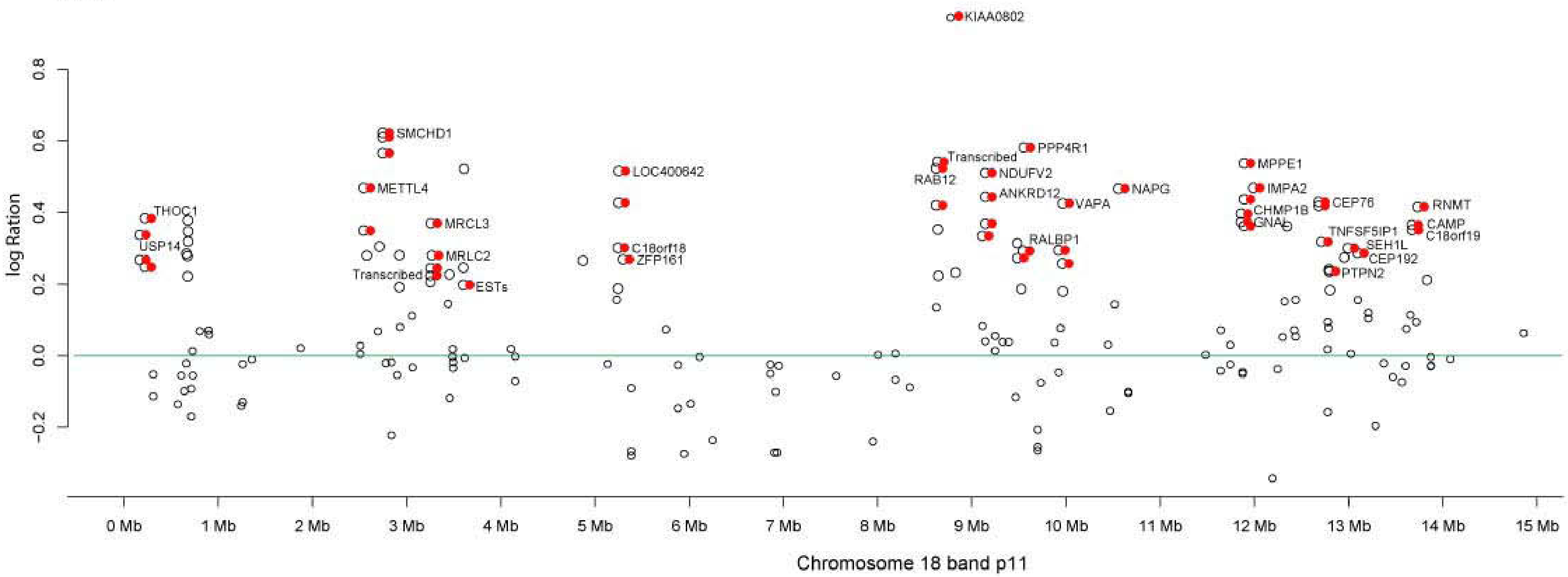

KIAA0802
SMCHD1
PPP4R1
Transcribed
MPPE1
LOC400642
RAB12
NDUFV2
METTL4
IMPA2
NAPG
ANKRD12
THOC1
CEP76
RNMT
VAPA
CHMP1B
MRCL3
GNAL
CAMP
C18orf19
USP14
TNFSF5IP1
RALBP1
SEH1L
C18orf18
MRLC2
ZFP161
CEP192
Transcribed
PTPN2
ESTs
log Ration
0.8
0.6
0.4
0.2
0.0
-0.2
0 Mb
1 Mb
2 Mb
3 Mb
4 Mb
5 Mb
6 Mb
7 Mb
8 Mb
9 Mb
10 Mb
11 Mb
12 Mb
13 Mb
14 Mb
15 Mb
Chromosome 18 band p11

Fig. 1k

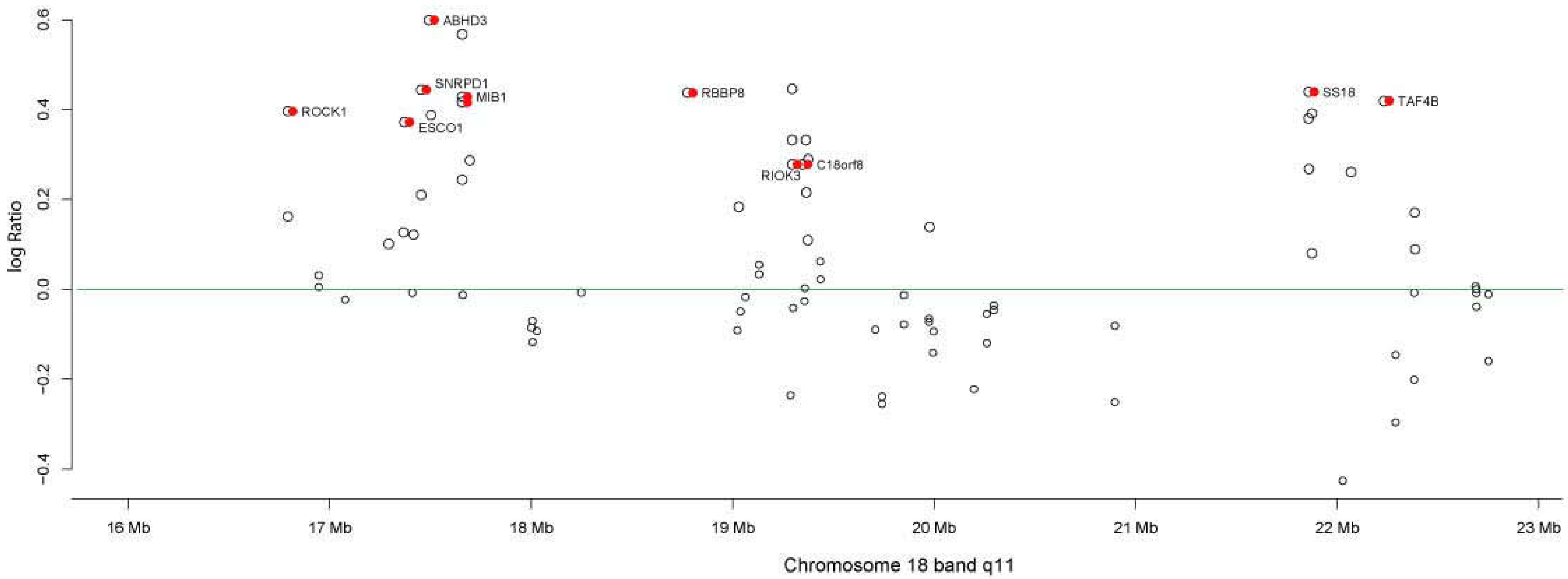
ABHD3
SNRPD1
MIB1
ROCK1
ESCO1
RBBP8
C18orf8
RIOK3
SS18
TAF4B
0.6
0.4
0.2
0.0
−0.2
−0.4
log Ratio
16 Mb
17 Mb
18 Mb
19 Mb
20 Mb
21 Mb
22 Mb
23 Mb
Chromosome 18 band q11

Fig. 1l

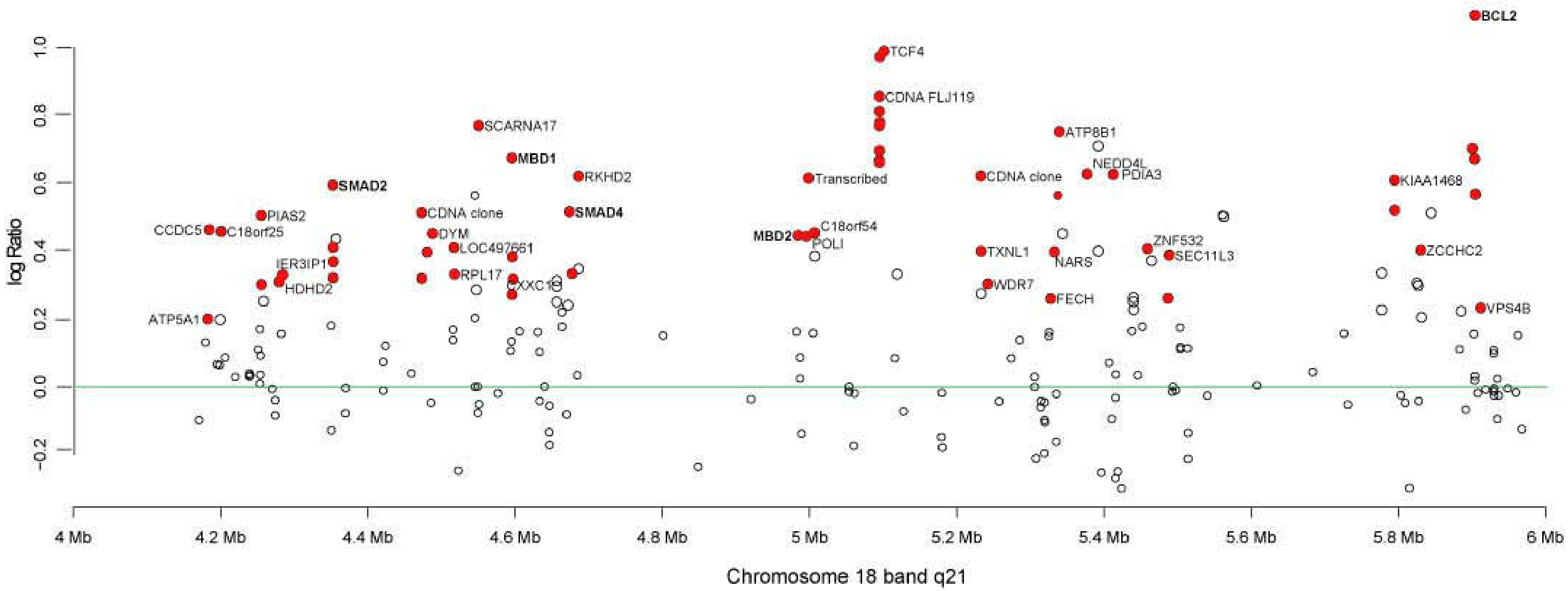

log Ratio
Chromosome 18 band q21
BCL2
TCF4
CDNA FLJ119
SCARNA17
MBD1
RKHD2
SMAD2
SMAD4
Transcribed
CDNA clone
ATP8B1
NEDD4L
PDIA3
KIAA1468
PIAS2
CCDC5
C18orf25
DYM
LOC497661
C18orf54
MBD2
POLI
TXNL1
NARS
ZNF532
SEC11L3
ZCCHC2
IER3IP1
HDHD2
RPL17
CXXC1
WDR7
FECH
ATP5A1
VPS4B

Fig. 1m

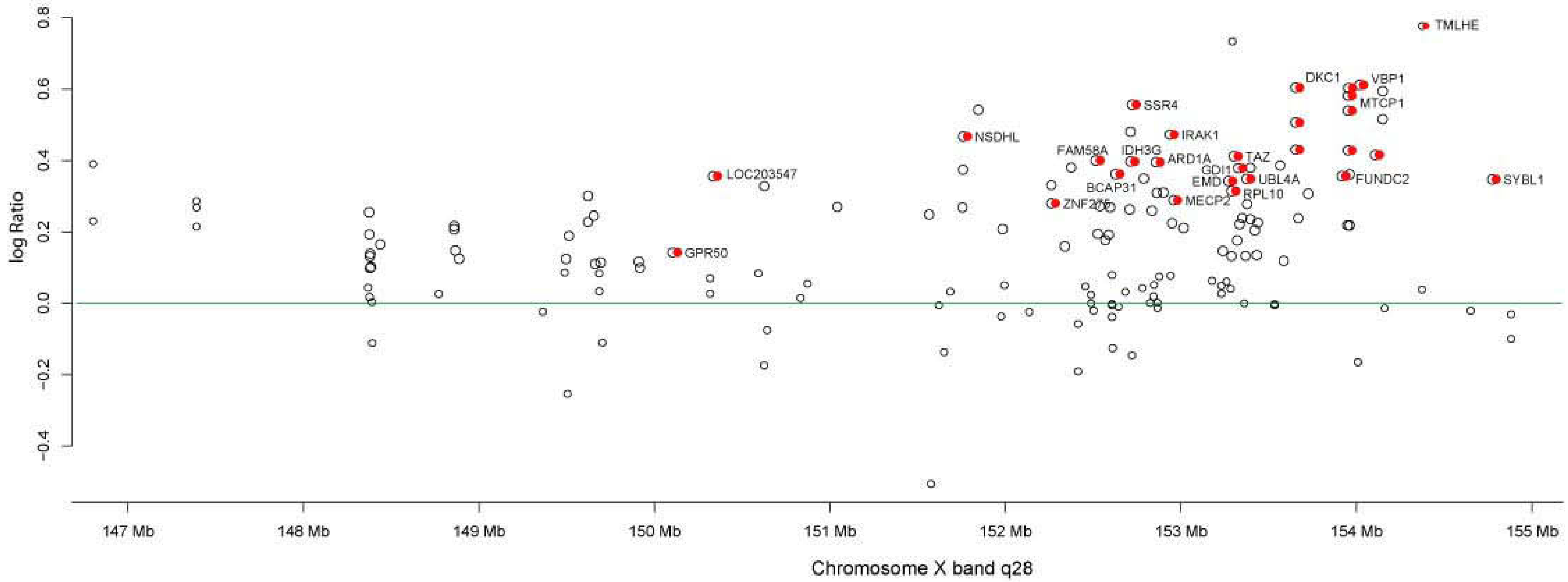
TMLHE
DKC1
VBP1
MTCP1
SSR4
NSDHL
IRAK1
FAM58A
IDH3G
ARD1A
TAZ
GDI1
LOC203547
BCAP31
EMD
UBL4A
FUNDC2
SYBL1
RPL10
ZNF275
MECP2
GPR50
log Ratio
Chromosome X band q28
147 Mb
148 Mb
149 Mb
150 Mb
151 Mb
152 Mb
153 Mb
154 Mb
155 Mb

10 References

1. Leich E, Haralambieva E, Zettl A, et al. Tissue microarray-based screening for chromosomal breakpoints affecting the T-cell receptor gene loci in mature T-cell lymphomas. J Pathol. 2007;213:99-105.
2. Swerdlow SH, Campo, E., Harris, N.L., Jaffe, E.S., Pileri, S., Stein, H., Thiele, J., Vardiman, J.W. (Eds.). WHO classification of tumors of haematopoietic and lymphoid tissues. Lyon: IARC; 2008.
3. Fugmann SD, Lee AI, Shockett PE, Villey IJ, Schatz DG. The RAG proteins and V(D)J recombination: complexes, ends, and transposition. Annu Rev Immunol. 2000;18:495-527.
4. Shaffer AL, Rosenwald A, Staudt LM. Lymphoid malignancies: the dark side of B-cell differentiation. Nat Rev Immunol. 2002;2:920-932.
5. Pasqualucci L, Neumeister P, Goossens T, et al. Hypermutation of multiple proto-oncogenes in B-cell diffuse large-cell lymphomas. Nature. 2001;412:341-346.
6. Robbiani DF, Bothmer A, Callen E, et al. AID is required for the chromosomal breaks in c-myc that lead to c-myc/IgH translocations. Cell. 2008;135:1028-1038.
7. Armstrong SA, Look AT. Molecular genetics of acute lymphoblastic leukemia. J Clin Oncol. 2005;23:6306-6315.
8. Feldman AL, Law M, Grogg KL, et al. Incidence of TCR and TCL1 gene translocations and isochromosome 7q in peripheral T-cell lymphomas using fluorescence in situ hybridization. Am J Clin Pathol. 2008;130:178-185.
9. Gesk S, Martin-Subero JI, Harder L, et al. Molecular cytogenetic detection of chromosomal breakpoints in T-cell receptor gene loci. Leukemia. 2003;17:738-745.
10. Martin-Subero JI, Wlodarska I, Bastard C, et al. Chromosomal rearrangements involving the BCL3 locus are recurrent in classical Hodgkin and peripheral T-cell lymphoma. Blood. 2006;108:401-402; author reply 402-403.
11. Lefranc M-PL, Lefranc G. The T cell receptor Facts Book. London, UK: Academic Press; 2001.
12. Lefranc M-PL, Lefranc G. The Immunoglobulin Facts Book. London, UK: Academic Press; 2001.
13. Ehlert JE, Kubbutat MH. Apoptosis and its relevance in cancer therapy. Onkologie. 2001;24:433-440.
14. Chao DT, Korsmeyer SJ. BCL-2 family: regulators of cell death. Annu Rev Immunol. 1998;16:395-419.
15. Pro B, Leber B, Smith M, et al. Phase II multicenter study of oblimersen sodium, a Bcl-2 antisense oligonucleotide, in combination with rituximab in patients with recurrent B-cell non-Hodgkin lymphoma. Br J Haematol. 2008;143:355-360.
16. Solal-Celigny P, Roy P, Colombat P, et al. Follicular lymphoma international prognostic index. Blood. 2004;104:1258-1265.
17. Davies AJ, Rosenwald A, Wright G, et al. Transformation of follicular lymphoma to diffuse large B-cell lymphoma proceeds by distinct oncogenic mechanisms. Br J Haematol. 2007;136:286-293.
18. Elenitoba-Johnson KS, Gascoyne RD, Lim MS, Chhanabai M, Jaffe ES, Raffeld M. Homozygous deletions at chromosome 9p21 involving p16 and p15 are associated with histologic progression in follicle center lymphoma. Blood. 1998;91:4677-4685.

19. Lossos IS, Alizadeh AA, Diehn M, et al. Transformation of follicular lymphoma to diffuse large-cell lymphoma: alternative patterns with increased or decreased expression of c-myc and its regulated genes. Proc Natl Acad Sci U S A. 2002;99:8886-8891.
20. Eray M, Postila V, Eeva J, et al. Follicular lymphoma cell lines, an in vitro model for antigenic selection and cytokine-mediated growth regulation of germinal centre B cells. Scand J Immunol. 2003;57:545-555.
21. Byers RJ, Sakhinia E, Joseph P, et al. Clinical quantitation of immune signature in follicular lymphoma by RT-PCR-based gene expression profiling. Blood. 2008;111:4764-4770.
22. Carreras J, Lopez-Guillermo A, Fox BC, et al. High numbers of tumor-infiltrating FOXP3-positive regulatory T cells are associated with improved overall survival in follicular lymphoma. Blood. 2006;108:2957-2964.
23. Farinha P, Masoudi H, Skinnider B F, et al. Analysis of multiple biomarkers shows that lymphoma-associated macrophage (LAM) content is an independent predictor of survival in follicular lymphoma (FL). Blood. 2005;106:2169-2174.
24. Wahlin BE, Sander B, Christensson B, Kimby E. CD8+ T-cell content in diagnostic lymph nodes measured by flow cytometry is a predictor of survival in follicular lymphoma. Clin Cancer Res. 2007;13:388-397.
25. Dave SS, Wright G, Tan B, et al. Prediction of survival in follicular lymphoma based on molecular features of tumor-infiltrating immune cells. N Engl J Med. 2004;351:2159-2169.
26. Bende RJ, Smit LA, van Noesel C J. Molecular pathways in follicular lymphoma. Leukemia. 2007;21:18-29.
27. Jaffe E. S. HNL, Stein H., Vardiman J.W. (Eds.). World Health Organization Classification of Tumors. Pathology and Genetics of Tumours of Haematopoetic an Lymphoid Tissues. Lyon: IARC Press; 2001.
28. Heckman CA, Duan H, Garcia PB, Boxer LM. Oct transcription factors mediate t(14;18) lymphoma cell survival by directly regulating bcl-2 expression. Oncogene. 2006;25:888-898.
29. Pasqualucci L, Bhagat G, Jankovic M, et al. AID is required for germinal center-derived lymphomagenesis. Nat Genet. 2008;40:108-112.
30. Viardot A, Barth TF, Moller P, Dohner H, Bentz M. Cytogenetic evolution of follicular lymphoma. Semin Cancer Biol. 2003;13:183-190.
31. Horsman DE, Connors JM, Pantzar T, Gascoyne RD. Analysis of secondary chromosomal alterations in 165 cases of follicular lymphoma with t(14;18). Genes Chromosomes Cancer. 2001;30:375-382.
32. de Jong D. Molecular pathogenesis of follicular lymphoma: a cross talk of genetic and immunologic factors. J Clin Oncol. 2005;23:6358-6363.
33. Hoglund M, Sehn L, Connors JM, et al. Identification of cytogenetic subgroups and karyotypic pathways of clonal evolution in follicular lymphomas. Genes Chromosomes Cancer. 2004;39:195-204.
34. McDonnell TJ, Korsmeyer SJ. Progression from lymphoid hyperplasia to high-grade malignant lymphoma in mice transgenic for the t(14; 18). Nature. 1991;349:254-256.
35. McDonnell TJ, Deane N, Platt FM, et al. bcl-2-immunoglobulin transgenic mice demonstrate extended B cell survival and follicular lymphoproliferation. Cell. 1989;57:79-88.
36. Albinger-Hegyi A, Hochreutener B, Abdou MT, et al. High frequency of t(14;18)-translocation breakpoints outside of major breakpoint and minor cluster regions in

follicular lymphomas: improved polymerase chain reaction protocols for their detection. Am J Pathol. 2002;160:823-832.
37. Leich E, Hartmann EM, Burek C, Ott G, Rosenwald A. Diagnostic and prognostic significance of gene expression profiling in lymphomas. Apmis. 2007;115:1135-1146.
38. Guo Y, Karube K, Kawano R, et al. Bcl2-negative follicular lymphomas frequently have Bcl6 translocation and/or Bcl6 or p53 expression. Pathol Int. 2007;57:148-152.
39. Horsman DE, Okamoto I, Ludkovski O, et al. Follicular lymphoma lacking the t(14;18)(q32;q21): identification of two disease subtypes. Br J Haematol. 2003;120:424-433.
40. Jardin F, Gaulard P, Buchonnet G, et al. Follicular lymphoma without t(14;18) and with BCL-6 rearrangement: a lymphoma subtype with distinct pathological, molecular and clinical characteristics. Leukemia. 2002;16:2309-2317.
41. Zha H, Raffeld M, Charboneau L, et al. Similarities of prosurvival signals in Bcl-2-positive and Bcl-2-negative follicular lymphomas identified by reverse phase protein microarray. Lab Invest. 2004;84:235-244.
42. Tagawa H, Karube K, Guo Y, et al. Trisomy 3 is a specific genomic aberration of t(14;18) negative follicular lymphoma. Leukemia. 2007;21:2549-2551.
43. Katzenberger T, Ott G, Klein T, Kalla J, Muller-Hermelink HK, Ott MM. Cytogenetic alterations affecting BCL6 are predominantly found in follicular lymphomas grade 3B with a diffuse large B-cell component. Am J Pathol. 2004;165:481-490.
44. Ott G, Katzenberger T, Lohr A, et al. Cytomorphologic, immunohistochemical, and cytogenetic profiles of follicular lymphoma: 2 types of follicular lymphoma grade 3. Blood. 2002;99:3806-3812.
45. Gribben JG, Freedman A, Woo SD, et al. All advanced stage non-Hodgkin's lymphomas with a polymerase chain reaction amplifiable breakpoint of bcl-2 have residual cells containing the bcl-2 rearrangement at evaluation and after treatment. Blood. 1991;78:3275-3280.
46. Trainor KJ, Brisco MJ, Wan JH, Neoh S, Grist S, Morley AA. Gene rearrangement in B- and T-lymphoproliferative disease detected by the polymerase chain reaction. Blood. 1991;78:192-196.
47. Kanda M, Suzumiya J, Ohshima K, et al. Analysis of the immunoglobulin heavy chain gene variable region of intravascular large B-cell lymphoma. Virchows Arch. 2001;439:540-546.
48. Mao Z, Quintanilla-Martinez L, Raffeld M, et al. IgVH mutational status and clonality analysis of Richter's transformation: diffuse large B-cell lymphoma and Hodgkin lymphoma in association with B-cell chronic lymphocytic leukemia (B-CLL) represent 2 different pathways of disease evolution. Am J Surg Pathol. 2007;31:1605-1614.
49. Barrans SL, O'Connor SJ, Evans PA, et al. Rearrangement of the BCL6 locus at 3q27 is an independent poor prognostic factor in nodal diffuse large B-cell lymphoma. Br J Haematol. 2002;117:322-332.
50. Barrans SL, Evans PA, O'Connor SJ, Owen RG, Morgan GJ, Jack AS. The detection of t(14;18) in archival lymph nodes: development of a fluorescence in situ hybridization (FISH)-based method and evaluation by comparison with polymerase chain reaction. J Mol Diagn. 2003;5:168-175.
51. Barrans SL, Evans PA, O'Connor SJ, et al. The t(14;18) is associated with germinal center-derived diffuse large B-cell lymphoma and is a strong predictor of outcome. Clin Cancer Res. 2003;9:2133-2139.

52. Paternoster SF, Brockman SR, McClure RF, Remstein ED, Kurtin PJ, Dewald GW. A new method to extract nuclei from paraffin-embedded tissue to study lymphomas using interphase fluorescence in situ hybridization. Am J Pathol. 2002;160:1967-1972.
53. Ott G, Katzenberger T, Greiner A, et al. The t(11;18)(q21;q21) chromosome translocation is a frequent and specific aberration in low-grade but not high-grade malignant non-Hodgkin's lymphomas of the mucosa-associated lymphoid tissue (MALT-) type. Cancer Res. 1997;57:3944-3948.
54. Pirc-Danoewinata H, Onderka E, Porenta G, et al. Phorbol-12,13-dibutyrate improves the quality of cytogenetic preparation in lymphoid malignancies. Cancer Genet Cytogenet. 1995;80:129-134.
55. Peto R, Pike MC. Conservatism of the approximation sigma (O-E)2-E in the logrank test for survival data or tumor incidence data. Biometrics. 1973;29:579-584.
56. Knutsen T. Cytogenetic mechanisms in the pathogenesis and progression of follicular lymphoma. Cancer Surv. 1997;30:163-192.
57. Haralambieva E, Kleiverda K, Mason DY, Schuuring E, Kluin PM. Detection of three common translocation breakpoints in non-Hodgkin's lymphomas by fluorescence in situ hybridization on routine paraffin-embedded tissue sections. J Pathol. 2002;198:163-170.
58. Schlegelberger B, Zhang Y, Weber-Matthiesen K, Grote W. Detection of aberrant clones in nearly all cases of angioimmunoblastic lymphadenopathy with dysproteinemia-type T-cell lymphoma by combined interphase and metaphase cytogenetics. Blood. 1994;84:2640-2648.
59. Katzenberger T, Kalla J, Leich E, et al. A distinctive subtype of t(14;18)-negative nodal follicular non-Hodgkin lymphoma characterized by a predominantly diffuse growth pattern and deletions in the chromosomal region 1p36. Blood. 2009;113:1053-1061.
60. Bea S, Ribas M, Hernandez JM, et al. Increased number of chromosomal imbalances and high-level DNA amplifications in mantle cell lymphoma are associated with blastoid variants. Blood. 1999;93:4365-4374.
61. Subramanian A, Tamayo P, Mootha VK, et al. Gene set enrichment analysis: a knowledge-based approach for interpreting genome-wide expression profiles. Proc Natl Acad Sci U S A. 2005;102:15545-15550.
62. Mootha VK, Lindgren CM, Eriksson KF, et al. PGC-1alpha-responsive genes involved in oxidative phosphorylation are coordinately downregulated in human diabetes. Nat Genet. 2003;34:267-273.
63. Shaffer AL, Wright G, Yang L, et al. A library of gene expression signatures to illuminate normal and pathological lymphoid biology. Immunol Rev. 2006;210:67-85.
64. Subramanian A, Kuehn H, Gould J, Tamayo P, Mesirov JP. GSEA-P: a desktop application for Gene Set Enrichment Analysis. Bioinformatics. 2007;23:3251-3253.
65. Klein U, Goossens T, Fischer M, et al. Somatic hypermutation in normal and transformed human B cells. Immunol Rev. 1998;162:261-280.
66. Lossos IS, Tibshirani R, Narasimhan B, Levy R. The inference of antigen selection on Ig genes. J Immunol. 2000;165:5122-5126.
67. Rosenwald A, Wright G, Chan WC, et al. The use of molecular profiling to predict survival after chemotherapy for diffuse large-B-cell lymphoma. N Engl J Med. 2002;346:1937-1947.
68. Dave SS, Fu K, Wright GW, et al. Molecular diagnosis of Burkitt's lymphoma. N Engl J Med. 2006;354:2431-2442.

69. Wright G, Tan B, Rosenwald A, Hurt EH, Wiestner A, Staudt LM. A gene expression-based method to diagnose clinically distinct subgroups of diffuse large B cell lymphoma. Proc Natl Acad Sci U S A. 2003;100:9991-9996.
70. Lam LT, Davis RE, Pierce J, et al. Small molecule inhibitors of IkappaB kinase are selectively toxic for subgroups of diffuse large B-cell lymphoma defined by gene expression profiling. Clin Cancer Res. 2005;11:28-40.
71. Shaffer AL, Lin KI, Kuo TC, et al. Blimp-1 orchestrates plasma cell differentiation by extinguishing the mature B cell gene expression program. Immunity. 2002;17:51-62.
72. Weller S, Braun MC, Tan BK, et al. Human blood IgM "memory" B cells are circulating splenic marginal zone B cells harboring a prediversified immunoglobulin repertoire. Blood. 2004;104:3647-3654.
73. McHugh RS, Whitters MJ, Piccirillo CA, et al. CD4(+)CD25(+) immunoregulatory T cells: gene expression analysis reveals a functional role for the glucocorticoid-induced TNF receptor. Immunity. 2002;16:311-323.
74. Kovanen PE, Rosenwald A, Fu J, et al. Analysis of gamma c-family cytokine target genes. Identification of dual-specificity phosphatase 5 (DUSP5) as a regulator of mitogen-activated protein kinase activity in interleukin-2 signaling. J Biol Chem. 2003;278:5205-5213.
75. Shaffer AL, Rosenwald A, Hurt EM, et al. Signatures of the immune response. Immunity. 2001;15:375-385.
76. Su AI, Wiltshire T, Batalov S, et al. A gene atlas of the mouse and human protein-encoding transcriptomes. Proc Natl Acad Sci U S A. 2004;101:6062-6067.
77. Rosenwald A, Wright G, Wiestner A, et al. The proliferation gene expression signature is a quantitative integrator of oncogenic events that predicts survival in mantle cell lymphoma. Cancer Cell. 2003;3:185-197.
78. Baechler EC, Batliwalla FM, Karypis G, et al. Interferon-inducible gene expression signature in peripheral blood cells of patients with severe lupus. Proc Natl Acad Sci U S A. 2003;100:2610-2615.
79. Liu D, Umbach DM, Peddada SD, Li L, Crockett PW, Weinberg CR. A random-periods model for expression of cell-cycle genes. Proc Natl Acad Sci U S A. 2004;101:7240-7245.
80. Whitfield ML, Sherlock G, Saldanha AJ, et al. Identification of genes periodically expressed in the human cell cycle and their expression in tumors. Mol Biol Cell. 2002;13:1977-2000.
81. Cho RJ, Huang M, Campbell MJ, et al. Transcriptional regulation and function during the human cell cycle. Nat Genet. 2001;27:48-54.
82. Basso K, Klein U, Niu H, et al. Tracking CD40 signaling during germinal center development. Blood. 2004;104:4088-4096.
83. Lindstedt M, Lundberg K, Borrebaeck CA. Gene family clustering identifies functionally associated subsets of human in vivo blood and tonsillar dendritic cells. J Immunol. 2005;175:4839-4846.
84. Mitchell TC, Hildeman D, Kedl RM, et al. Immunological adjuvants promote activated T cell survival via induction of Bcl-3. Nat Immunol. 2001;2:397-402.
85. Mathas S, Johrens K, Joos S, et al. Elevated NF-kappaB p50 complex formation and Bcl-3 expression in classical Hodgkin, anaplastic large-cell, and other peripheral T-cell lymphomas. Blood. 2005;106:4287-4293.
86. Kuppers R, Dalla-Favera R. Mechanisms of chromosomal translocations in B cell lymphomas. Oncogene. 2001;20:5580-5594.

87. Schwaenen C, Viardot A, Berger H, et al. Microarray-based genomic profiling reveals novel genomic aberrations in follicular lymphoma which associate with patient survival and gene expression status. Genes Chromosomes Cancer. 2009;48:39-54.
88. Al-Assar O, Rees-Unwin KS, Menasce LP, et al. Transformed diffuse large B-cell lymphomas with gains of the discontinuous 12q12-14 amplicon display concurrent deregulation of CDK2, CDK4 and GADD153 genes. Br J Haematol. 2006;133:612-621.
89. Siebert R, Gesk S, Harder S, et al. Deletions in the long arm of chromosome 10 in lymphomas with t(14;18): a pathogenetic role of the tumor supressor genes PTEN/MMAC1 and MXI1? Blood. 1998;92:4487-4489.
90. Vaandrager JW, Schuuring E, Raap T, Philippo K, Kleiverda K, Kluin P. Interphase FISH detection of BCL2 rearrangement in follicular lymphoma using breakpoint-flanking probes. Genes Chromosomes Cancer. 2000;27:85-94.
91. Elenitoba-Johnson KS, Jenson SD, Abbott RT, et al. Involvement of multiple signaling pathways in follicular lymphoma transformation: p38-mitogen-activated protein kinase as a target for therapy. Proc Natl Acad Sci U S A. 2003;100:7259-7264.
92. Schraders M, de Jong D, Kluin P, Groenen P, van Krieken H. Lack of Bcl-2 expression in follicular lymphoma may be caused by mutations in the BCL2 gene or by absence of the t(14;18) translocation. J Pathol. 2005;205:329-335.
93. Duan H, Heckman CA, Boxer LM. The immunoglobulin heavy-chain gene 3' enhancers deregulate bcl-2 promoter usage in t(14;18) lymphoma cells. Oncogene. 2007;26:2635-2641.
94. Xiang H, Wang J, Boxer LM. Role of the cyclic AMP response element in the bcl-2 promoter in the regulation of endogenous Bcl-2 expression and apoptosis in murine B cells. Mol Cell Biol. 2006;26:8599-8606.
95. Karube K, Ying G, Tagawa H, et al. BCL6 gene amplification/3q27 gain is associated with unique clinicopathological characteristics among follicular lymphoma without BCL2 gene translocation. Mod Pathol. 2008;21:973-978.
96. Nanjangud G, Rao PH, Teruya-Feldstein J, et al. Molecular cytogenetic analysis of follicular lymphoma (FL) provides detailed characterization of chromosomal instability associated with the t(14;18)(q32;q21) positive and negative subsets and histologic progression. Cytogenet Genome Res. 2007;118:337-344.
97. Alizadeh AA, Eisen MB, Davis RE, et al. Distinct types of diffuse large B-cell lymphoma identified by gene expression profiling. Nature. 2000;403:503-511.
98. Naresh KN. MUM1 expression dichotomises follicular lymphoma into predominantly, MUM1-negative low-grade and MUM1-positive high-grade subtypes. Haematologica. 2007;92:267-268.
99. Falini B, Fizzotti M, Pucciarini A, et al. A monoclonal antibody (MUM1p) detects expression of the MUM1/IRF4 protein in a subset of germinal center B cells, plasma cells, and activated T cells. Blood. 2000;95:2084-2092.
100. Martinez A, Pittaluga S, Rudelius M, et al. Expression of the interferon regulatory factor 8/ICSBP-1 in human reactive lymphoid tissues and B-cell lymphomas: a novel germinal center marker. Am J Surg Pathol. 2008;32:1190-1200.
101. Katzenberger T, Kalla J, Leich E, et al. A distinctive subtype of t(14;18) negative nodal follicular non-Hodgkin lymphoma characterized by a predominantly diffuse growth pattern and deletions in the chromosomal region 1p36. Blood. 2008.
102. Zurawski SM, Vega F, Jr., Huyghe B, Zurawski G. Receptors for interleukin-13 and interleukin-4 are complex and share a novel component that functions in signal transduction. Embo J. 1993;12:2663-2670.

103. Du X, Ho M, Pastan I. New immunotoxins targeting CD123, a stem cell antigen on acute myeloid leukemia cells. J Immunother. 2007;30:607-613.
104. Del Porto P, Bruno L, Mattei MG, von Boehmer H, Saint-Ruf C. Cloning and comparative analysis of the human pre-T-cell receptor alpha-chain gene. Proc Natl Acad Sci U S A. 1995;92:12105-12109.
105. Batten M, Ghilardi N. The biology and therapeutic potential of interleukin 27. J Mol Med. 2007;85:661-672.
106. Kim BK, Surti U, Pandya A, Cohen J, Rabkin MS, Swerdlow SH. Clinicopathologic, immunophenotypic, and molecular cytogenetic fluorescence in situ hybridization analysis of primary and secondary cutaneous follicular lymphomas. Am J Surg Pathol. 2005;29:69-82.
107. Streubel B, Scheucher B, Valencak J, et al. Molecular cytogenetic evidence of t(14;18)(IGH;BCL2) in a substantial proportion of primary cutaneous follicle center lymphomas. Am J Surg Pathol. 2006;30:529-536.
108. Ross CW, Ouillette PD, Saddler CM, Shedden KA, Malek SN. Comprehensive analysis of copy number and allele status identifies multiple chromosome defects underlying follicular lymphoma pathogenesis. Clin Cancer Res. 2007;13:4777-4785.
109. Lo Cunsolo C, Casciano I, Banelli B, Tonini GP, Romani M. Refined chromosomal localization of the putative tumor suppressor gene TP73. Cytogenet Cell Genet. 1998;82:199-201.
110. Li QL, Ito K, Sakakura C, et al. Causal relationship between the loss of RUNX3 expression and gastric cancer. Cell. 2002;109:113-124.
111. White PS, Kaufman BA, Marshall HN, Brodeur GM. Use of the single-strand conformation polymorphism technique to detect loss of heterozygosity in neuroblastoma. Genes Chromosomes Cancer. 1993;7:102-108.
112. Ellmeier W, Aguzzi A, Kleiner E, Kurzbauer R, Weith A. Mutually exclusive expression of a helix-loop-helix gene and N-myc in human neuroblastomas and in normal development. Embo J. 1992;11:2563-2571.
113. Shapiro DN, Sublett JE, Li B, Valentine MB, Morris SW, Noll M. The gene for PAX7, a member of the paired-box-containing genes, is localized on human chromosome arm 1p36. Genomics. 1993;17:767-769.
114. Enomoto H, Ozaki T, Takahashi E, et al. Identification of human DAN gene, mapping to the putative neuroblastoma tumor suppressor locus. Oncogene. 1994;9:2785-2791.
115. Nelson MA, Ariza ME, Yang JM, et al. Abnormalities in the p34cdc2-related PITSLRE protein kinase gene complex (CDC2L) on chromosome band 1p36 in melanoma. Cancer Genet Cytogenet. 1999;108:91-99.
116. Shendure J, Ji H. Next-generation DNA sequencing. Nat Biotechnol. 2008;26:1135-1145.
117. Sultan M, Schulz MH, Richard H, et al. A global view of gene activity and alternative splicing by deep sequencing of the human transcriptome. Science. 2008;321:956-960.

11 Appendix

11.1 Abbreviations

ABC	Activated B-cell like
ACTN1	Actinin, Alpha-1
AILT	Angioimmunoblastic T-cell lymphoma
ALL	acute lymphoblastic lymphoma
ALCL	Anaplastic large cell lymphoma
AML1/RUNX1	Acute myeloid leukemia/ Runt-related transcription factor 1
APES	3-aminopropyltriethoxysilane
B	B-lymphocyte
BAC	Bacterial artificial chromosome
BAD	BCL2 antagonist of cell death
BAK	BCL2 antagonist killer 1
BAX	BCL2-associated X protein
BCL2	B-cell lymphoma 2
BCL6	B-cell lymphoma 6
BCL2A1/Bfl1	BCL2 related protein A1
B-CLL	B-chronic lymphocytic leukemia
BCL_{XL}	BCL2 like 1
BCL11A	B-cell CLL/lymphoma 11A
BCL11b	B-cell CLL/lymphoma 11B
BCR	B-cell receptor
BH	BCL2 homology
BID	BH3 interacting domain death agonist
BIK	BCL2 interacting killer
BIM	BCL2-like 11
BL	Burkit lymphoma
BRB	Biometric research branch
BSA	Bovine serum albumin

°C	Degree Celsius
C3AR	Complement component 3a receptor
CCND1	Cyclin D1
CDK4	Cyclin dependent kinase 4
CDK6	Cyclin dependent kinase 6
CDKN2A/	
p16(INK4)/p14(ARF)	Cyclin dependent kinase inhibitor 2A
CD7	T-cell antigen CD7
CD8B1	T-cell glycoprotein CD8B1
CD10/MME	Membrane melalloendopeptidase
CD19	B-lymphocyte antigen CD19
CD20/MS4A1/B1	B-lymphocyte surface antigen B1
CD21 /CR2	Complement component receptor-2
CD22	B-cell antigen CD22
CD79a/MB1/IGA	B-lymphocyte specific MB1 protein/
CDC2L1	Cell division cycle 2-like 1
CDC2L6	Cell division cycle 2-like 6
CED9	Cell death abnormal
	Immunoglobulin associated alpha
CEP1	Centromer probe for chromosome 1
CEP7	Centromer probe for chromosome 7
CGH	Comparative genomic hybridization
CHOP	Chemotherapeutic treatment regime with Cyclophosphamide, Hydroxydaunorubicin, Vincristin (Oncovin), Predniso(lo)n
cm2	square centimeter
CNAG	Copy number analyzer for gene chip
CNAT	Copy number analysis tool
DAN	Differential screening-selected gene abberant in neuroblastoma
DAPI	4,6-Diamidino-2-phenylindol
dATP	Deoxyadenosine triphosphate
DC	Dendritic cell

dCTP	Deoxycytosine triphosphate
ddH2O	Destilled water
del	deletion
dGTP	Deoxyguanosine triphosphate
Dig	Digoxigenine
DISC	Death receptor induced complex
DMSO	Dimethyl sulfoxide
DNA	Desoxyribonucleic acid
dNTP	Desoxyribonukleosid triphosphate
DTT	Dithiothreitol
dTTP	Deoxythymidine triphosphate
dUTP	Deoxyuridine triphosphate
DLBCL	Diffuse large B-cell lymphoma
ECOG	Eastern Cooperative Oncology Group
E2F	E2F transcription factor
EDTA	Ethylenediaminetetraacetic acid
EGL1	Endoglucanase
EtOH	Ethanol
FCGR1A/IGFR1	Immunoglobulin G Fc receptor 1
FDR	False discovery rate
FICTION	Fluorescence Immunophenotyping and Interphase Cytogenetics as a Tool for the Investigation of Neoplasms
FISH	Fluorescence in situ hybridization
FDC	Follicular dendritic cell
FFPE	Formalin fixed and n embedded
FL	Follicular Lymphoma
FLIPI	Follicular Lymphoma International Prognostic Index
FOXO3A	Forkhead box O3A
FR1	Framework region1
FR2	Framework region 2
FR3	Framework region 3
g	gravitation

GC	Germinal center
GCB	Germinal center B-cell like
GCOS	Gene Chip Operating Software
GSEA	Gene set enrichment analysis
GTYPE	Gene Chip Genotyping Analysis Software
GZMB	Granzyme B
h	Hours
HCL	hairy cell leukemia
HOX11A	Homeobox A11
Icr	intermediate cluster region
ID3	Inhibitor of DNA binding 3
IG	Immunoglobulin
IgA	Immunoglobulin A
IgD	Immunoglobulin D
IgG	Immunoglobulin G
IgH	Imunoglobuline heavy chain
Igk	Immunoglobuline kappa
Igl	Immunoglobulin lambda
IgL	Imunoglobuline light chain
IgM	Immunoglobulin M
IgVH	Immunoglobulin variable heavy chain
IHC	Immunohistochemistry
iHOP	Information Hyperlinked over Proteins
IMGT	ImMunoGeneTics
IR1	Immuneresponse 1
IR2	Immuneresponse 2
IRF4/MUM1	Interferon regulating factor 4
ITK/EMT	Interleukin-2-inducible T-cell kinase/ Expressed mainly in T-cells
JH	Joining region of the Ig heavy chain
Ki67	cell proliferation antigen
LB	Luria-Bertani
LDH	Lactate dehydrogenase

LEF1	Lymphoid enhancer-binding factor 1
LGMN	Legumain
LOH	Loss of heterozygosity
M	Molar
MAP3K7	Mitogenic-activated protein kinase kinase kinase 7
MAX	Myc associated factor X
Mb	Mega base
MBD1	Methyl-CpG-binding domain protein 1
MBD2	Methyl-CpG-binding domain protein 2
Mbr	major breakpoint region
Mcr	minor cluster region
MCL	Mantle cell lymphoma
MCL1	Mantle cell lymphoma 1
MCR	Minimal chromosomal region
MES	2-(*N*-morpholino)ethanesulfonic acid
µg	Microgramm
mg	Milligramm
min	Minutes
ml	Milliliter
µm	Micrometer
mM	Millimolar
mm	Millimeter
MM	Multiple Myeloma
MOPS	3-(N-morpholino)propanesulfonic acid
MSigDB	Molecular Signature Database
MYC	Avian myelocytomatosis viral oncogene homolog
NFKB	Nuclear factor kappa B
NHL	Non Hodgkin Lymphoma
NK	Natural killer
NP-40	Tergitol-type NP-40
p	Probability
PAX5	Paired box gene 5

PAX7	Paired box gene 7
PBS	Phosphate buffered saline
PCD	Programmed cell death
PCR	Polymerase chain reaction
PEA3	
PLAGL1	Pleomorphic adenoma gene-like 1
PTCL (NOS)	Peripheral T-cell lymphoma (not otherwise specified)
PTEN	Phosphatase and tensin homolog
RAG1	Recombination activating gene 1
RAG2	Recombination activating gene 2
REAL	Revised European American Lymphoma
RNA	Ribonucleic acid
RT	Room temperature
RUNX3	Runt-related transcription factor 3
SAPE	Streptavidin, R-phycoerythrin conjugate
SEPT10	Septin 10
SHM	Somatic hypermutation
SMAD2	Mothers against decaplentaplegic, drosophila, homolog of, 2
SMAD4	Mothers against decaplentaplegic, drosophila, homolog of, 4
SNP	Single nucleotide polymorphism
SPSS	Statistical Package for the Social Science software
SRF	Serum response factor
SSC	Saline sodium citrate
T	T-lymphocyte
t	Translocation
TAE	Tris acetate + EDTA
TBK1	Tank binding kinase 1
TCF4	Transcription factor 4
TCR	T-cell receptor
TE	Tris-EDTA
Th	T-helper

TLR5	Toll like receptor 5
TLX1	T-cell leukemia homeobox 1
TMA	Tissue Microarray
TMACL	Tetramethylammonium chloride
TNFR2	Tumor necroses factor receptor 2
TNSF13B	Tumor necrosis factor ligand superfamily, member 13B
TP53	Tumor protein p53
TP73	Tumor protein 73
T-PLL	T-cell prolymphocytic leukemia
TR	Target retrieval
USF/2	Upstream stimulatory factor 2
VDJ	Variable Diversity Joining
VH	Variable heavy chain
Vκ	Variable kappa chain
Vλ	Variable lambda chain
WHO	World Health Organisation
YAC	Yeast artificial chromosome

11.4 Publications/Oral presentations

Research articles

1. Ellen Leich, Itziar Salaverria, Silvia Bea, Andreas Zettl, George Wright, Victor Moreno, Randy D. Gascoyne, Wing-Chung Chan, Rita M. Braziel, Lisa M. Rimsza, Dennis D. Weisenburger, Jan Delabie, Elaine S. Jaffe, Thomas A. Lister, Andrew J. Norton, Louis M. Staudt, Elena M. Hartmann, Hans-Konrad Mueller-Hermelink, Elias Campo, German Ott, and Andreas Rosenwald. **Follicular Lymphomas with and without Translocation t(14;18) Differ in Gene Expression Profiles and Genetic Alterations**. Blood First Edition Paper, prepublished online May 26, 2009; DOI 10.1182/blood-2009-01-198580

2. Rasa Beinoraviciute-Kellner, Katharina Schlereth, Markus Sauer, Anne Catherine Bretz, Justus Beck, Ellen Leich, Birgit Samans, Martin Eilers, Caroline Kisker, Andreas Rosenwald, Thorsten Stiewe. **DNA binding cooperativity of p53 is essential for apoptosis but not cell cycle arrest**. In Revision for publication in Cancer Research.

3. Gattenlöhner S, Stühmer T, Leich E, Reinhard M, Etschmann B, Völker HU, Serfling E, Bargou RC, Einsele H and Müller-Hermelink, H-K. **Specific detection of CD56 (NCAM) isoforms for the identification of aggressive malignant neoplasms with progressive development**. The American Journal of Pathology. 2009 April;174(4):1160-71

4. Tiemo Katzenberger, Jorg Kalla, Ellen Leich, Heike Stocklein, Elena Hartmann, Sandra Barnickel, Swen Wessendorf, M. Michaela Ott, Hans Konrad Muller-Hermelink, Andreas Rosenwald, and German Ott. **A distinctive subtype of t(14;18) negative nodal follicular non-Hodgkin lymphoma characterized by a predominantly diffuse growth pattern and deletions in the chromosomal region 1p36**. Blood. 2009 Jan 29; 113 (5): 1053-61

5. Heike Stöcklein, Grit Hutter, Jörg Kalla, Elena Hartmann, Yvonne Zimmermann, Tiemo Katzenberger, Patrick Adam, Ellen Leich, Sylvia Höller, Hans Konrad Müller-Hermelink, Andreas Rosenwald, German Ott and Martin Dreyling. **Genomic deletion and promoter methylation status of Hypermethylated in Cancer 1 (HIC1) in mantle cell lymphoma**. Journal of Hematopathology. 2008 Sept; 1: 85-95.

6. Philip J Brown, Sally L Ashe, Ellen Leich, Christof Burek, Sharon Barrans, James A Fenton, Andrew S Jack, Karen Pulford, Andreas Rosenwald, Alison H Banham. **Potentially oncogenic B-cell activation induced smaller isoforms of FOXP1 are highly expressed in the activated B-cell-like subtype of DLBCL**. Blood. 2008 Mar 1;111(5):2816-24.

7. Stefan Nagel, Ellen Leich, Hilmar Quentmeier, Corinna Meyer, Maren Kaufmann, Hans Drexler, Andreas Rosenwald and Roderick MacLeod. **Amplification at 7q22 targets cyclin-dependent kinase 6 in T-cell lymphoma**. Leukemia. 2008 Feb;22(2):387-92

8. Ellen Leich, Eugenia Haralambieva, Andreas Zettl, Andreas Chott, Thomas Rüdiger, Sylvia Höller, Hans-Konrad Müller-Hermelink, German Ott, Andreas Rosenwald. **Tissue microarray-based screening for chromosomal breakpoints affecting the T-cell receptor gene loci in mature T-cell lymphomas**. J Pathol. 2007 Sep;213(1):99-105.

9. Adam P, Steinlein C, Schmid M, Haralambieva E, Stocklein H, Leich E, Rosenwald A,
Muller-Hermelink HK, Ott G. **Characterization of chromosomal aberrations in diffuse large B-cell lymphoma (DLBL) by G-banding and spectral karyotyping (SKY)**. Cytogenet Genome Res. 2006;114(3-4):274-8.

Review Articles

Leich E, Hartmann EM, Burek C, Ott G, Rosenwald A. **Diagnostic and prognostic signifi-cance of gene expression profiling in lymphomas**. APMIS. 2007 Oct;115(10):1135-46.

Book Chapters

Ellen Leich, Elena Hartmann, Andreas Rosenwald, German Ott. **Gene expression profiling in lymphoma**. Lymphoma in the 21 century, Publicidad Permanyer S.L, in press.

Published Abstracts

1. Ellen Leich, Itziar Salaverria et al.. **Follicular Lymphomas with and without Translocation t(14;18) Differ in Gene Expression Profiles and Genetic Alterations**. Blood (ASH Annual Meeting Abstracts) 110: 360.

2. Stefan Nagel, Ellen Leich, Hilmar Quentmeier, Corinna Meyer, Andreas Zettl, Hans G. Drexler, Andreas Rosenwald, and Roderick A.F. MacLeod. **Amplification at 7q22 Targets CDK6 in T-Cell Lymphoma**. Blood (ASH Annual Meeting Abstracts) 110: 3563.

3. Ellen Leich, Itziar Salaverria et al.. **Follicular Lymphomas with and without Translo-cation t(14;18) Differ in Gene Expression Profiles and Genetic Alterations**. Der Pathologe, Springer Berlin/Heidelberg, 2008 May, 29: 1-100 (Supplement 1) , Do-047

4. Ellen Leich, Itziar Salaverria et al.. **Follicular Lymphomas with and without Translo-cation t(14;18) Differ in Gene Expression Profiles and Genetic Alterations**. J Hematopathol, Springer Berlin/Heidelberg, 2008 Jul, 1: 161-256 (Number 2), LS 44

Oral Presentations

- Congress of the American Society of Hematology (ASH), Atlanta, 2007
- Meeting of the Deutsche Gesellschaft für Pathologie (DGP), Berlin, 2008
- Meeting of the Interdisziplinäres Zentrum für Klinische Forschung (IZKF), Bad Staffelstein, Kloster Banz, 2008
- Congress of the European Association of Hematopathology (EAHP), Bordeaux, 2008
- Invitated speaker at the Transregio 17-Retreat, Beilngries, 2009
- Invitated speaker in the Institue of Pathology, Verona, 2009

11.5 ***Ehrenwörtliche Erklärung***

Hiermit versichere ich, dass ich die vorliegende Dissertation selbständig angefertigt und keine anderen als die angegebenen Quellen und Hilfsmittel verwendet habe.

Diese Arbeit wurde in gleicher oder ähnlicher Form noch zu keinem anderen Prüfungsverfahren vorgelegt.

Ich erkläre, dass ich bisher keine akademischen Grade erworben oder zu erwerben versucht habe.

Würzburg, 02.06.09

Ellen Leich

11.6 ***Acknowledgments***

I would like to thank Professor Hans-Konrad Müller Hermelink for giving me the opportunety to accomplish my Ph. D. thesis in the Institute of Pathology.

Furthermore, I would like to thank my supervisors Priv.-Doz. Andreas Rosenwald and Professor German Ott for their outstanding support during my Ph. D. thesis regarding the choice of topics and the experimental design as well as for the good working atmosphere.

Following this, I would also like to thank my supervisor from the Faculty of Biology, Priv.-Doz. Dr. Robert Hock who kindly agreed to act as the second reviewer of my thesis.

Many thanks are also directed towards Professor Elias Campo, a long-standing collaborator of our lab, and the people of his lab in Barcelona, especially Dr. Itziar Salaverria and Dr. Silvia Bea who helped with the generation of the CGH data and Dr. Victor Moreno for his contribution to the statistical analysis.

Furthermore, I would like to acknowledge all colleagues of the Lymphoma and Leukemia Molecular Profiling Project (LLMPP), especially Dr. George Wright for his statistical contributions.

Of utmost importance were of course also the professional and social support of my colleagues Irina Eichelbrönner, Theodora Nedeva, Juliana Helfrich, Heike

Brückner, Inge Klier, Doris Hetzer, Katharina Schlereth, Dr. Alberto Zamo, Dr. Heike Horn, Dr. Elena Hartmann and Dr. Eugenia Haralambieva.

Moreover, I would like to thank Petra Stempfle and her colleagues who performed the immunohistochemical stainings and Sabine Roth who helped me with the FICTION analysis.

Furthermore, I am grateful to my study colleagues and friends Sylvie Braun and Dr. Dana Specht who supported me in all situations of life during our study period.

Many thanks go also to Dr. Michalina Adamski, Dr. Andreas Immelmann, Dr. Benjamin Dälken, Dr. Joanna Tripp and Dr. Markus Fauth who contributed to my scientific education.

Since not everything in live is straight-lined, there are also several other persons to whom I am grateful and who contributed significantly, although not directly, to the success of my Ph. D. thesis.

Among those:

Wolfgang Kövel, Stefan Düll and Shukran Schaub.

My dear friends Dana Specht, Christiane Abt, Susanne Kögel and most importantly Eva Markwig.

My parents Hans and Doris Leich, my sister Ines Leich and my grandmother Luzia Leich as well as the rest of my family who gave me backing in all situations of life.

And of course I am indebted to my beloved and very understanding husband Abdel-Ilah Zbat who was and is always there for me.

11.7 *Danksagung*

Zunächst möchte ich mich bei Prof. Dr. Hans-Konrad Müller-Hermelink bedanken, der mir die Möglichkeit gab meine Dr. Arbeit in seinem Institut anzufertigen.

Meinen Betreuern Priv.-Doz. Andreas Rosenwald und Prof. German Ott danke ich vielmals für ihre herausragende professionelle Unterstützung bei der Auswahl der Themen und dem experimentellen Design sowie für die sehr angenehme Zusammenarbeit.

In Anlehnung daran möchte ich mich auch herzlich bei meinem Betreuer Priv.-Doz. Dr. Hock, aus der Biologischen Fakultät, bedanken, der sich freundlicherweise dazu bereit erklärt hat, das Zweitgutachten meiner Dr. Arbeit zu übernehmen.

Mein Dank richtet sich auch an Prof. Dr. Elias Campo aus Barcelona, ein langjähriger Kollaborationspartner unserer Arbeitsgruppe und an seine Mitarbeiter, insbesondere Dr. Itziar Salaverria and Dr. Silvia Bea die bei der Aufbereitung der CGH Daten geholfen haben und Dr. Victor Moreno danke ich für seinen Beitrag zu den statistischen Analysen.

Außerdem möchte ich mich bei allen Kollegen des Lymphoma and Leukemia Molecular Profiling Project (LLMPP) bedanken, insbesondere bei Dr. George Wright für seine große Unterstützung bei den statistischen Auswertungen.

Von besonderer Bedeutung war natürlich auch die berufliche und soziale Unterstützung meine Kollegen Irina Eichelbrönner, Theodora Nedeva, Juliana Helfrich, Heike Brückner, Inge Klier, Doris Hetzer, Katharina Schlereth, Dr. Alberto Zamo, Dr. Heike Horn, Dr. Elena Hartmann und Dr. Eugenia Haralambieva.

Darüber hinaus danke ich Petra Stempfle und ihren Kollegen für die Anfertigung der immunohistochemischen Färbungen und Sabine Roth für ihre Hilfe bei der FICTION Analyse.

Meinen Studienkollegen und Freunden Sylvie Braun und Dr. Dana Specht danke ich für die schöne Studienzeit und die stete persönliche und fachliche Unterstützung.

Des Weiteren möchte ich Dr. Andreas Immelmann, Dr. Michalina Adamski, Dr. Benjamin Dälken, Dr. Joanna Tripp und Dr. Markus Fauth für ihren Beitrag zu meiner wissenschaftlichen Ausbildung danken.

Da im Leben nicht alles nach Plan verläuft, gibt es noch einige Menschen denen ich sehr dankbar bin und die, wenn auch nicht direkt, in großem Maße zum Gelingen meiner Dr.-Arbeit beigetragen haben.

Darunter:

Wolfgang Kövel, Stefan Düll und Shukran Schaub.

Meine lieben Freunde Dana Specht, Christiane Abt, Susanne Kögel und vor allem Eva Markwig.

Meine Eltern Hans und Doris Leich, meine Schwester Ines Leich, meine Großmutter Luzia Leich, sowie meine restliche Familie, die mir in jeder Lebenssituation den Rücken gestärkt haben.
Und natürlich nicht zu vergessen mein geliebter und sehr verständnisvoller Ehemann Abdel-ilah Zbat, der immer für mich da war und ist und dem ich für seine selbstlose Unterstützung zutiefst zu Dank verpflichtet bin.